HYDROLYSIS OF ALUMINUM IN SYNTHETIC CATION EXCHANGE RESINS AND DIOCTAHEDRAL VERMICULITE

by

Stuart Brady Cotton, B.S.

Thesis submitted to the Graduate Faculty of the
Virginia Polytechnic Institute
in candidacy for the degree of

DOCTOR OF PHILOSOPHY

in

AGRONOMY

July 1965

Blacksburg, Virginia

INTRODUCTION

The introduction to the subject matter and the relation that it bears to the investigations undertaken and to the general field of agronomy is treated in the first section along with the review of pertinent literature. In the review of literature section, most of the previous work that is deemed pertinent to all that follows is outlined. The actual experimental work undertaken falls into three broad categories, but all three relate to the general investigation of hydrolysis of aluminum as affected by environments differing in charge density. The presentation of the experimental results and their discussion is preceded by the section outlining the methods, materials, and procedures used in each section. The relationship between all three categories is brought out in the final conclusion.

TABLE OF CONTENTS

TABLE OF CONTENTS (cont.)

TABLE OF CONTENTS (cont.)

TABLE OF CONTENTS (cont.)

TABLES

TABLES (cont.)

FIGURES

FIGURES (cont.)

FIGURES (cont.)

FIGURES (cont.)

REVIEW OF THE LITERATURE

The agronomic importance of aluminum in soils has long been recognized, though its exact nature is yet to be defined. Jenny (1961) has recently reviewed the interesting history in his article appropriately titled Soil Acidity Merry-go-round. The more recent developments, with particular emphasis on the chemistry of aluminum bonding, have been presented by Jackson (1963). These reviews cover the many aspects of aluminum chemistry including the hydrolysis of aluminum which is of specific interest in this study. Most workers agree that the hydrated triple charged aluminum ion hydrolyzes, initially producing a double charged ion and possibly a single charged ion having the general formula $Al_x(OH)_{3x-y}^{y+}$, but here agreement ends. The initially produced single charged ions are thought by some to undergo slow polymerization with the size of the end product being determined by the system pH (Brosset, 1952, Brosset, et al., 1954, Schofield and Taylor, 1954). Many structures, formulas, and sizes of polymeric forms of aluminum have been suggested by these and other authors (Tanabe, 1954; Matijevic and Tezac, 1953; Ruff and Tyree, 1958).

Recently, Frink and Peech (1963) have attempted to explain aluminum hydrolysis according to a simple three stage mechanism dependent on the solubility product of gibbsite, the thermodynamically preferred form of aluminum hydroxide. The variety of polymeric basic ions that have been postulated by other authors are said to be "transient stages in the aggregation of molecular Al(OH) and are representative of solutions not in equilibrium". Though these studies are all of interest to the

present effort, lack of agreement between them makes them of limited applicability.

Two of the many directions taken by the investigations of aluminum hydrolysis as related to cation exchangers will be discussed here because of their close bearing to the studies undertaken. One of these has dealt primarily with synthetic cation exchange resins and the other with naturally occurring minerals exhibiting cation exchange properties.

Hydrolysis of aluminum related to synthetic cation exchangers: Hsu and Rich (1960) investigated hydrolysis of aluminum on the synthetic exchanger, Dowex 50-X8, by studying the effect of treatment with solutions varying in degree of aluminum hydrolysis, referred to by them as OH/Al ratio. After equilibration for various times with these solutions, the cation exchange capacity decreased and the aluminum on the exchanger was found to be in two forms. One form, readily replaced by salt solutions, was referred to as exchangeable aluminum and the other, removed only by strong acids or excess base, was termed fixed aluminum. On removal of the fixed aluminum with acid, the cation exchange capacity was regenerated and the fixed aluminum was found to be in 3 to 1 ratio (equivalent basis) to the decrease in exchange capacity. The effect of solution OH/Al ratio and solution volume was studied and led to the conclusion that $Al(OH)_3$ was not blocking the exchange sites because the exchange capacity decrease continued to bear the same relationship to the quantity of aluminum fixed. That there was a saturation point for fixed aluminum was considered as additional supporting evidence.

The constant ratio observed was thought to have resulted from the fixation of ions having an average of two hydroxyl groups per aluminum. Hydrolysis and polymerization of aluminum in solution and the selectivity properties of the resin with respect to size and shape were both deemed important properties of the system. An aluminum hydroxy-polymer containing six aluminum ions bonded to each other through two hydroxyl ions in a ring structure was proposed as the principal species involved in aluminum fixation. Hsu and Rich point out that the pore diameter (8 A) of the resin as determined by Kunin (1958) was about the same as the diameter of the ring structure proposed.

The ring structure diagrammed by Hsu and Rich (1960), developed in consultation with M. L. Jackson according to the accompanying acknowledgement, is an adaptation of a structure proposed by Brosset et al. (1954, p. 1923) who used a similar double ring structure to illustrate $Al_6(OH)_{15}^{+3}$ (OH/Al ratio: 2.5). Brosset et al. concluded, after exhaustive study, that this double ring structure is "the most probable main reaction product in the hydrolysis of Al^{3+} in the acid range." Brosset (1954) acknowledges the originator of the ring structure diagrammed as being Wells (1950, p. 417); the diagram also appears in Wells (1962, p. 552) along with a review of the gibbsite structure which it depicts.

The constancy of the OH/Al ratio of the fixed aluminum found was thought to result from a stabilizing effect which prevented further hydrolysis. The stabilizing effect was attributed to the high negative charge of the resin. This investigator's effort is an extension of this work in that the investigation of aluminum fixation in resins of

different charge density is a logical consequence of the results reported.

Hydrolysis of aluminum in naturally occurring minerals: Both exchangeable and nonexchangeable aluminum exist in the interlayer region of expansible layer silicates and are important in soil chemistry. This importance is due to the controlling effect of these forms of aluminum on pH, and their indirect effect on ammonium and potassium fixation in addition ot their importance in the chemistry of sulphates and phosphates.

Fixed aluminum was investigated in montmorillonite systems by Slaughter and Milne (1960), Shen and Rich (1962), and Barnhisel and Rich (1963) along lines similar to the investigation of resins discussed above. On expansion to an interplanar spacing of 18 A, montmorillonite contains an aqueous region which is 8 A thick and may be continuous in two dimensions and has a charge density relatively lower than that of the exchange resin investigated by Hsu and Rich. Under certain conditions, the expansion may be as great as 40 A and greater (MacEwan, 1961, p. 172). Fixed aluminum in the interlayer region of montmorillonite was found by Shen and Rich (1962) to have the same linear relationship to decrease in cation exchange capacity as was found in the resin systems. The aluminum removed by dilute acid was used as a measure of fixed aluminum. It was pointed out that all the $Al(OH)_3$ was not removed as evidenced by differential thermal analysis. The evidence still supported the presence of positively charged hydroxy groups having a 2 to 1 OH/Al ratio as the agents responsible for cation exchange capacity reduction.

It was noted that pH for a minimum exchange capacity was less in the montmorillonite systems than in the resin systems. Comparable differences in hydrolysis have been noted by Coleman et al. (1960). The greater effectiveness of Dowex 50 in suppressing hydrolysis was attributed to its greater charge density which at once retained aluminum strongly and repelled similarly charged hydroxyl ions. The reasoning for the latter argument is the somewhat weaker of the two in light of the concept of proton transfer along the hydrogen bond, ("quantum mechanical tunneling") reviewed by Jackson (1963) with specific emphasis on aluminum chemistry.

The montmorillonite system was further investigated by Barnhisel and Rich (1963) who extended the work of Slaughter and Milne, obtaining greater detail on the formation of crystalline gibbsite ($Al(OH)_3$) after aging solutions of hydrolyzed aluminum. The aluminum interlayer stability, which was equated with its persistence, decreased with increased time of aging and increase in OH/Al ratio of the solutions used. The quantity of gibbsite formed was found to increase as the interlayer material disappeared. This led to the conclusion that large gibbsite sheets formed in the interlayer space, possibly promoting additional expansion of montmorillonite as they grew beyond the 8 A available. The gibbsite was said to be released by a mechanism involving the "tendency of sodium to split off the gibbsite sheet from the montmorillonite". The disappearance of the triple charged aluminum flocculating agent from the solution with increased time and OH/Al ratio and resultant creation of conditions for expansion of the montmorillonite in a dilute (0.03 N)

NaCl environment was not considered with respect to the release of interlayer material. According to the theoretical presentation of Frink and Peech (1963), the dissolution of the interlayer with concurrent precipitation of gibbsite in the aqueous phase would be a possible mechanism.

The effects of fixed aluminum on the mineralogical properties of vermiculite were extensively investigated by Rich (1960). Vermiculite differs from montmorillonite by having a smaller interplanar spacing (14 A). Among the differences noted between this system and the montmorillonite system was the much slower rate of reaction during titration with base. "Slower diffusion within the interlayer space of vermiculite because of the smaller distance between silicate sheets, the larger particle size, the higher charge density" were thought to be responsible for this behavior. Vermiculite is probably intermediate between montmorillonite and the high charge cation exchange resins (Dowex 50 X8) used by Hsu and Rich (1960).

Recently, Hsu and Bates (1964) have reported on the fixation of hydroxy-aluminum polymers by vermiculite from solutions varying in OH/Al ratio. Treatment with solutions with a ratio less that 2.1 resulted in fixation of polymers with a ratio close to 2. As the solution ratio increased, the ratio calculated for the polymers fixed also increased. They indicate that these polymers are more strongly held in vermiculite than in montmorillonite. The "single ring" "OH-Al polymers" in solution are said to be 5 A in thickness and approximately 10 to 14 A in diameter, a size which permits them to enter the vermiculite interlayer space.

The ratio of x-ray diffraction intensity obtained for the 7 A and 14 A peaks was used by Rich (1960) to indicate changes in the interlayer space, following the work of Bassett (1958). To satisfy the interlayer charge, additional aluminum must enter the interlayer space as the aluminum hydrolyzes to fixed aluminum. This increase in the electron population of the interlayer is thought to affect the coherent scattering of x-rays so as to increase the 7 A reflection, thereby increasing the 7 A/14 A ratio. The data reported reflect a 7 fold change in the ratio resulting from an 8 day hydrolysis treatment.

The use of this ratio to infer population of interlayers has been used recently by Frink (1965), who sites Bradley (1953) as a reference on the subject. After discussing diagrammed form factors and phase relationships for 14 A minerals, Bradley (1953, p. 730, Fig. 7) states that "Deficiencies of interlayer scattering matter strengthen first order and weaken second and third order" reflections. This statement is clearly intended as an illustration of the diagram and not a generality for it is followed by another statement: "Excesses have opposite effects".

Following the discussion of this figure, Bradley (1953, p. 730) states the following: "Algebraic sums of the products of relative electron densities by their respective phase angles cosines establish the scattering amplitudes of the respective orders of diffraction". Specific knowledge of the scattering amplitudes for vermiculite clearly can come only from a determination of "the algebraic sums of products" mentioned. The fact that vermiculite is deficient in interlayer material in comparison with the chlorite illustrated can only emphasize this point.

The exchange resins, montmorillonite, and trioctahedral vermiculite so far characterized with respect to aluminum fixation behavior, are similar to soil materials. These non-soil materials have been used because they can be obtained in pure form, thus eliminating many confounding factors. However, layer silicates with aluminum interlayers have been identified in soils by several workers. Rich and Obenshain (1955) described a "vermiculite-like" clay mineral whose variable degree of collapse on K-saturation is indicative of interlayer aluminum. This material, reportedly, was derived from the dioctahedral vermiculite identified in the lower horizons. Pearson and Ensminger (1949), Brown (1953, 1954), Jeffries et al. (1953), and Klages and White (1957) were among the first to report the material later termed "intergradational vermiculite-chlorite" by Jackson (1959).

Dixon and Jackson (1962), in recent studies of "intergradient chlorite-expansible layer silicates", suggest that interlayers may be preferentially developed in vermiculite rather than montmorillonite. This result is attributed to the greater "stearic pinching" associated with the higher charge of vermiculite. In the same report these investigators succeed in "only partial filling of the interlayer space" with "hydroxy-aluminohydronium" and attribute the result to "blocking of aluminum entrance".

Cook and Rich (1962) and Rich and Cook (1963) report on the weathering of muscovite and paragonite to dioctahedral vermiculite similar to the mineral described by Rich and Obenshain (1955) and Rich (1958). The techniques employed involved prolonged boiling in salt

solutions and showed promise of eventually providing a relatively pure material derived from the soil for use in soil chemistry studies. Though the expansion of the mica was by no means complete since the method was by no means perfected, the basic information as to the characteristics of the more easily expansible materials had been obtained. Thus it became an objective of the present effort to prepare as pure a specimen of soil derived dioctahedral vermiculite with which to better characterize aluminum hydrolysis in this type of soil material. If the material could be obtained in pure enough form, the comparison of theoretical and observed scattering amplitudes mentioned above was planned. In this quest, much was inferred from what is known about trioctahedral vermiculite and other micaceous minerals.

Structure of vermiculite: A comprehensive picture of the structure of trioctahedral vermiculite is presented by Mathieson and Walker (1954), and later refined by Mathieson (1958). The literature pertinent to vermiculite studies has been reviewed by Walker (1951) and more recently by Walker (1961). From structural analysis, much information has been gained as to the precise nature of the alumino-silicate network, but the nature of the interlayer region, which is of primary interest in the studies undertaken, has not been so clearly defined. In general, the bond distances and angles along with the atomic coordinates of the silicate network have been found not to vary much from vermiculite to vermiculite. In fact, the atomic coordinates reported for the silicate network of muscovite (Radoslovich, 1960) vary only slightly from the values reported for vermiculites. Mathieson (1958) reports the following

coordinates along the c axis for the 14.36 A phase of Mg-vermiculite, having chosen the octahedral magnesium as the origin: octahedral O: 1.06 A, tetrahedral Si: 2.73 A, and tetrahedral oxygen: 3.28 A. The average positions reported by Radoslovich (1960), which probably better represent dioctahedral vermiculite because muscovite is dioctahedral, are as follows: octahedral O: 1.06 A, tetrahedral Si: 2.74 A, and basal O: 3.32 A.

The nature of the interlayer is not nearly as precisely documented. Existing concepts of the interlayer region are based to a large extent on the octahedral coordination of the hydrated magnesium ion described by Bernal and Fowler (1933). This concept has been incorporated with the concepts proposed by Hendricks and Jefferson (1938) which call for an interlamellar water layer to be composed of water molecules joined into hexagonal groups in an extended hexagonal net. This configuration is determined by the triad nature of the water molecule and the forces holding it together are attributed to the hydrogen bonds. One-fourth of the hydrogens available are not required in the structure and are available to bond the layer to the silicate network or another water layer. In vermiculite, two such water layers have been found to exist in the interlayer and are shifted with respect to each other so that close packing is possible, resulting in multiple octahedrally coordinated sites. Only a portion of these sites are filled with exchangeable cations. Controversy abounds on this subject and there is little agreement as to whether the forces promoting this water structure are inherent in the nature of the

water molecule (Hendricks and Jefferson) or result from the hydration of exchangeable cations and silicate network on which the water is adsorbed, once it has been absorbed into the interlayer (Mathieson and Walker, 1954). Bradley and Serratosa (1960) have attempted to integrate the two positions.

The quantity of water present in vermiculite is variable and at least four hydration states have been identified and reported by Walker (1956). These hydration states are characterized by the interplanar spacing that obtains for each state which is referred to as a phase in the literature. The 14.36 A phase has been accurately characterized by two dimensional structural analysis (Mathieson and Walker, 1954) so the other phases are related to it by hydration or dehydration. This phase was thought to have 12 water molecules in the interlayer for every cation, with six apparently coordinating about the exchangeable cation, and the remainder associated only with the silicate network, forming vacant octahedra. Upon hydration, the 14.85 A phase is formed with 16 water molecules per cation. This increase in interplanar spacing is accounted for by Walker (1956) as resulting from "rotation of water molecules weakening H_2O - O bonds". The weakened bond increases from 2.90 A in the 14.36 A phase to "about 3.1 A" in the 14.8 phase. In effect, the silicate layers spread, leaving the H_2O-Mg-H_2O layer in the middle. The magnesium ion, acting as an exchangeable cation, is surrounded by a hydration shell of octahedrally coordinated water molecules (Walker, 1954). In such a structure, three water molecules can be thought of as being

located at the extremities of an equilateral triangle in one plane, and three in another triangle rotated 60° in another plane. This permits the water molecules of each plane to be close packed with respect to the molecules in the other plane. The two planes constitute the planes of the water layers parallel to the basal oxygens of the silicate structure. The distance between the planes through the centers of the water layers approximates 2.28 A, and the O-O bond distance was found to be 2.76 A (Mathieson, 1958) in agreement with the O-O bond lengths found by Shallcross and Carpenter (1957) and Hono and Shimaoka (1957) in ice.

From this description, it can be seen that the hydrated magnesium octahedron presents its smallest dimension (2.28 A, 2.76 A) to the silicate network (Walker, 1956). This permits a smaller interplanar spacing than would obtain if the octahedra were rotated 60°, resulting in the separation of layers by a double diameter of water (2 x 2.76 A).

In the contraction of the 14.36 A phase to the 13.82 A phase, the occupancy of sites by the interlayer cation is thought to change and to be the same as in the subsequent dehydration phase, which is 11.59 A. The two layers of water are still present in the 13.89 A phase, but Walker (1956) claims the cations have migrated to new sites near the silicate layer surfaces over the triads of oxygens. Such an arrangement of water molecules in contact with a cation forms an imperfect octahedron with the underlying basal oxygens. As pointed out by Walker, such a structure would be asymmetric if the cations were associated preferentially with one of the two sheets. If, however,

the cations were associated with alternate sides in a random fashion, a one dimensional projection on a line perpendicular of the ab plane would be symmetric.

It is to be noted that in his recent review, Walker (1961) indicates that, with the exception of the 14.36 A phase, the structures presented are "postulated structures" and that the "configuration of the interlayer regions of other phases ... have not been determined in detail."

Walker (1961) indicates that the 14.3 phase is the one more or less at equilibrium when "air dry" and expands only slowly when immersed in water. The time given for this expansion is in the order of days. The spacing reported for aluminum saturated trioctahedral vermiculite is 14.0 and the aluminum saturated vermiculite does not expand in water. These relationships were considered in detail in the assumption of structures used in the comparison of diffractions amplitudes calculated for soil derived dioctahedral vermiculite with the amplitudes observed in the study that follows.

HYDROLYSIS OF ALUMINUM IN CATION EXCHANGE RESINS

Materials and Methods

The choice of materials and methods used was dictated by the objective which was to investigate the effect of charge density on the fixation of aluminum by synthetic cation exchange resins. To this end, exchange resins with different amounts of cross linkage were selected and treated with solutions of hydrolyzed aluminum.

Preparation of solutions: In order to prevent additional metallic cations from confounding the interpretation of the results, hydrolyzed aluminum solutions were prepared by adding aluminum metal to $AlCl_3$ solutions. Solutions of hydrolyzed aluminum whose OH/Al ratio ranged from 0.25 to 2.25 were prepared by dissolving varying amounts of Alcoa aluminum foil in normal aluminum chloride. This is a slow reaction involving the oxidation of aluminum and release of hydrogen gas and goes to completion in the case of the lower OH/Al ratio solution in about five days, but may take as long as a month for the high ratio solution. If the solutions are heated, the reaction proceeds much more rapidly, but produces a hydrolyzed aluminum precipitate instead of the clear solution desired. A desired OH/Al ratio was achieved by combining in a known volume of distilled water, aluminum chloride and aluminum foil in quantities satisfying the two following equations simultaneously:

$$R = \frac{3X}{X + Y}$$

$$C = X + Y$$

where R is the desired OH/Al ratio, C is the desired concentration in

moles of aluminum per liter, X is the moles of aluminum (as foil) added per liter to produce 3X moles of OH, and Y is the moles of aluminum chloride added per liter. The normality of the solutions prepared and the quantities added are given in Table 1. The higher ratio solutions were prepared in greater concentration to reduce the time of reaction and to reduce the rate of hydrolysis of the dissolved aluminum. These solutions were not stable, but three months were required for them to yield the precipitate that rendered them unusable. The solutions were diluted to approximately 0.1 N just prior to the beginning of each experiment.

Aluminum determination: The aluminum content of these solutions and in the various extracts was determined by a method adapted from that proposed by Krupskii et al. (1961). This method is based on the ability of EDTA to complex aluminum and iron at pH 4.8 and the ability of iron to produce a colored complex with sulphosalicylic acid. An appropriate aliquot is transferred to a 125 ml Erlenmeyer flask to which standardized EDTA is added in slightly greater quantity than required to complex all the aluminum. After addition of 25 ml pH 4.8, 2 N, NH_4OH buffer, and bringing the solution to a boil on a hot plate and cooling, the excess EDTA is titrated with standardized acidic ferric iron solution to the first indication of the brown end point. Aliquots of acid solutions were neutralized prior to addition of EDTA.

Determination of OH/Al ratio: The base titer required to convert the aluminum in the solution to be analysed to aluminum hydroxide was determined by titrating appropriate aliquots to the phenothalein end

Table 1. Solutions of aluminum used in hydrolysis studies.

OH/Al ratio	Normality prepared	Aluminum foil		Aluminum chloride	
	Eq/l	moles/l	gms/l	moles/l	gms/l
0.00	1	--	--	0.3333	80.48
0.25	1	0.02775	0.7487	0.3052	73.70
0.75	1	0.08325	2.246	0.2497	60.30
1.25	2	0.2779	7.498	0.3891	93.94
1.75	3	0.5833	15.738	0.4167	100.60
2.25	4	0.9997	26.973	0.3332	80.46

point under an atmosphere of CO_2 free air with standardized NaOH. The OH initially present was calculated by subtracting the equivalents of base titer from the equivalents of aluminum found by analysis as above. The OH/Al ratio reported on a molar basis is obtained by dividing the OH present by 1/3 the aluminum values (meq) reported in the tables.

Preparation of cation exchange resins: Dowex 50 resins, 50 to 100 mesh, with varying amounts of cross linkage (X1, X4, and X8) were used to obtain varying charge density. Unfortunately, pore size and consequent water content and cation exchange capacity on a weight basis also varied (Kunin, 1958).

The strongly acidic Dowex 50 exchange resins are sulfonated styrene-divinylbenzene beads. The difference in charge density results from different degrees of "crosslinkage" which obtains in resins of different divinylbenzene composition. In Dowex: Ion Exchange, it states: "The fraction of divinylbenzene in the bead determines to what extent the ion exchange resin is free to shrink and swell." Low cross linkage resins will take up many times their weight in water and swell into a "jelly-like mass" in which the sulfonic acid groups (RSO_3^-) are immersed. Using data obtained from Dowex: Ion Exchange, (p. 17 and p. 19) on wet volume exchange capacities and percent water content, charge densities were calculated for the resins used. For the Dowex X1, X4, and X8 resins used, the charge densities were calculated to be 0.57, 1.9, and 3.4 meq/cc of water in the resin.

The resins were saturated with the desired cation and washed with distilled water, thoroughly drained, and allowed to dry in the air until

excess water had evaporated. The resins were stored wet in tightly stoppered glass jars and the cation exchange capacity determined after several days. This method was adopted to avoid effects drying might have on aluminum saturated resins. All samples of a type of resin for the principal experiment were weighed on the same day to avoid differences in water content. The weights were adjusted to obtain the same exchange capacity in all samples, but some variation in water content of the resins did result in small differences. These differences were only revealed when total exchange capacity was determined at the end of the experiment.

Cation saturation of resins: Aluminum saturation was accomplished by washing the hydrogen saturated resins with a minimun of 25 symmetries of aluminum as the normal chloride salt in seven washes. The pH of each wash was compared to the pH of the unused aluminum chloride (about 3.2) and when no difference was detectable, the resin was considered aluminum saturated. Potassium saturation was accomplished by leaching the hydrogen resin with 0.5 N KOH and the progress followed by testing the effluent with phenothelein indicator. This method was adopted when the above procedure indicated that potassium saturation with the chloride salt could be accomplished only with difficulty, if at all. Some of the earlier exploratory experiments indicated that potassium saturation had not been accomplished with five N KCl washes. The resins were washed free of salt or base as indicated respectively, by a $AgNO_3$ or pH test.

Hydrolysis treatment: Freshly diluted 0.1 N hydrolyzed aluminum solutions were added with a 100 ml pipette to 200 ml glass test tubes

containing the weighed resin samples. Both potassium and aluminum saturated resins were treated. The stoppered test tubes were placed on a slow moving shaker for the reaction times of 36 hours or 2 weeks.

Separation of solution and resin: At the end of the reaction time, the separation of solution and resin was effected by decanting the majority of the reaction solution into a plastic bottle for storage until analysis. The remainder of the solution and the resin sample were washed into 10 ml coarse fritted glass filtering funnels and quickly washed with distilled water until free of chloride as revealed by testing the effluent with $AgNO_3$. When precipitate was evident in the sample, it was removed from the funnel by flotation resulting from back washing the sample with water.

Analysis of resins: The filtering funnels were arranged in a group of six on an iron bar so that solutions flowing through them could be collected directly in 250 ml volumetric flasks. Tygon tubing with clamps used to restrict the flow rate conducted the solution from the funnel to the volumetric flask. Exchangeable aluminum was removed from the resin by leaching with 200 ml of the normal chloride salt of either magnesium or potassium. Magnesium sulfate was used in the earlier investigations. The flow rate was adjusted so that the leaching time was approximately 3 hours. The volumetric flasks were made to volume with distilled water and the solution analysed for aluminum and potassium. The resins were washed until free of chlorides and were then leached for approximately 8 hours with 200 ml 3 N HCl insuring complete dissolution of aluminum. This solution, collected as before, was analysed for aluminum and potassium

(or magnesium). The aluminum found is reported as fixed aluminum.

Potassium analysis: Potassium was determined by using a Beckman DU emission spectrophotometer to compare the solutions obtained with standards of known potassium content and identical salt and acid composition. The potassium determination was used as a measure of the cation exchange capacity (CEC_K) of the sample after treatment.

Magnesium determination: Magnesium was analysed by the Versene titration method outlined by Jackson (1956, p. 288) using the same EDTA solutions used for aluminum analysis to complex the magnesium at pH 10. Considerable difficulty was experienced with this method when aluminum was not removed as the hydroxide precipitate. Even after aluminum removal, precise results were not obtained.

Analysis of reaction solutions: The reaction solutions were analysed for aluminum and when present, potassium, by the methods described above. When precipitate was evident, the solution containers were agitated vigorously prior to obtaining the aliquot for analysis. The solutions were acidified and the aluminum precipitate digested on a hot plate prior to making solutions to volume for potassium analysis.

pH determination: The pH of the reaction solutions was determined and compared with the values obtained for a sample of the solutions that had not been used. The pH determinations were made on a Beckman, Model G, pH meter using a newly purchased glass electrode and Fisher pH 4.00 and 7.00 standard buffer solutions. Each reported value is the average of two separate determinations that were repeatable within 0.02 pH units. Electrodes were carefully washed and blotted dry with absorbent

tissue after testing each sample and 25 ml volumes of solution were used.

Accountability of aluminum: For each sample, the solution phase was analysed for aluminum before and after the reaction and the exchangeable and fixed aluminum were determined. As part of the calculations, the sum of the reaction solution aluminum, exchangeable aluminum and fixed aluminum was compared to the sum of original solution aluminum and aluminum added in the resin. This comparison was used as a check on the determinations.

OH/Al ratio calculation: The OH/Al ratio of the fixed aluminum is calculated with the assumption that the aluminum is countering only the negative charge associated with the decrease in cation exchange capacity. The remainder of the triple charge of the aluminum ion is satisfied by hydroxyl ions. Thus, the quantity of hydroxyl ions associated with the fixed aluminum is calculated by subtracting the decrease in cation exchange capacity from the equivalents of aluminum found. The ratio is reported on a molar basis.

Results and Discussion

A certain amount of exploratory investigation preceeds the development of techniques of analysis and selection of appropriate methods. Though this study was characterized by a great deal of such unproductive effort, a small portion will be presented here because it lends some weight to the conclusions reached. These observations, which were incidental to the main experiment, will be presented first.

Solution OH/Al ratio change during reaction: The analysis of the solutions prepared was undertaken primarily to see how closely the predicted solution OH/Al ratio was achieved. As can be seen by comparison of the first and last columns of Table 2, the result was satisfactory for the purpose of the experiment. Comparison of this ratio in the solutions before and after reaction reveals that in all but the lowest ratio solution, the ratio increased during the reaction with the potassium saturated Dowex X8 resin. These data can be interpreted as resulting from triple charged aluminum entering the resin in exchange for potassium and leaving in the solution phase, aluminum associated with hydroxyl ions. If fixation of polymeric forms is taking place, relatively more triple charged aluminum is leaving the solution than the aluminum associated with hydroxyl ions. The lower ratio resulting in the 0.25 solution resulted from the potassium saturated resins having a hydrogen ion fraction remaining as the result of saturation using N KCl instead of the KOH used in later investigations.

Table 2 also includes data on the back titration of the samples with standardized HCl after addition of 0.5 N NaF as called for in the

Table 2. Comparison of solution OH/Al ratio before and after reaction. (Dowex X8, K saturated, 1 week treatment).

OH/Al ratio	Al	Base titer	Acid titer		Determined OH/Al ratio
			30 min	12 hrs	
		meq/100 ml			
		Stock solution			
(Predicted)					
0.25	10.02	9.06	8.64	9.06	0.29
0.75	10.10	7.54	7.14	7.57	0.76
1.25	10.02	5.77	5.43	6.04	1.27
1.75	10.21	4.18	3.86	5.17	1.77
2.25	11.79	2.84	2.94	4.23	2.28
		Reaction solution			
(Initial)					
0.25	4.04	3.96	3.76	3.88	0.06
0.75	3.88	2.47	2.28	2.55	1.91
1.25	2.92	1.06	0.44	1.30	1.92
1.75	5.18	1.11	1.22	2.38	2.35
2.25	7.78	0.86	0.67	1.24	2.65

aluminum determination method proposed by Yuan (1959).

The fluoride ions are supposed to complex all the aluminum, releasing the hydroxyls which are then titrated. As can be seen from the table, the fluoride ions generally do not release all of the base just added, much less the hydroxyls associated with aluminum. When the titrated sample is allowed to stand for 12 hours, more of the hydroxyl ions are released, but only slightly more than the base titer. In addition to revealing that this method is useless for determining partially hydrolyzed aluminum, these data indicate that the hydroxy-aluminum complex present in these clear solutions is a discrete entity not easily destroyed. Even though partially hydrolyzed aluminum is thought of as a good buffer or proton sink, it is apparent that these solutions only exhibit this characteristic with a long reaction time. Brosset et al. (1954) has reported that when acid is added to an aged hydrolyzed aluminum solution with an OH/Al ratio equal to 2.5, the hydrogen ions react very slowly. It is clear from Table 2 that stable polynuclear complexes are present throughout the range of OH/Al ratios investigated.

Effect of solution age: In the exploratory phase of the study, magnesium sulphate solutions were used to replace exchangeable aluminum to permit the determination of potassium that might be trapped by the fixed aluminum and to determine if any chloride accompanied the hydroxyl ions associated with the fixed aluminum. Both these investigations yielded negative results, but hydrolyzed aluminum solutions of different ages were used in the experiments and produced different quantities of

fixed aluminum. These data, presented in Table 3, show that the younger solution produces more fixed aluminum in the Dowex X8 resins even when other variables are imposed on the treatment. These results indicate that the hydrolysis of aluminum in the solution is related to the production of fixed aluminum since those solutions that have undergone more hydrolysis (older solutions) yield less fixed aluminum. It is interesting to note that the activity of aluminum in the solutions of different age appears to be the same since the same amount of potassium is exchanged in resins of the same batch. Also of interest is that about the same quantity of exchangeable aluminum is found regardless of solution age. These results favor an alternate interpretation based on the size of the aluminum species rather than hydrolysis. In the solutions of greater age, hydrolysis may have produced aluminum polymers of greater size than in the younger solution and fewer of these polymers can enter the resin to become fixed. To decide which interpretation is best supported by the data, the amount of aluminum in solution must be considered. It is noted that the younger solutions all have less aluminum remaining in the solution phase, yet these different quantities of aluminum are in equilibrium with the same quantities of aluminum on the resin and have exchanged the same amount of potassium. This indicates that a greater proportion of the aluminum remaining in the younger solutions is active in cation exchange and that the difference between the two solutions results from more hydrolysis taking place after the initiation of the exchange reaction in the younger solutions.

Effect of extracting solution pH: The displacement of exchangeable

Table 3. Effect of solution age and pH of extracting solution on forms of aluminum Dowex X8, 1.25 initial solution OH/Al ratio, 1 week reaction time.

Age of solution	Resin batch	$MgSO_4$ solutions pH		Al				K			CEC_{Mg}
		Initial	Final	Soln.	Exch.	Fixed	Total	Soln.	Resin.	Total	
years						meq/sample					
2	A*	4.00	4.30	4.53	5.15	0.494	10.17	5.02	1.14	6.16	6 70
0.1	A*	4.00	4 35	4.06	5.22	.740	10.02	5.01	1.15	6.16	6.56
2	B	4.00	4.30	4.45	4.92	.730	10.10	4.74	.888	5.63	5.66
0.1	B	4.00	4.30	4.13	4.92	.992	10.05	4 75	.862	5.61	5.54
2	B	5.75	4.30	4.57	4.65	.798	10.12	4.70	.908	5.61	5.66
0.1	B	5.75	4.30	4.15	4.78	1.13	10.06	4.73	.908	5.64	5.75

* Larger sample weights of resin batch A were used.

aluminum with N $MgSO_4$ resulted in change of the extracting solution pH as can be seen in the last two lines in Table 3. Since this increase in hydrogen ion concentration could be caused by hydrolysis of aluminum on the resin or could be only the effect of aluminum in solution, analyses were carried out with extracting solutions adjusted to pH 4. The low pH solutions underwent a decrease in hydrogen ion concentration as evidenced by increase in pH to 4.3 in spite of an increase in aluminum concentration which would tend to lower the pH. Since less fixed aluminum was found with the more acid solutions, some dissolution could be taking place using the lower pH solution as well as hydrolysis taking place with the salt solution having the higher pH. The conclusion from this investigation was that a slightly buffered salt such as magnesium sulfate yielded unsatisfactory results since the aluminum on the resin was altered by the leaching treatment.

Effect of extracting solution cation: Since the use of magnesium was still desirable to study the trapping of potassium, a comparison of the chloride salts of magnesium and potassium as extracting solutions was undertaken and the results are presented in Table 4. That these two unbuffered salts with identical anions produce different results is immediately apparent from the differences in exchangeable and fixed aluminum found. Since these resins were treated identically up to the time of replacing the exchangeable aluminum, the effect can only be due to the cation used in the displacing salt solution. The loss in exchangeable aluminum was approximately equivalent to the gain in fixed aluminum, indicating that one form was converted to the other by

Table 4. Comparison of $MgCl_2$ and KCl exchangeable aluminum and associated fixed aluminum, CEC reduction, and OH/Al ratio in aluminum saturated Dowex X8 resin after 2 week hydrolysis treatment.

Soln. OH/Al ratio	Exch. Al			Fixed Al			CEC change		OH/Al ratio	
	MgCl	KCl	Change	MgCl	KCl	Change	MgCl	KCl	MgCl	KCl
					meq					
0.00	5.46	5.54	-0.08	0.34	0.28	+0.06	-0.07	-0.25	--	--
0.25	5.04	5.28	-0.24	1.41	1.34	+0.07	-0.40	-0.55	1.83	1.72
0.75	4.93	5.14	-0.21	2.16	1.84	+0.32	-0.66	-0.51	2.08	2.17
1.25	4.84	5.10	-0.26	2.30	1.92	+0.38	-0.77	-0.64	1.99	2.00
1.75	4.66	5.02	-0.36	2.73	2.26	+0.47	-0.83	-0.74	2.08	2.02
2.25	4.58	4.93	-0.35	3.01	2.24	+0.57	-0.98	-0.75	2.03	1.99

magnesium ion induced hydrolysis. Magnesium ion, being more highly hydrated than potassium, probably has a much slower rate of diffusion within the resin matrix. This would result in a slower rate of replacement of aluminum ions which could permit hydrolysis in the same fashion slow replacement with salt solutions permits hydrolysis (Pratt and Bair, 1961).

It is to be noted with emphasis that the product of this salt induced hydrolysis does not differ significantly in OH/Al ratio from the fixed aluminum present after KCl extraction for all solutions tested. Thus, if this property of aluminum polymers present in the solution which somehow enter the resin or grow in the resin, it is not different from the product produced within the resin by hydrolysis.

Comparison of analyses of resins differing in cross linkage: The analyses of resins differing in cross linkage (X8, X4, X1), initially saturated with potassium and aluminum, after two reaction times constituted the main experimental effort. The data obtained are presented in tabular form in Tables 7 - 12, and comparisons are made in Figures 1 - 3 and Tables 5 and 6.

It is an unchallengeable postulate that the total charge of the exchangeable cations must equal the cation exchange capacity. Inspection of the comparisons drawn in Table 5 indicates that excess cation charge exists in violation of this postulate if all the exchangeable aluminum ions are considered to be triple charged. The only rational conclusion is that all the aluminum exchanged is not triple charged and that what appears to be excess charge, is countered by hydroxl ions. With this

Table 5. Difference between exchangeable cations and cation exchange capacity in potassium saturated resins treated with hydrolyzed aluminum solutions.

Initial OH/Al ratio	Exch. Al + K on resin	CEC_K	Excess cations	Exch. Al OH/Al ratio	Exch. Al + K on resin	CEC_K	Excess cations	Exch. Al OH/Al ratio
	meq/sample				meq/sample			
	Dowex X1 resin							
	After 36 hours				After 2 weeks			
0.00	5.95	5.35	0.60	0.34	5.63	5.30	0.33	0.20
0.25	5.90	5.08	0.72	0.41	6.49	5.17	0.32	0.20
0.75	5.16	4.70	0.46	0.31	5.02	4.75	0.27	0.18
1.25	4.72	4.40	0.32	0.24	4.81	4.25	0.56	0.42
1.75	4.20	4.15	0.05	0.05	4.25	4.00	0.25	0.26
2.25	4.14	4.03	0.10	0.33	3.95	3.83	0.12	0.40
	Dowex X4 after 2 weeks				Dowex X8 after 2 weeks			
0.00	5.68	5.55	0.13	0.08	6.00	5.85	0.15	0.09
0.25	5.56	5.23	0.33	0.20	5.59	5.50	0.09	0.06
0.75	4.96	4.60	0.36	0.24	4.85	4.80	0.05	--
1.25	4.57	4.40	0.17	0.12	4.63	4.65	--	--
1.75	4.10	4.10	--	--	4.84	4.65	0.19	--
2.25	3.99	4.08	--	--	4.68	4.75	--	--

Table 6. Difference between exchangeable aluminum and cation exchange capacity in aluminum saturated resins treated with hydrolyzed aluminum solution.

Resin type	Initial OH/Al ratio					
	0.00	0.25	0.75	1.25	1.75	2.25
			After 36 hours			
Dowex X1	-0.16	0.04	0.07	0.09	0.13	0.26
Dowex X4	-0.13	0.02	0.07	0.07	0.02	-0.05
Dowex X8	-0.01	0.13	-0.06	0.05	0.06	-0.02
			After 3 weeks			
Dowex X1	-0.15	-0.06	0.14	0.17	0.08	0.18
Dowex X4	-0 12	-0.08	-0.14	0.02	0.01	0.03
Dowex X8	0.11	0.12	0.06	-0.05	-0.14	-0.11

assumption, the OH/Al ratios were calculated and presented for comparison in the table. These ratios represent the average composition and could result from the exchangeable ions being a mixture of triple charged, single charged $(Al(OH)_2^+$ and double charged $Al(OH)^{2+}$ ions in the proper proportions. Multicharged units sharing hydroxls are possible, but it is hard to conceive of such a unit being exchangeable.

It is noteworthy that the amount of hydroxyls associated with exchangeable cations decreases as either the time of reaction or hydroxy:aluminum ratio is increased. This is revealed best by the comparison of the two analyses of the X1 resin, though the same behavior is apparent with the X4 resin. The behavior is less pronounced with the higher charge density (X4) and may not be present at all with the highest charge density tested (X8). Table 6 indicates that this phenomenon may be totally absent in the aluminum saturated resins. Since the data seem to follow a trend that recurs in several analyses, an all-inclusive explanation is required.

If aluminum hydroxide adsorbed on the surface of the resins were somehow released at the time of cation exchange, the analysis would yield results high in aluminum. If this were to be the case, the amount released would be expected to be at a minimum at low OH/Al ratios and at a maximum at the high ratios where aluminum hydroxide would be more probable. This cannot be the explanation because the observed trend is exactly the opposite and the excess present in the X1 resin, 0.25 OH/Al ratio, 36 hour treatment is six times the fixed aluminum present.

The following interpretation is made using the trend observed

with different charge densities as a key. Lower density is synonymous with the exchange sites being further apart. If the exchange sites were far enough apart, triple charged aluminum would be hydrolyzed as separate molecules and would not form $Al_x(OH)_{3x-y}^{y+}$ by hydroxy bridges, and single $Al(OH)_2^+$ ions could conceivably be exchangeable. The absence of the excess of cations over cation exchange capacity in the aluminum saturated series would indicate that the charge density is not diffuse enough to permit this. But consider that the potassium ions remaining on the exchanger in the series originally potassium saturated are randomly distributed on the exchange sites. In this case, areas could exist where aluminum ions would be surrounded, not by aluminum ions to which they could bond on hydrolysis, but by potassium ions. This could, in effect, isolate some aluminum ions, making the hydrolyzed unit exchangeable. As the charge density increases, this isolation would be less effective since the aluminum ions would be closer to each other and could bond around or over the potassium ions. Furthermore, the effect would be expected to decrease with increasing OH/Al ratio of the solutions used because the higher OH/Al ratios could promote the growth of larger units around each individual hydrolyzed aluminum unit. With increasing time of reaction, the units would have more time to grow and become non-exchangeable. The hypothesis just presented explains all the observed trends in the data.

If the potassium resins are considered alone, the data can also be explained in terms of the presence of aluminum polymers in the solution which was one of the possible mechanisms proposed by Hsu and Rich (1962). It could be argued that only small polymers are exchangeable

and that these are present in greater quantity at the low OH/Al ratios. If this were the case, these polymers would also be present in the aluminum saturated resins where they have been shown to be absent.

If the isolation of the aluminum ions is accepted as the reason for their exchangeability, the converse must also be true. This implies that the fixed nature of aluminum is generated within the resin by hydrolysis, and is due primarily to the large size of the unit having ionic bonds to the exchanger.

Such an interpretation of the nature of fixed aluminum would not require any particular OH/Al ratio to support it. That this ratio is variable and can exceed the 2 to 1 ratio by more than the values obtained by Hsu and Rich (1962) is evidenced by the calculations presented in the last columns of Tables 7 - 12. The ratio of 2 to 1 is fairly well reproduced for the X8 resins, but does not obtain for the other types and has the greatest variability at the shortest reaction times. The overall range in OH/Al ratio is from 1.72 to 2.46 with the resins with lower charge density having the higher OH/Al ratios, but the distinction between the X4 and X1 types is not clear.

The difference between the X1 and X8 resins is brought out even more clearly in Figures 1 and 2. In both potassium and aluminum saturated resins, the relative amount of fixed aluminum increases more rapidly for the X8 resin and levels off, whereas the fixed aluminum in the X1 resins continues to increase as the OH/Al ratio is increased. The same behavior is noted for the changes in cation exchange capacity plotted for the X1 and X8 resins in Figure 3. Here again, the faster

rate, followed by a leveling off, is noted for the X8, compared to a slower but continuing rate for the X1.

The differences resulting from initial cation saturation are brought out by comparing Figures 1 and 2. Figure 1 reveals that when no other cation is present, both fixed and exchangeable aluminum, when plotted as percent of total aluminum in the system, do not show much difference, though the general trend, resulting in lower charge density material fixing more aluminum at higher OH/Al ratios, is still detectable. In Figure 2, however, the higher quantity of exchangeable aluminum in the lower charge density material is clearly demonstrated. This difference is almost entirely accounted for by this aluminum associated with hydroxyl ions which would be fixed in the X8 resin and is exchangeable in the X1. The difference between the exchangers in potassium affinity is about one percent of potassium present when treated with identical aluminum solutions, and apparently does not affect the quantity of exchangeable aluminum found.

The relatively greater ability of the lower charge density material to fix aluminum in resins originally potassium saturated probably results from the higher pH of this system. At the higher pH, aluminum in the low charge density material continues to be fixed by hydrolysis, whereas the build-up of aluminum in the X8 resins levels off markedly.

The data for the X4, not presented in Figures 1 - 3, reveals the intermediate behavior of this resin with intermediate charge density. The behavior of the X4 resins is not distinctly nor consistently like either of the other two, and was omitted from the figures to make the

Figure 1—Relationship of fixed aluminum to total aluminum in the system and exchangeable aluminum to original cation exchange capacity in Dowex 50 X8 and X1 aluminum saturated resins after two week hydrolysis treatment.

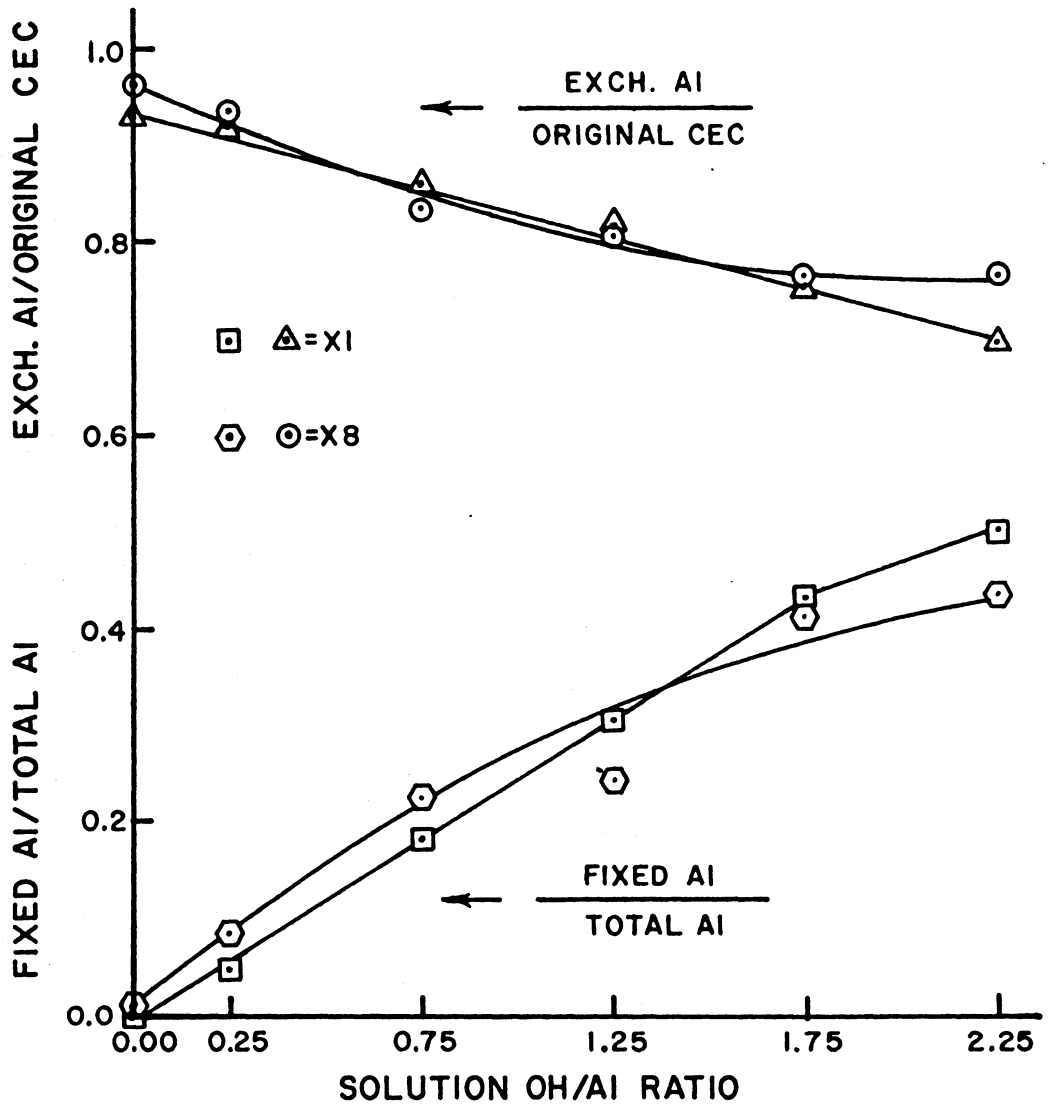
EXCH. AI/ORIGINAL CEC
FIXED AI/TOTAL AI
1.0
0.8
0.6
0.4
0.2
0.0
EXCH. AI
ORIGINAL CEC
△=X1
⊙=X8
FIXED AI
TOTAL AI
0.00
0.25
0.75
1.25
1.75
2.25
SOLUTION OH/AI RATIO

Figure 2—Relationship of fixed aluminum to total aluminum in the system and exchangeable aluminum to original cation exchange capacity in Dowex 50 X8 and X1 potassium saturated resins after two week hydrolysis treatment.

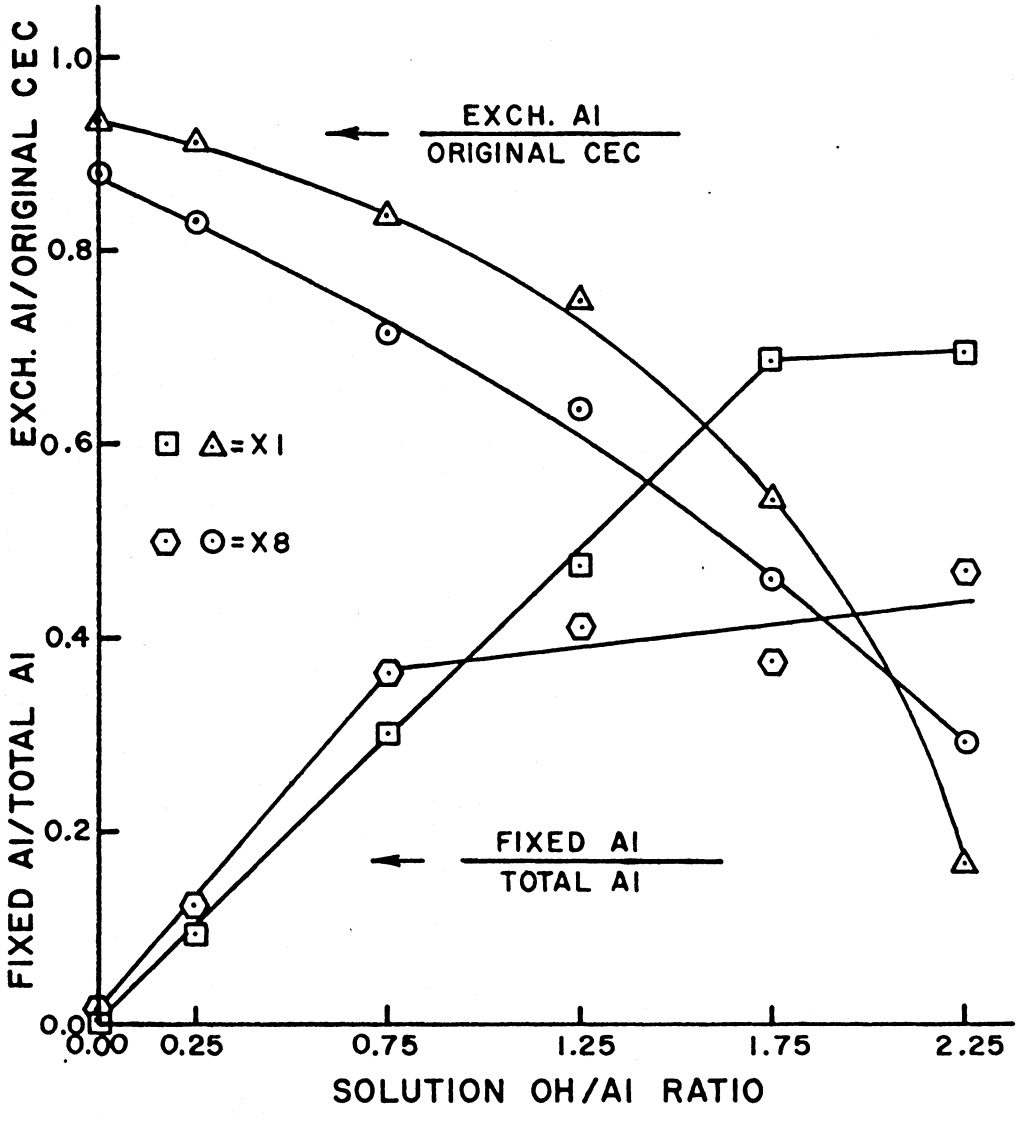
EXCH. AI/ORIGINAL CEC
1.0
0.8
0.6
0.4
0.2
0.0
EXCH. AI
ORIGINAL CEC
△=X1
⊙=X8
FIXED AI/TOTAL AI
FIXED AI
TOTAL AI
0.00
0.25
0.75
1.25
1.75
2.25
SOLUTION OH/AI RATIO

Figure 3—Comparison of decrease in cation exchange capacity in X8 and X1 resins saturated with aluminum or potassium after 2 week hydrolysis treatment.

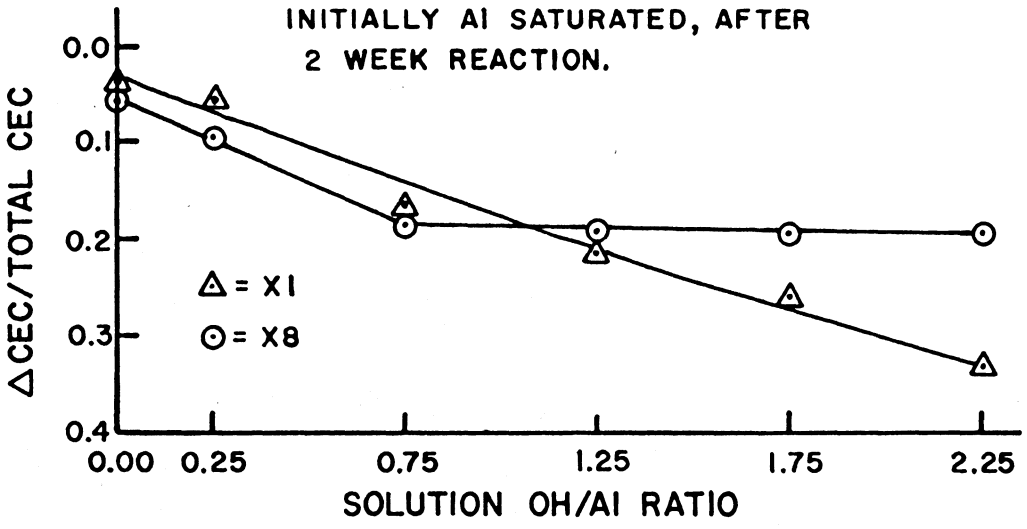
INITIALLY Al SATURATED, AFTER
2 WEEK REACTION.
ΔCEC/TOTAL CEC
0.0
0.1
0.2
0.3
0.4
△ = X1
⊙ = X8
0.00
0.25
0.75
1.25
1.75
2.25
SOLUTION OH/Al RATIO

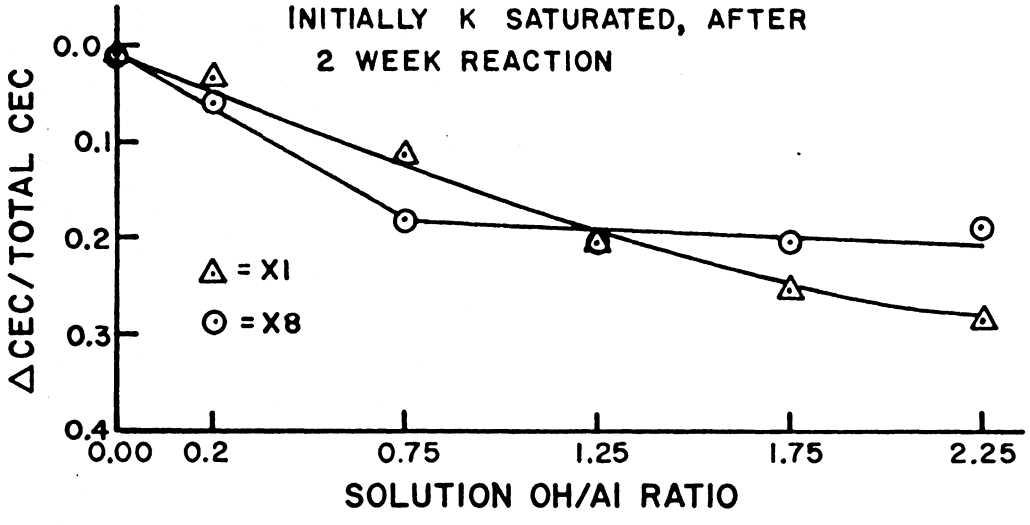
INITIALLY K SATURATED, AFTER
2 WEEK REACTION
ΔCEC/TOTAL CEC
0.0
0.1
0.2
0.3
0.4
△ = X1
⊙ = X8
0.00
0.2
0.75
1.25
1.75
2.25
SOLUTION OH/Al RATIO

existing differences more evident.

The data for the 2 week reaction time was used to illustrate the maximal development of the difference. As can be seen from Tables 7 - 12, the change with time involves an increase in fixed aluminum along with a decrease in cation exchange capacity, resulting in little change in OH/Al ratio.

Though many interpretations are possible, all must include some factor limiting fixation of aluminum and change in cation exchange capacity in the high charge density resins. This limiting factor could be space. Lack of space could prohibit aluminum from incorporating increasing amounts of aluminum into larger units during hydrolysis and additional space could permit it. The lower charge density resins have more space between charge sites and can accommodate larger $Al_x(OH)^{y+}_{3x-y}$ units with a lower charge to volume ratio. Such a hypothesis requires the fixed aluminum associated with lower charge density materials to have a higher OH/Al ratio, a hypothesis that is supported by the data. The additional pore space associated with lower cross linkage resin (Kunin, 1958), may also contribute additional space for growth.

Summary: The data and discussion presented add to the previous work of Hsu and Rich (1962) in two main aspects: (1) Exchangeable aluminum from Dowex resins is not limited to the triple charged aluminum species; (2) Fixed aluminum in Dowex resins may have other than a 2 to 1 OH/Al ratio. The data on salt induced hydrolysis would indicate that fixed aluminum in X8 resin has the 2 to 1 OH/Al ratio regardless of the method of formation. The gibbsite-like structure proposed by Hsu

and Rich (1962) may well exist in the X8 resin, but does so because the charge per unit volume (surface charge density) of such a unit is accommodated by the charge density of the resin. As the charge density decreases, larger units of the same general structure ($Al_x(OH)^{y+}_{3x-y}$), but with a higher OH/Al ratio and lower surface charge density are accommodated.

The existence of exchangeable aluminum with a finite hydroxy-aluminum ratio and the hypothesis presented accounting for this exchangeability suggest that the aluminum fixation in Dowex resins is due to stearic hindrance of the exchange, and implies that if this stearic hindrance were not present, exchange of hydrolyzed aluminum is possible. Such a situation could exist in expanded montmorillonite clays prepared by Barnhisel and Rich (1963) where a low charge density and relatively much greater space permits the growth of very large $Al_x(OH)^{y+}_{3x-y}$ units. On release into solution, these units are large enough to diffract x-rays, producing characteristic gibbsite reflections. The mechanism for their final release into solution could be cation exchange.

Finally, the data obtained on the effect of solution age suggest that hydrolysis in place can account for the growth of the fixed aluminum rather than the migration of polymers present in the solution.

Table 7. Analyses of aluminum saturated Dowex 50 X1 after reaction times of 36 hours and 2 weeks in hydrolyzed aluminum solutions of various OH/Al ratios.

Reaction solution				Resin				
Initial OH/Al ratio	pH		Al	Al		CEC_K		OH/Al ratio
	Change	Final	Change	Exch.	Fixed	Post reaction	Change	
				meq/sample				
				After 36 hours				
0.00	-0.36	3.05	0.53	4.54	0.05	4.70	0.30	--
0.25	-0.38	3.44	-0.40	4.72	0.83	4.68	0.32	1.85
0.75	-0.39	3.51	-2.00	4.37	2.74	4.30	0.70	2.24
1.25	-0.43	3.52	-3.56	4.14	4.45	4.05	0.95	2.36
1.75	-0.43	3.59	-4.62	4.03	5.55	3.90	1.10	2.40
2.25	-0.43	3.79	-4.03	4.06	4.97	3.80	1.20	2.27
				After 2 weeks				
0.00	-0.19	3.20	0.30	4.77	0.08	4.92	0.18	--
0.25	-0.33	3.49	-0.32	4.74	0.75	4.80	0.30	1.80
0.75	-0.32	3.58	-1.93	4.39	2.78	4.25	0.85	2.08
1.25	-0.36	3.59	-3.61	4.17	4.62	4.00	1.10	2.30
1.75	-0.40	3.62	-5.22	3.85	6.56	3.77	1.33	2.38
2.25	-0.46	3.76	-6.19	3.56	7.54	3.38	1.72	2.32

Table 8. Analyses of aluminum saturated Dowex 50 X4 after reaction times of 36 hours and 2 weeks in hydrolyzed aluminum solutions of various OH/Al ratios.

Reaction Solution				Resin				
Initial OH/Al Ratio	pH		Al	Al		CEC_K		OH/Al ratio
	Change	Final	Change	Exch.	Fixed	Post reaction	Change	
				meq/sample				
				After 36 hours				
0.00	-0.30	3.03	-0.02	5.37	0.18	5.50	--	--
0.25	-0.48	3.32	-0.84	5.22	1.09	5.20	-0.30	2.17
0.75	-0.43	3.42	-2.53	4.80	3.18	4.73	-0.77	2.18
1.25	-0.44	3.50	-4.16	4.55	5.18	4.48	-1.02	2.40
1.75	-0.46	3.63	-4.42	4.37	5.55	4.35	-1.15	2.38
2.25	-0.27	4.04	-2.90	4.65	3.92	4.70	-0.80	2.38
				After 2 weeks				
0.00	-0.12	3.12	-0.04	5.33	0.13	5.45	-0.05	--
0.25	-0.30	3.50	-0.75	5.17	1.13	5.25	-0.25	2.30
0.75	-0.25	3.60	-2.42	4.74	3.18	4.88	-0.62	2.42
1.25	-0.26	3.68	-4.08	4.37	5.22	4.35	-1.15	2.36
1.75	-0.35	3.74	-5.48	4.06	6.95	4.05	-1.45	2.37
2.25	-0.31	4.00	-3.25	4.48	4.26	4.45	-1.05	2.28

Table 9. Analyses of aluminum saturated Dowex 50 X8 after reaction times of 36 hours and 2 weeks in hydrolyzed aluminum solutions of various OH/Al ratio.

Reaction solution				Resin				
Initial OH/Al ratio	pH		Al	Al		CEC_K		OH/Al
	Change	Final	Change	Exch.	Fixed	Post reaction	Change	ratio
				meq/sample				
				After 36 hours				
0.00	-0.31	3.09	-0.05	5.54	0.28	5.55	-0.25	--
0.25	-0.56	3.29	-0.89	5.28	1.34	5.15	-0.50	1.72
0.75	-0.45	3.45	-1.25	5.14	1.84	5.20	-0.51	2.17
1.25	-0.40	3.58	-1.36	5.10	1.92	5.05	-0.64	2.00
1.75	-1.32	3.72	-1.27	5.02	2.26	4.96	-0.74	2.02
2.25	-0.25	4.01	-1.58	4.93	2.24	4.95	-0.75	1.99
				After 2 weeks				
0.00	-0.30	3.10	-0.00	5.61	0.31	5.50	-0.30	--
0.25	-0.51	3.33	-0.76	5.42	1.35	5.30	-0.55	1.77
0.75	-0.47	3.43	-2.49	4.84	3.62	4.78	-1.05	2.13
1.25	-0.46	3.47	-2.64	4.68	3.88	4.73	-1.13	2.12
1.75	-0.51	3.57	-2.75	4.46	4.24	4.60	-1.15	2.19
2.25	-0.57	3.70	-2.87	4.44	4.28	4.55	-1.20	2.16

Table 10. Analyses of potassium saturated Dowex 50 X1 after reaction times of 36 hours and 2 weeks in hydrolyzed aluminum solution of various OH/Al ratios.

Reaction solution					Resin					
Initial OH/Al ratio	pH		Al	K	Al		K	CEC_K		OH/Al ratio
	Change	Final			Exch.	Fixed		Post reaction	Change	
					meq/sample					
After 36 hours										
0.00	-0.17	3.24	4.65	4.68	5.28	0.11	0.67	5.35	--	--
0.25	-0.27	3.50	3.98	4.70	5.25	1.02	0.65	5.08	-0.28	2.18
0.75	-0.20	3.60	2.42	4.70	4.51	2.94	0.65	4.70	-0.65	2.34
1.25	-0.12	3.78	0.95	4.60	3.96	5.00	0.75	4.40	-0.95	2.43
1.75	0.60	4.57	0.39	4.00	2.85	6.71	1.35	4.15	-1.20	2.46
2.25	1.07	5.20	2.00	2.16	0.95	7.29	3.19	4.03	-1.32	2.46
After 2 weeks										
0.00	-0.06	3.35	4.70	4.74	5.02	0.13	0.61	5.30	-0.05	--
0.25	-0.15	3.62	4.04	4.74	4.88	0.93	0.61	5.17	-0.18	2.42
0.75	-0.08	3.72	2.44	4.80	4.47	2.98	0.55	4.75	-0.60	2.38
1.25	-0.03	3.87	1.46	4.54	4.00	4.97	0.81	4.25	-1.10	2.34
1.75	0.43	4.40	0.17	4.00	2.90	6.95	1.35	4.00	-1.35	2.39
2.25	1.19	5.32	1.40	2.28	0.90	7.78	3.05	3.83	-1.52	2.42

Table 11. Analyses of potassium saturated Dowex 50 X4 after reaction times of 36 hours and 2 weeks in hydrolyzed aluminum solutions of various OH/Al ratios.

Reaction solution					Resin					
Initial OH/Al ratio	pH		Al	K	Al		K	CEC_K		OH/Al ratio
	Change	Final			Exch.	Fixed		Post reaction	Change	
					meq/sample					
					After 36 hours					
0.00	-0.28	3.13	4.63	4.88	5.11	0.06	0.62	5.50	--	--
0.25	-0.41	3.46	4.06	4.84	4.94	1.03	0.66	5.30	-0.20	2.41
0.75	-0.35	3.60	2.52	4.88	4.45	3.10	0.62	4.75	-0.75	2.27
1.25	0.28	4.28	3.14	4.68	4.31	2.54	0.82	4.90	-0.60	2.29
1.75	0.50	4.72	1.97	4.04	2.87	5.35	1.46	4.50	-1.00	2.44
2.25	1.14	5.50	3.84	1.96	0.96	5.32	3.54	4.38	-1.12	2.37
					After 2 weeks					
0.00	-0.30	3.10	4.66	4.84	5.02	0.05	0.66	5.55	--	--
0.25	-0.36	3.49	4.04	4.86	4.92	1.04	0.64	5.23	-0.27	2.22
0.75	-0.36	3.61	2.61	4.88	4.34	3.08	0.62	4.60	-0.90	2.11
1.25	-0.20	3.50	0.78	4.82	3.89	5.20	0.68	4.40	-1.10	2.38
1.75	0.02	4.30	0.20	4.24	2.84	7.05	1.26	4.10	-1.40	2.40
2.25	1.07	5.40	1.47	2.32	0.81	7.64	3.18	4.08	-1.42	2.44

Table 12. Analyses of potassium saturated Dowex 50 X8 after 2 weeks in hydrolyzed aluminum solution of various OH/Al ratios.

Reaction solution					Resin					
Initial OH/Al ratio	pH		Al	K	Al		K	CEC_K		OH/Al ratio
	Change	Final			Exch.	Fixed		Post reaction	Change	
					meq/sample					
					After 2 weeks					
0.00	-0.34	3.07	4.67	5.00	5.15	0.12	0.85	5.85	--	--
0.25	-0.45	3.40	4.02	5.12	4.86	1.22	0.73	5.50	-0.35	2.14
0.75	-0.30	3.61	2.26	5.20	4.20	3.66	0.65	4.80	-1.05	2.14
1.25	-0.20	3.80	2.09	4.96	3.74	4.12	0.89	4.65	-1.20	2.13
1.75	0.46	4.54	3.71	3.72	2.71	3.86	2.13	4.65	-1.20	2.23
2.25	1.33	5.62	3.99	1.88	0.71	4.28	3.97	4.75	-1.10	2.24
2.25	1.39	5.68	4.13	1.80	0.71	4.20	4.05	4.85	-1.00	2.28

HYDROLYSIS OF ALUMINUM IN DIOTAHEDRAL VERMICULITE

Materials and Methods

Objectives of sample preparation: The use of intensity data to infer structure, requires certain characteristics of the sample. The goal in sample preparation then was to obtain pure dioctahedral vermiculite of known chemical composition from a soil source that satisfied these prerequisites. In addition, the sample had to be one that could be made regular enough to diffract incident x-rays so as to produce at least eight, and preferably twelve or more diffraction maxima of measurable intensity. Any knowledge of the nature of soil materials will indicate that this desired sample is an uncommon one.

Selection of material: Initially, an effort was made to expand micaceous material which approached ideal muscovite in structure and chemical composition. Some of this material was obtained from soil sources and some from grinding fresh muscovite. Though these samples met all of the prerequisites, the effort to expand the micaceous material met with very little success. For this reason, materials that had been already partially expanded by nature and might more properly be called hydrous micas were investigated. A large number of soil mica diffraction patterns are represented by Rich (1955), and from this report, suitable material was selected. High intensity of the x-ray peaks for mica and the lack of intensive weathering to 14 A component were predominant considerations in the choice. The quantity available, unfortunately, had to be a consideration in the choice. Much of the work was done with the sample that is classified

as No. 57 in the report and is the C1 - B3 horizon of the Nason soil from Orange County and will be referred to as "Nason IC". When the original supply of this sample was nearly exhausted, an unsuccessful attempt to relocate the original site was made. This effort yielded the sample referred to herein as "Nason IIC" and came from approximately the same horizon position in a road bank near the site of the original sample. When the nature of this sample was known, an additional attempt to reproduce the original sample was made by separating the 5-2 micron and 20-5 micron fraction from the soil sample of the horizon immediately above the original sample. This effort was moderately successful and yielded similar material which will be referred to as "Nason IB". Much of the chemical analysis was performed on this sample in order to economize the original material.

Initial treatment: X-ray diffraction considerations dictate that the 2-20 micron particle size be used since this range offers maximum intensity of diffraction and a minumum of absorption. In an effort to retain standard particle sizes for comparison with other work, the 2-5 micron and 5-20 micron fractions were selected for use. The particle sizes were separated by the method outlined by Jackson (1956), appropriately abbreviated after removal of free oxides by the method of Aguilera and Jackson (1953). Some of the Nason IB sample of the desired fraction was available and apparently had been prepared by the above method.

Initial purification; Selective dissolution: Since the (001) peaks of kaolinite coincide with alternate vermiculite peaks, it is

imperative that the sample be free of kaolinite. It is desirable that the sample be free of quartz, but if a known, small amount of quartz is present, appropriate corrections can be made. Two selective dissolution methods described below were investigated and evaluated in terms of kaolinite removal, interlayer aluminum material, and damage to the sample.

Selective dissolution of kaolinite and interlayer aluminum by the method proposed by Hashimoto and Jackson (1960) was employed using the Nason IC sample. One hundred milligram sample was heated to 400 C in a ceramic crucible in an electric furnace. The material was then dispersed in 250 ml 0.5 N NaOH, boiled for five minutes, cooled in a water bath, centrifuged and washed free of base. This sample was magnesium saturated and x-ray diffraction patterns obtained before and after glycerol solvation and after heating to various temperatures.

Simultaneous selective dissolution of quartz in addition to kaolinite and interlayer aluminum by the method proposed by Black and Rich (1963) to remove aluminum interlayers was attempted using both a leaching method and a batch treatment method. In both cases, all equipment used was made of plastic materials since the 0.1 N HCl, 0.2 N NH_4Cl, 0.5 N NH_4F solution used dissolves glass.

An inverted four liter plastic bottle was used as reservoir for the solution in the leaching mechanism. Rubber tubing attached to the mouth of the bottle opened into a plexiglass tube of four centimeter diameter which was held by rubber bands to a funnel, holding down a Millipore filter underlaid by a regular filter paper. The

sample, consisting of not more than about 200 milligrams of the material to be treated, was sedimented on the Millipore filter paper. Clamps pinching off the rubber tubing were then released permitting the flow of solution. With material from 2 to 20 microns and Millipore filter paper of 0.45 millimicron pore size, the flow rate was approximately 4 liters per twenty-four hours.

The batch treatment method employed a 20 liter plastic bottle filled with ten liters of solution and a 500 milligram sample. A magnetic stirrer was used to stir the solution, but it was effective only for samples smaller than 5 microns. For the larger material, frequent manual agitation was necessary. A treatment time of twenty-four hours was used, after which the sample was permitted to sediment, the bulk of the solution siphoned off, and the sample poured into centrifuge bottles, washed five times with distilled water and dried after a methanol wash. X-ray diffraction patterns of the material, predominantly NH_4 saturated, were made in addition to standard ones after magnesium saturation.

Preparation methods - mica expansion study: Numerous attempts to expand mica and hydrous mica were made using either a continuous leaching technique or a batch process. At the outset, the temperature was considered to be an important factor so all techniques used employed solutions at or near the boiling point. Removal of reaction products was considered to be of equal importance, so in the batch treatments, solutions were changed daily.

Continuous leaching: The equipment for continuous leaching

consisted of a cell containing the sample, a pump to force solutions through the cell, glass and rubber tubing serving as connectors, and a hot water bath thermostatically controlled at 95 C. The cell was constructed by connecting two fine pore size fritted glass filtering funnels mouth to mouth with standard high pressure automotive radiator hose, suitably clamped to prevent leakage. The sample was placed in the cell prior to construction and the cell dismantled to examine the sample at weekly intervals. With the particle sizes used, there was no noticeable loss of sample due to passage through the cell. Glass tubing and rubber connectors were used to connect the cell to a solution pump in such a way that the cell remained immersed in the hot bath, and the solution traveled through a sufficient length of tubing prior to entering the cell to allow the solution to attain the temperature of the bath. A Harvard Apparatus Co. infusion pump or a Brewer automatic pipet equipped with interval timer were used to force the solution through the cell at approximately 100 milliliters per hour.

Batch treatment: Two differing batch treatment methods were used. One employed a hot plate to heat the solutions, and the other employed an autoclave. The solution and sample to be boiled were placed in a florence flask or erlenmeyer with a reflux condenser attached to the top. Initially, two quart Mason jars were used for autoclaving solutions, with occasional loss of sample due to breakage. Gallon plastic bottles (Nalgene, Boston, round) were later substituted for the Mason jars. The autoclave was operated at 20 psi and always

returned to atmospheric pressure by gradual cooling rather than by opening the pressure release valves to prevent boiling over of the solutions.

Evaluation of reagents - X-ray analysis: Two different approaches to evaluating the expanding effectiveness of a solution were used. Initally, the samples were treated for varying lengths of time and the changes in the sample evaluated from comparison of x-ray diffraction patterns of samples saturated with the appropriate cations. This is the only practical method for evaluation of the continuous leaching techniques since the large volumes of solution used dilute the potassium released below the limits detectable by chemical analysis.

The solutions used in conjunction with the leaching technique are as follows:

n-Butyl amine hydrochloride: Normal solution prepared by adding 100 ml n-butyl amine to 200 ml of distilled water to which 1 equivalent HCl (82 ml conc.) was added slowly under a hood; the solution was adjusted to approximately pH 7 and distilled water added to make the solution to one liter volume. One gram of sodium citrate was added as a buffer and solution adjusted to pH 5.

Acid n-butyl amine hydrochloride: the above solution with excess acid was used to achieve pH 2.

Multi-sized cation solution: 0.3 N n-butyl amine hydrochloride, 0.3 N NaCl, 0.3 N MgCl, 0.1 N sodium citrate, adjusted to pH 2.

In addition to those listed above, the solutions used in the batch treatment method were neutral, one normal solutions of sodium

citrate, sodium chloride, barium chloride.

Potassium Release: In an effort to measure the relative effectiveness of the neutral salts, the alternative method of testing the solution after treatment was used. Fifty milligram samples of Nason IC were autoclaved in 10 ml volumes of the normal salt solutions for two and twelve hour intervals. Two additional 25 ml washes with barium chloride were made. Since only small amounts of potassium were to be released into concentrated salt solutions, this potassium had to be separated from the extracting solution for determination; this is particularly true in the case of N $BaCl_2$. An adaptation of the methods proposed by Scott and Reed (1960) based on the insolubility of potassium tetraphenol boron in water and its high solubility in acetone-water mixtures was tested on known standards and used to evaluate potassium release by the normal neutral salt solutions.

To determine the recovery of potassium by the method, a 5 ml aliquot of 5 ppm standard solution is pipetted into a 10 ml graduated pointed centrifuge tube. One ml .05 N sodium tetraphenol boron solution is added, thoroughly mixed by swirling, centrifuged (1000 rpm for 10 min.), decanted and washed three times with 2 ml 0.002 N sodium tetraphenol boron solution. The precipitate was dissolved by adding half and half mixture of acetone and water, making the solution to a 5 ml volume using the centrifuge tube calibration. This solution was compared to the standard solution using a Beckman Model DU flame emission spectrophotometer, and the results reported in Table B-3. The unknown samples were prepared in an identical manner by taking 5 ml

aliquots from the solution to be tested. The results are reported in Tables 13 and 14.

Evaluation of time of treatment and solution concentration: In the interest of finding the most economical method to remove potassium from hydrous mica with respect both to time and quantity of reagent used, the following experiment was undertaken. Four 100 mg samples of 5-2 micron Nason IC were weighed out into gallon Nalgen bottles. The treatment times used were 24 hours and two weeks; the solutions used were 0.1 $\underline{N}$ $BaCl_2$ and $\underline{N}$ $BaCl_2$. Two liter volumes of solution were used in all cases. The barium saturated samples were washed three times with distilled water after the samples had been concentrated by sedimentation and siphoning of the barium solutions. The effectiveness of the treatments was evaluated in terms of the change of x-ray diffraction patterns.

Expansion of hydrous mica; general procedure: Since the method of expanding the micas has not been fully tested, the general procedure adopted incorporated testing of the material at different stages in the treatment. One-fourth gram samples were autoclaved in three liter volumes of normal, reagent grade, barium chloride in gallon Nalgen bottles with loose caps. After each twelve hour period, the autoclave steam supply was turned off and the chamber allowed half an hour to return to atmospheric pressure by cooling. The containers were removed, allowed to cool, and the supernatant solution siphoned off. The sample from several containers can then be concentrated in one centrifuge bottle to be washed three times with distilled water. The wet sample

is then appropriately split and returned to rinsed containers to which three liters of the barium chloride solution have been added. At least five such treatments were made prior to examining the progress of the barium saturated sample by means of evaluating the x-ray diffraction pattern. Samples of the material were magnesium saturated by washing five times with N MgCl in order to further evaluate the progress of the expansion during the preliminary development of the method. Approximately ten treatments are required to produce homogeneous material with the sample sizes and solution volumes given above.

Cation saturation of dioctahedral vermiculite: The standard method of washing five times with the normal chloride salt of the cation desired was used initially. When it became apparent that this method did not give satisfactory results with the barium saturated dioctahedral vermiculite, the practice of placing the last two washes in the autoclave for an hour or more was used. To obtain complete magnesium saturation of a barium saturated sample, N $MgSO_4$ was used in the last wash. All samples were saturated with magnesium prior to saturation with any other cation. Where possible, an autoclave treatment was incorporated in saturation procedure.

Aluminum saturation: Since the aluminum saturated samples were the ones of greatest interest for structural analysis, much attention was devoted to the matter of aluminum saturation. In order to avoid hydrolysis, a magnesium saturated sample was soaked in a single wash of normal aluminum chloride for one week to achieve aluminum saturation. This sample was later compared to one that had been washed eight times

in normal aluminum chloride. After saturation, the samples were not washed salt-free as is the usual procedure in cation saturation, but were given one rapid wash, centrifuged, and either poured onto a glass slide for x-ray analysis or dried for storage after a single methanol wash.

Hydrolysis of aluminum saturated samples: Two methods of hydrolyzing the aluminum in aluminum saturated samples were employed. The first samples were placed on a sintered glass filtering funnel, and partially hydrolyzed aluminum solution (OH/Al ratio = 1.75, described on page 26) delivered to the funnel from a separatory funnel. The flow through the funnel was regulated with a clamp on tubing attached to the funnel. The treatment adopted for subsequent samples was washing with the partially hydrolyzed 0.5 N aluminum solutions (OH/Al ratio = 1.75) with examination of the progress after each wash. Additional treatments were made with the same solution but made more vigorous by boiling the solution overnight and autoclave treatments as described in the earlier section dealing with mica expansion. The progress of the hydrolysis was followed by potassium saturating a small portion of the sample and interpreting the collapsing effect of various heat treatments. For the purpose of comparison with the efforts of other workers, a twenty milligram sample of Wyoming Bentonite (2-.2 microns) was boiled in 0.5 N aluminum solution as described above.

Elution analysis: In order to estimate the effectiveness of the aluminum saturation method which incorporated many normal aluminum chloride washes, the washes were analysed. Lithium and magnesium

saturated samples weighing 100 mg were placed in weighed 100 ml plastic centrifuge tubes and were washed with exactly 50 ml $\underline{N}$ $AlCl_3$, placed on an equipoise shaker for twelve hours, centrifuged, and the supernatant poured off and kept for analysis. The tubes were weighed to determine the correction factor to be applied to the analysis of the next wash and the procedure repeated eight times. The analysis for both lithium and magnesium was carried out with a Model 303 Perkin Elmer atomic adsorption spectrophotometer. The first two washes required dilution of the sample, but the remaining washes were run directly. Two sets of standards had to be prepared with appropriate concentrations of aluminum chloride since preliminary investigation showed that aluminum in the concentrations present interferes with the determinations.

Total analysis: The most direct method to determine the extent of cation exchange is total analysis of the sample being treated. This approach was used to investigate the exchange of magnesium by sodium and lithium; 100 mg magnesium saturated samples were boiled in 300 ml of normal solution of the salts and the completeness of the exchange evaluated by total analysis. Since the quantity of sample available was severely limited, a method for total analysis utilizing only a ten milligram sample was developed. This method is possible utilizing the Kahn micro balance which can weigh the small sample with an accuracy of one-half percent, and the Perkin Elmer Model 303 which can accurately determine small amounts of the elements of interest. The air dry ten milligram samples weighed out in aluminum boats were dried at 110 C and 350 C and weight loss used to determine water loss. Structural

water was determined by heating the sample to 550 C. Additional structural water loss was estimated by heating to 800 C in a specially constructed gold foil boat. The samples were digested in 0.5 ml. perchloric acid and 5 ml hydrofluoric acid in a platinum crucible in a sand bath following the procedure outlined by Jackson (1958). The samples were taken up in 2 ml 6 N HCl; heating of the samples on a steam plate was required to dissolve the precipitate.

Potassium determination: The samples were transferred to 25 ml volumetric flasks, made to volume with water, and these solutions analysed directly for potassium by comparison against suitable standards utilizing a Beckman Model DU emission spectrophotometer. Since the high standard was 4 ppm (equivalent to 1% K in the sample), the instrument was set for maximum sensitivity and a slit setting of 0.1 was employed. The standards and samples were read without any attempt to calibrate the scale. A scale reading of more than fifty units was obtained for the high standard, insuring that potassium contents of 0.02% would be detected.

Magnesium, iron, barium, lithium determination: The Perkin Elmer Model 303 atomic adsorption spectrophotometer was used for the analysis of these elements. Barium analysis was carried out directly from the 25 ml volumetric, affording a detection limit of 0.05% in spite of the lack of sensitivity of the instrument with respect to this element. For the magnesium, iron, and lithium determination, 5 ml of sample were diluted in 50 ml volumetric flasks so that they would fall within the range of accurate determination by the atomic adsorption spectrophotometer, making the detection limit for these elements 0.002%. For

all of the above determinations, the standard settings set forth in the instruction manual were used.

Aluminum determination: The determination of aluminum was made employing the method proposed by Jones and Thurman (1959) on a 2 milliliter aliquot of the diluted sample prepared above using a Beckman Model DB spectrophotometer. This procedure permits aluminum contents up to 50% to be determined and has a detection limit of 0.5%.

Selection of reagents: After the importance of the presence of small amounts of potassium in the reagent used was recognized, the careful testing of a reagent for potassium prior to use was incorporated as part of the general procedure. To test reagents for small amounts of potassium impurity, a Bauch and Lomb strip chart recorder was used in conjunction with a Beckman Model DU spectrophotometer adapted for spectrum scanning. Solutions containing 1 ppm potassium in the normal solution of the salt to be tested were used as standards. All components were set for maximum sensitivity and the slit opened wide enough to give a deflection suitable for recording. The solution to be tested is aspirated while the spectrum is scanned from 750 to 800 millimicrons. Since a continuous recording is made on the chart paper, the background is easily determined; this permits the intensity due to the potassium added to the standard to be calculated by subtraction of the intensity found in the solution without potassium added. A quantitative estimate of the potassium present in the reagent can then be made. The accuracy and the detection limit of this procedure depend greatly on the enhancement effect of the salt tested on the emission of potassium.

Silica determination: The sodium carbonate fusion method set forth by Jackson (1958, p. 284) was adapted to the 10 mg sample size. Duplicate samples of 60 mesh Brazil quartz were used to calibrate the silica determination.

X-ray determination of quartz: Since quartz was known to be a contaminant, the quantity present was determined by comparing the intensity of the peak at 26.6° 2 θ in the sample with the intensity of the peak in a sample th which 5% 5-2 micron quartz standard had been added. The quartz standard was prepared by digesting in sodium pyrophosphate a sample of 5-2 micron separate from a soil high in quartz. The method followed was adapted from that outlined by Keily and Jackson (1965) for selective dissolution of all constituents in a soil sample except quartz and felspar.

X-ray diffraction studies: X-ray diffraction patterns for qualitative analysis were obtained using a General Electric XRD-3 instrument, and recorded logarithmically. Intensity data for quantitative analysis was obtained using an XRD-5 instrument with interval counter and printout. All intensity data reported is the average of five readings from which a background count was subtracted. The background was determined by averaging five counts obtained by step scanning on each side of the diffraction maxima, commencing 1.50° away from the maxima. Step scanning was used to obtain a better estimate of average background count.

Because the quantity of sample available was severely limited, only small quantities of sample were used to obtain the information

for qualitative study. The standard method of orienting the samples by pouring aqueous suspensions on glass slides was used. The procedure was used for the samples for quantitative study, but 100 mg samples were poured on 4 cm slides and confined to the central part of the slide by placing plastic tape strips on the edges of the slide. The tape was chosen so that its thickness was approximately equal to the thickness of the hydrated sample. Samples were hydrated by placing them in desiccators maintained at 100 percent relative humidity by the presence of water, and the samples were maintained at this humidity by an adaptation of the device described by Fink (1963).

RESULTS AND DISCUSSION

Sample Preparation

The overall objective of the investigation of different methods of sample preparation was achieved, but presentation of the diffraction patterns obtained before and after the successful treatment exclusively will not reveal all the knowledge obtained. Information gathered from some of the methods that failed will be presented for more than just mere documentation, for careful analysis of the material enlightens the interpretation of soil x-ray diffraction patterns and reveals something of the weathering processes in general.

Initial Purification: At the outset, an investigation of the selective dissolution method proposed by Hashimoto and Jackson was made in the hopes that, in addition to removing kaolinite, this treatment might make the potassium remaining in the hydrous mica more easily removable. Some representative diffraction patterns are presented in Figures 4, 5, and 7. The initial heat treatment to 400 C is supposed to dehydroxylate the kaolinite, making it easily digestible in hot 0.5 N NaOH; the disappearance of the 7 A peak is noted by comparing the untreated sample at the top of Figure 4 with any of the other patterns. The kaolinite free sample was then boiled in normal sodium citrate in an attempt to remove extraneous aluminous materials prior to magnesium saturation. The diffraction pattern obtained after this treatment also appears in Figure 4. The third order of this pattern clearly reveals that at least three components at different stages of

Figure 4—Comparison of untreated Nason IC 5-2 micron fraction (A) with the same material after selective dissolution of kaolinite by the method proposed by Hashimoto and Jackson (1960) followed by boiling in sodium citrate, glycerol solvation, and four hour heat treatment at 110 C (B) and 300 C (C).

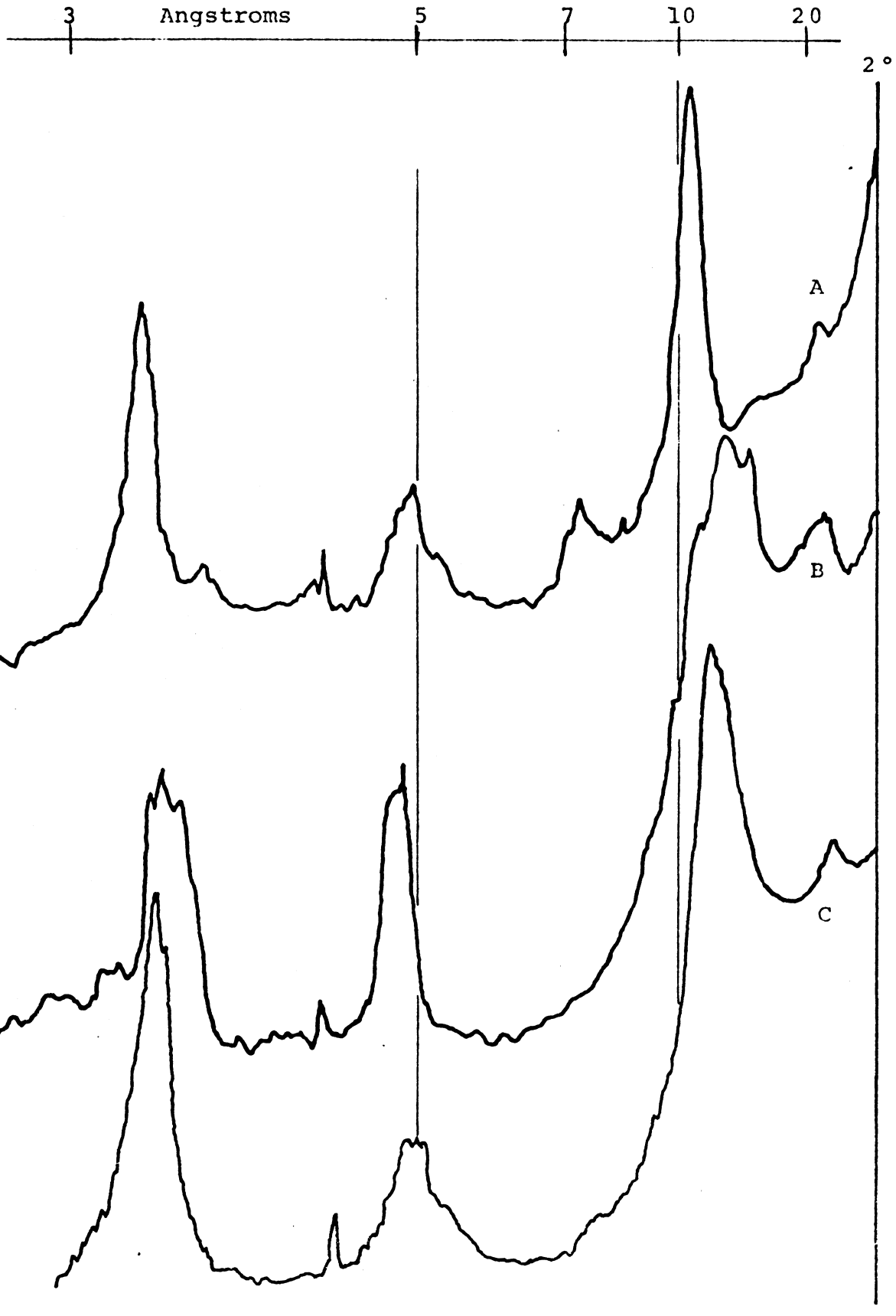
3
Angstroms
5
7
10
20
2°
A
B
C

Figure 5—Effect of leaching using sodium citrate on expansion of 5-2 micron magnesium saturated Nason IC after selective dissolution of kaolinite by method of Hashimoto and Jackson: five day treatment (A), ten day treatment (B), ten day treatment glycerol solvated (C), ten day treatment glycerol solvated and heated to 110 C (D).

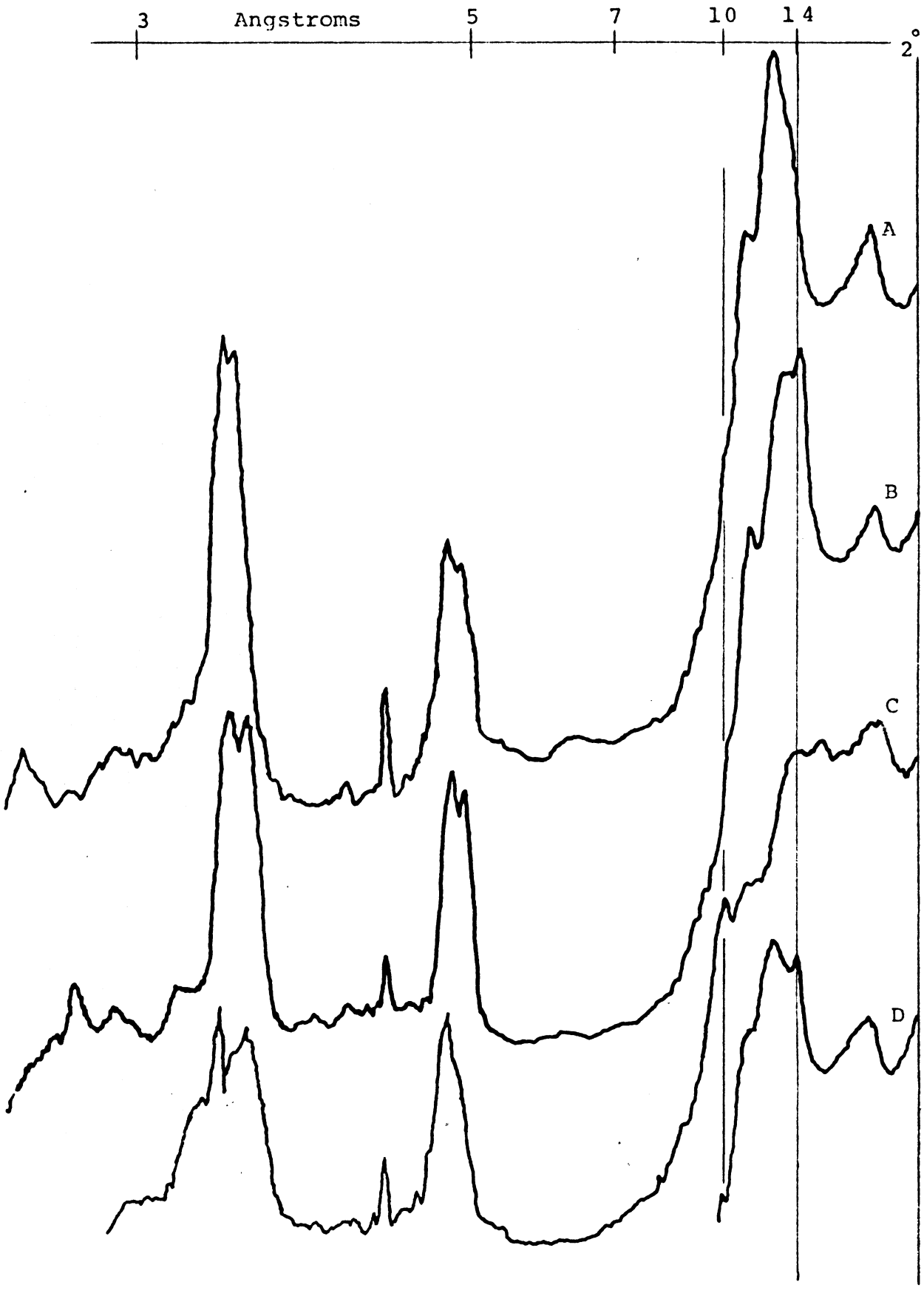
3
Angstroms
5
7
10
14
2°
A
B
C
D

Figure 6—Acid fluoride removal of kaolinite: four day leaching treatment of 5-20 micron Nason IC (A); same sample magnesium saturated (B).

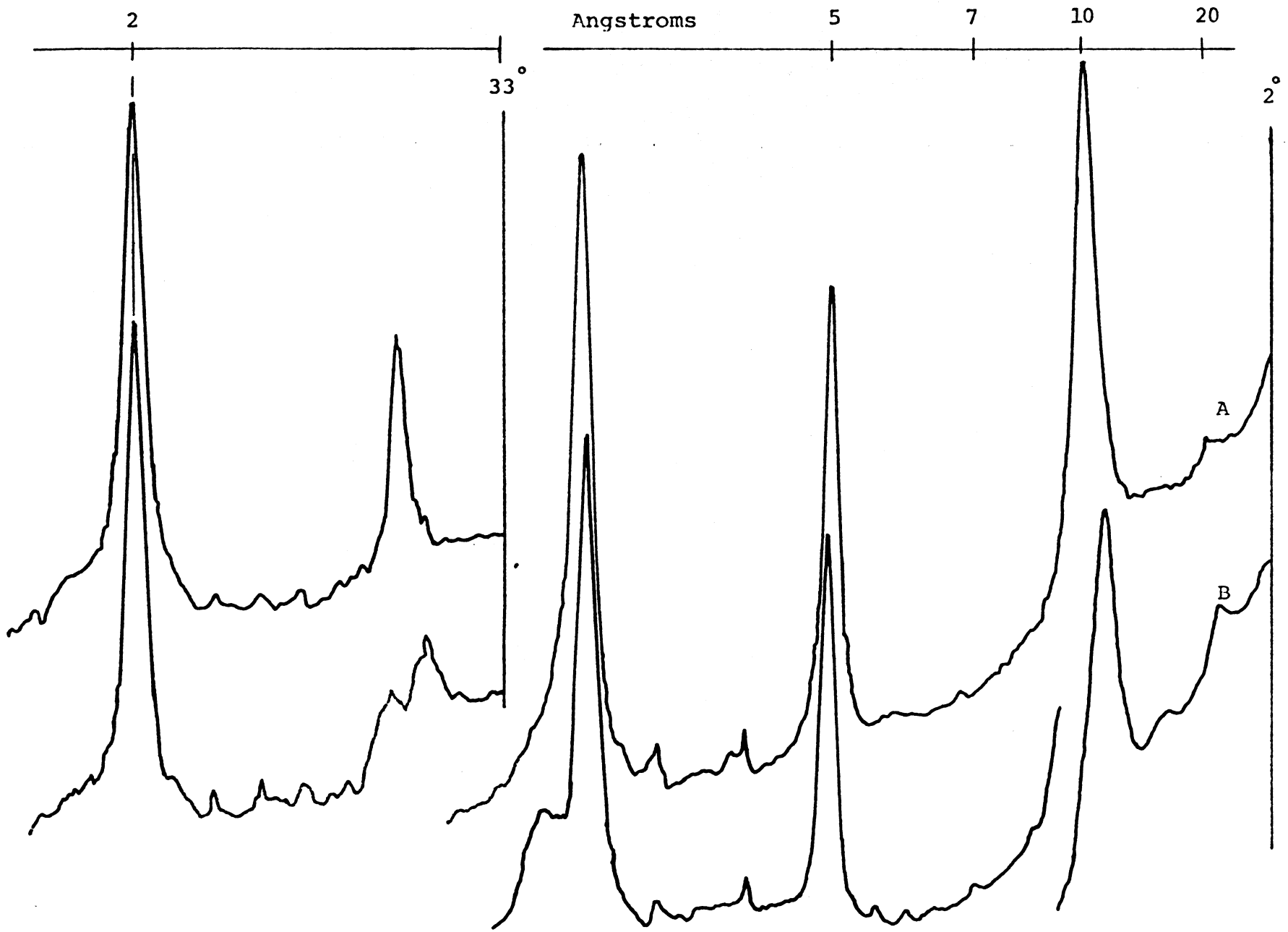
2
33°
Angstroms
5
7
10
20
2°
A
B

Figure 7—Effect of selective dissolution technique proposed by Hashimot and Jackson on crystallinity of 5-2 micron Nason IC as seen by sample leached five days by sodium citrate, magnesium saturated, heated to 550 C (A) compared with the sample without prior selective dissolution treatment, heated to 550 C (B).

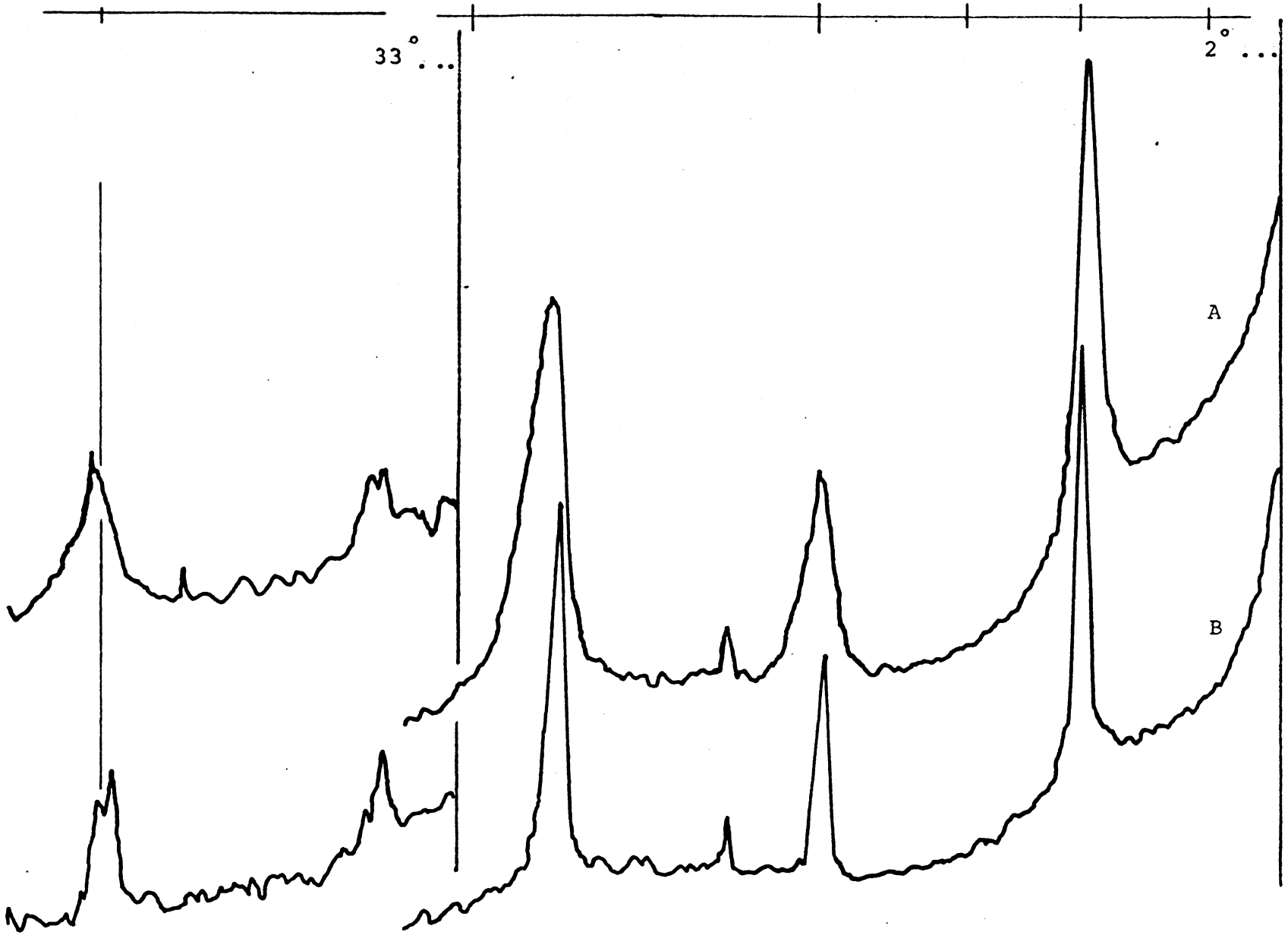
33°
2°
A
B

expansion are present in addition to considerable random interstratification; that one of these is approximately the desired 14 A is indicated by a slight peak. The third pattern in Figure 4 indicates the most serious drawback of this method. The magnesium saturated sample will not collapse to a regular 10 A phase when heated to 300 C. Since the sample had been treated with boiling hydroxide and boiling sodium citrate, one is tempted to rule out the normally encountered interlayer aluminum as the cause of this failure to collapse. It appears that the treatment has disrupted the mica structure in addition to dissolving the kaolinite. That this disruption of structure is caused by the selective dissolution methods proposed by Hashimoto and Jackson is well brought out in Figure 7, where samples with and without the treatment are compared after heating to 550 C. Additional treatment with sodium citrate followed by magnesium saturation and glycerol solvation yields material that produces the diffraction patterns presented in Figure 5. Examination of the third pattern reveals that one effect of the treatments has been to produce material with a wide variety of charge since there is a great variability of expansion. In addition, random interstratification of materials of widely differing spacings must predominate since the peaks are broad and the intensities low. All these results of the treatment make the method unsatisfactory for the endeavors of this study.

Unpublished work by Rich of the effects of continued treatment of the acid fluoride solution indicated that this combination of acids and salts was effective in dissolving kaolinite and quartz in

addition to the interlayer aluminum for which it was originally intended. When a 100 mg of Nason IC sample was leached with four liters of the solution and magnesium saturated, it produced the diffraction pattern shown in Figure 6. Comparison of this pattern obtained after sodium citrate treatment with those of Figures 4 and 5 reveals the extent of the difference between the two treatments. Both treatments remove kaolinite, but the acid fluoride treated material retains much of the regularity that is characteristic of unweathered material. Whereas the heat treated, sodium hydroxide-washed material must have been attacked on edges and faces of the mica platelets, the acid fluoride must attack only along edges, possibly dissolving away weathered fringes without disturbing the interior portion except to remove any interlayer aluminum compounds. It was noted that the leaching method, if prolonged, could remove essentially all the quartz and kaolinite in the sample, while leaving behind the micaceous material. Approximately one-half of the total sample by weight was dissolved by such a treatment. The batch treatment method, on the other hand, was not effective in removing quartz, though approximately the same sample solution volumes were used. From these observations one can conclude that the silica content required to stop dissolution of quartz is much lower than that required to stop dissolution of kaolinite. In the leaching method, fresh solution is continually supplied, permitting the dissolution of quartz. Since the presence or absence of quartz was not critical, and quartz was occasionally useful in calibrating diffraction patterns, the batch method of sample preparation was

considered preferable since it permitted the preparation of larger samples in a shorter time.

Expansion of Mica

Evaluation of Solutions: Since there is no known natural source of pure dioctahedral vermiculite, further study requiring the pure material could not progress unless this material was produced from dioctahedral mica. To this end, the solutions described in the previous section were concocted with previous knowledge and theories dictating the ingredients with the intent that treating hydrous mica with these solutions would produce dioctahedral vermiculite. Typical of the solutions investigated was the multi-sized cation solution. It was theorized that if cations of different sizes were present together, the small ones could work their way in between the mica platelets, exchanging for potassium, permitting some expansion and the entrance of a larger cation. The size ranged from that of the hydrogen ion, the smallest possible, provided by the low pH, to n-butyl amine, a fairly large one; sodium and magnesium were included because of their intermediate size. The leaching apparatus described in the previous section was constructed to keep potassium from building up in the solution and stopping the exchange reaction; citrate was added to complex any aluminum that might be released. A sample was leached with this solution at 95 C for two weeks and no change detected in the x-ray diffraction pattern. Solutions of neutral n-butyl amine and acid n-butyl amine were investigated in the same manner with the same result. Use of the autoclave and batch treatments did not alter the outcome. Apparently the good results obtained by Weiss and Kantner (1960) were primarily due to the long reaction times (1 year).

Sodium citrate used as a leaching solution did give some results as evidenced by Figures 5 and 8. Comparison of the five and ten day treatments in Figure 5 indicates that slow progress was being achieved. The ten day treatment diffraction pattern exhibits a distinct 14 A phase which is absent in the five day treatment. Consideration of Figure 8 indicates that though good progress seems to be made in the first five days, the twelve day treatment does not have much additional effect. There appear to be two kinds of material present originally: a ten A component and a randomly interstratified component with a peak at eleven A. The ten A component is not discernable in the magnesium saturated, untreated sample. The effect of the sodium citrate treatment is to alter the composition of the randomly interstratified component, making it richer in 14 A material, resulting in a shift of the peak from 8 to 7.6 degrees 2θ, permitting the 10 A peak to be resolved. The effect of additional treatment is only on the randomly interstratified component, causing further slight shifting to smaller angle of its peak. The peak at 3.7 degrees 2θ, which reaches its maximum development in the third pattern in Figure 8, is attributed to diffraction from randomly interstratified combinations of 10 and 14 A components. According to MacEwan et al. (1961, p. 416), the 11.8 A spacing represents approximately fifty-fifty random interstratification. More accurately, the peaks at 4.84 and 3.41 A represent 002/003 and 003/004 random interstratification of 10 and 14 A species corresponding to 60 and 62 percent ten A phase respectively. When the random interstratification approaches this

Figure 8—Effect of leaching with sodium citrate solution: acid fluoride treated 5-2 micron Nason IC, magnesium saturated, 25 C (A); same sample leached five days (B), and leached twelve days (C), in sodium citrate, magnesium saturated, 25 C.

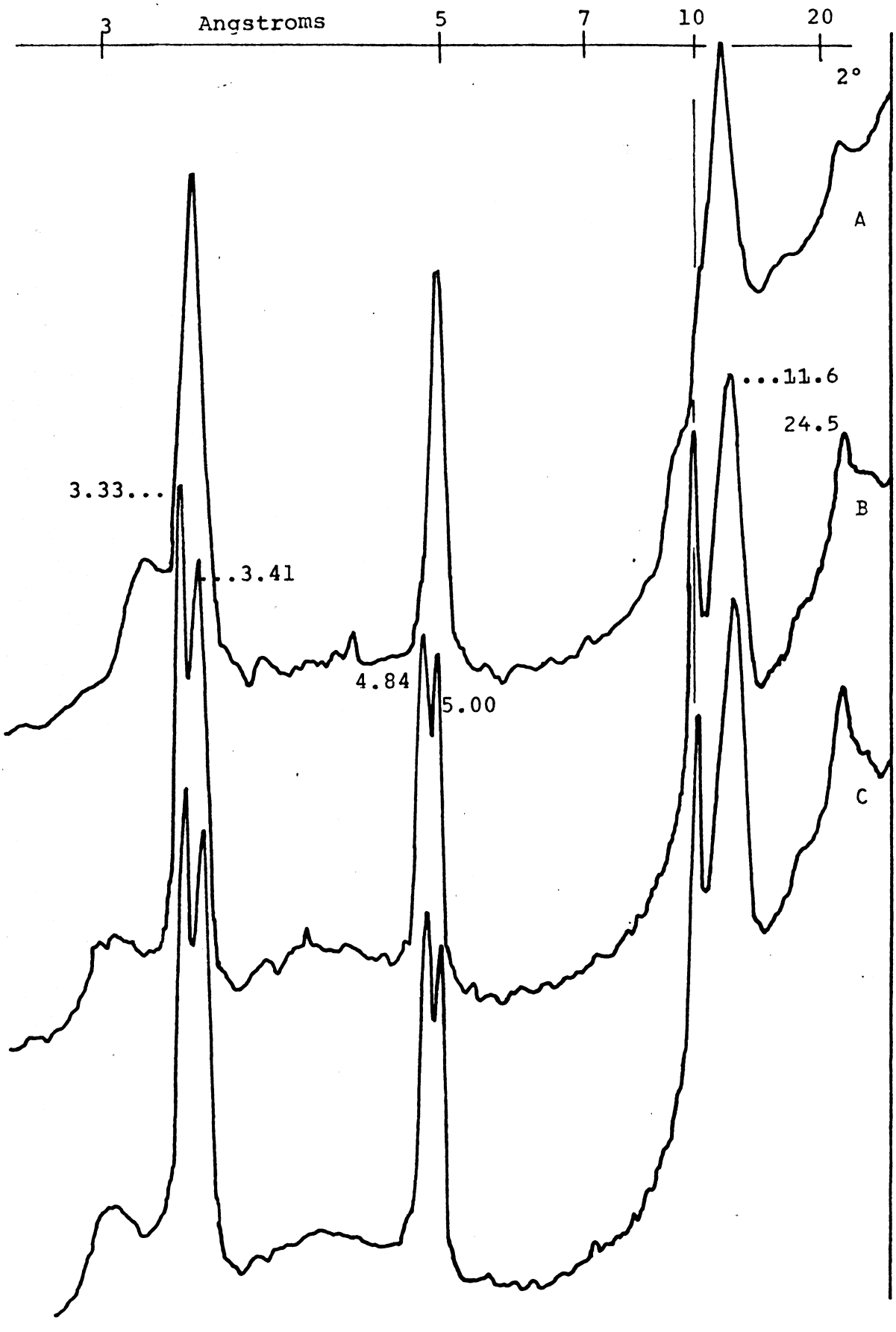
3
Angstroms
5
7
10
20
2°
A
...11.6
24.5
3.33...
B
...3.41
4.84
5.00
C

level, the probability of 10-14 A combinations existing as coherent, diffracting domains is at its highest. By way of illustration, if several packets of 10-14 sequence were randomly interstratified with packets of 14-14 sequence, diffraction of x-rays would be at a maximum at an angle corresponding to layer spacing intermediate between 28 and 24 A. This explanation is substantiated by the fact that higher order spacings are not observed, a requirement of some other explanations of similar low angle peaks. That this peak predominates when 50-50 random interstratification predominates, and that the peak dissipates as the expansion (or weathering) process progresses also tend to substantiate this explanation. This same phenomenon was interpreted by Cook (1962) as being a "regular interstratification of mica and vermiculite" in which the sodium replaced the potassium only in alternate layers, presumably because of different bond strengths obtaining in different layers resultant from the mica being a "2M" muscovite. Such a phenomenon would require 00ℓ reflections for ℓ=even integers integral with the 24 A spacing, the absence of which were neither mentioned or explained. The peaks representing the 002/003 and 003/004 random interstratification of 10-14 A species were present (Figure 17, p. 68), but apparently were not recognized as such. Furthermore, these peaks did shift in the manner expected for random interstratification of this type; the 002/003 peak moved to higher angles and the 003/004 peak moved to lower angles as the 14 A component increased.

In summary of the above discussion, it is noted that other workers have felt that sodium citrate treatments were effective in

expanding dioctahedral mica to some other mixed material, be it random or regular; if this were so, the method would be worthwhile pursuing. This experimenter believes that only the hydrous mica component is being altered to something richer in 14 A component, with little if any evidence of alteration of the 10 A component as reported by Cook and Rich (1962). Thus, with laboriously slow progress, many additional treatments might produce a mixture of 10 A material with 14 A material; such a result would not be satisfactory.

Potassium Release Studies: In order to obtain a more thorough understanding of the release of potassium and concurrent expansion of the mica with the intent of predicting the feasibility of mica expansion, analysis of the solutions after treatment of the micaceous material was attempted using several salts. Normal solutions of sodium chloride, sodium citrate, and barium chloride were used in treatments of varying length, and the results reported in Tables 13 and 14. The use of barium chloride was indicated by unpublished work by Rich showing barium as effective in potassium release. The method developed for this analysis leaves something to be desired as shown at the bottom of Table 14, but was adequate for revealing relative differences. The low recovery is due to dispersion and consequent loss of the potassium tetraphenol boron precipitate while being washed free of salts. This procedure is required to determine small quantities of potassium in normal barium chloride and practical for determinations in normal sodium chloride. Examination of Table 13 shows that increasing the time of treatment usually increased the amount removed,

Table 13—Potassium released by salts (normal solutions, 10 ml volume, 50 mg samples)

Treatment time	Sodium chloride	Sodium citrate	Barium chloride
hours	meq/100 g		
2	1.03	4.5	11.9
12	2.07	4.4	15.8
	ppm in solution		
2	0.75	1.8	3.8
12	1.80	1.7	6.3

Table 14—Potassium removed by normal barium chloride (25 ml volume, 12 hour treatment, 50 mg sample)

	Potassium	
	meq/100 g	ppm
1st wash	22.2	3.6
2nd wash	30.6	4.9

Standardization of method

	Potassium added	Potassium recovered
	ppm	
Blank	0.0	0.35
5 ppm standard	5.0	3.15

but the treatments did not remove much potassium even with the longest treatment time. Barium chloride appeared to be much more effective than the sodium salts. Comparison of Table 13 with Table 14 revealed that the concentration of potassium remains about the same with the same treatment time though the volume of the solution is doubled; this holds true for additional washes. This indicates that an equilibrium concentration of potassium may exist in these solutions which stops the reaction. With this in mind, small quantities of acid-fluoride treated dioctahedral mica were autoclaved in 3 liter volumes of barium chloride. The expansion was followed by examining the x-ray diffraction patterns after magnesium saturation of the sample; typical patterns are presented in Figure 9. Not only is the progressive expansion of the material evident from the comparison of the first three patterns, but it is also apparent that the whole sample is affected. There is no 10 A material in the end product detectable by examination of the bottom tracing in Figure 9. Figure 10 further substantiates this, for any 10 A material would be clearly evident by its higher orders which are totally absent in the topmost tracing. The behavior on heat treatment shown in Figure 10 is indicative of the purity and crystallinity of the product and shows aluminum interlayer material to be essentially absent by the collapse to 10 A at 110 C.

Time of Treatment and Solution Concentration: To determine the most productive method of preparing the expanded material, the effect of time of treatment and concentration of solution were studied, and the

Figure 9—Nason IC, 5-2 micron fraction, magnesium saturated, 25 C (A), after iron removal, acid fluoride treatment, a single barium chloride treatment, magnesium saturated by five washes and one autoclave treatment, 25 C (B), same sample after two barium chloride treatments and identical subsequent treatments (C), same sample after ten barium chloride treatments and three magnesium chloride autoclave treatments (D)

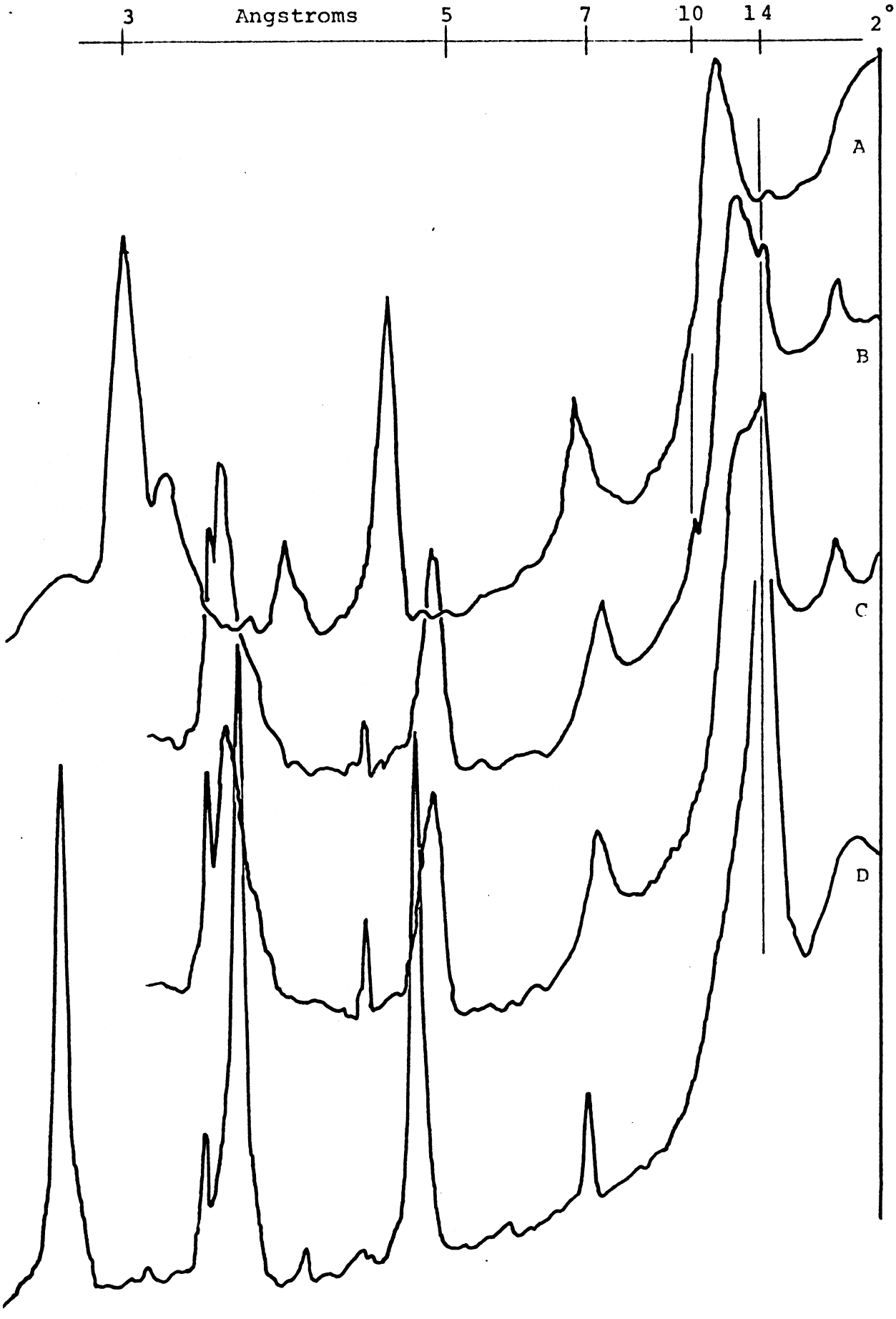
3
Angstroms
5
7
10
14
2°
A
B
C
D

Figure 10—Nason 1C, 5-2 micron fraction, purified, fully expanded by barium chloride treatment, 25 C (A), heated to 110 C (B), and 550 C (C).

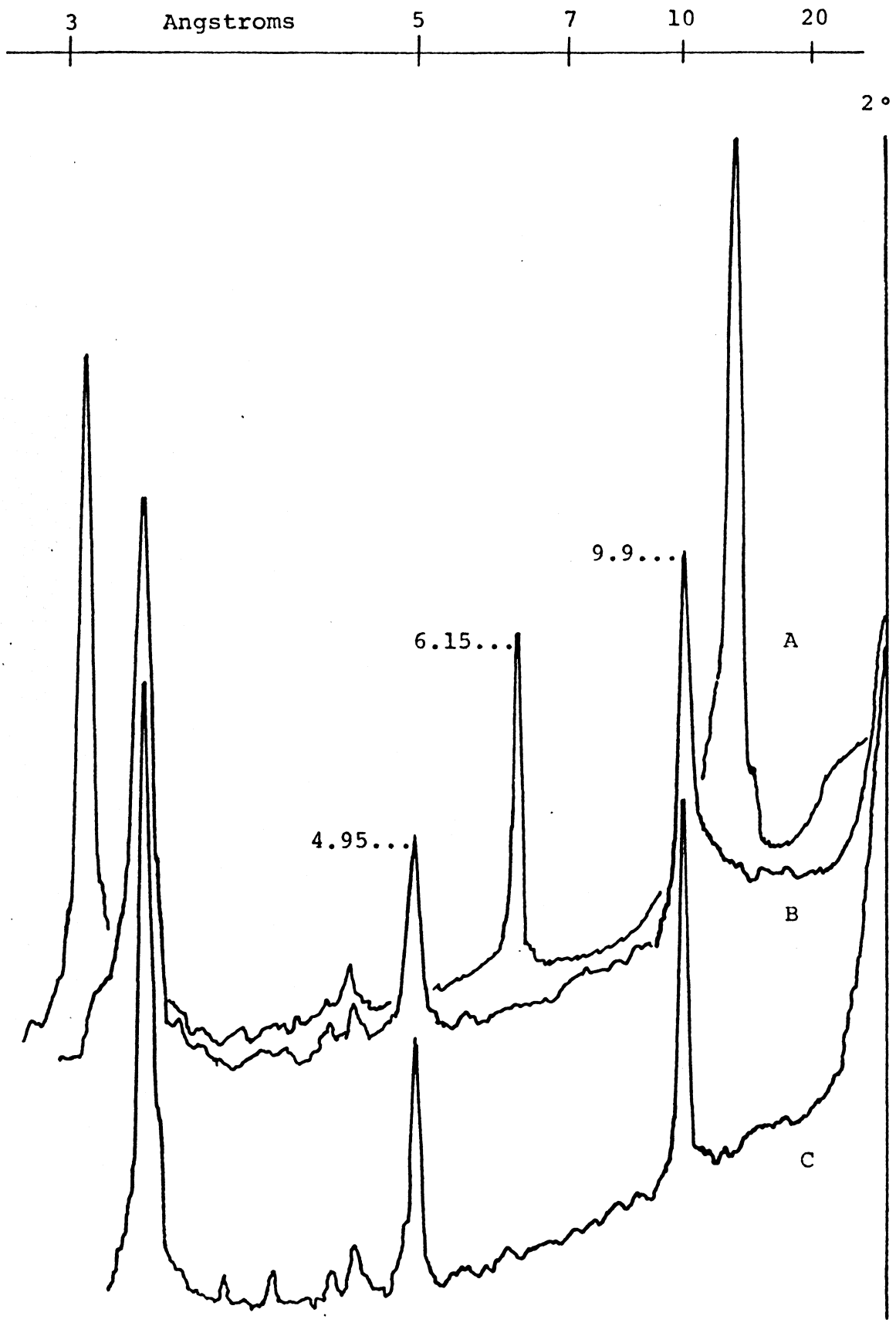
3
Angstroms
5
7
10
20
2°
9.9...
6.15...
4.95...
A
B
C

results are presented in Figure 11. The most striking result is how effective a single treatment can be if concentration and volume of solution are adequate; the bottom pattern indicates that the exchange reaction has gone nearly to completion as the result of a single, one day autoclave treatment. The high solution to sample ratio (3 liters/ 0.1 g) is, in part, responsible for this. Comparison of the top two patterns with the bottom one clearly indicates that, in spite of adequate solution volume and extended time of treatment, the treatments with 0.1 N $BaCl_2$ have not progressed as far as the one day treatment with the normal salt. The exchange reaction involving the removal of potassium from mica apparently must have an equilibrium constant of a different order of magnitude than the cation exchange reactions usually considered.

Samples Containing Paragonite: An attempt to relocate the site from which the original sample was taken failed, but similar material was obtained from a nearby location, apparently in the same geologic formation. The material, Nason IIC, has some important differences which can be readily seen in Figure 12. Though the material was indistinguishable from Nason IC before any treatment, the presence of paragonite was noted after initial purification. As the series of diffraction patterns illustrates, the paragonite resists expansion beyond the point where all the potassium mica has expanded. If changes in relative intensity can be used to measure changes in sample composition, comparison of the second and third patterns in Figure 12

Figure 11—Nason 1B, 5-2 micron fraction, purified, treated with 0.1 N $BaCl_2$ for one day (A), two weeks (B), same sample treated with 1 N $BaCl_2$ for one day (C).

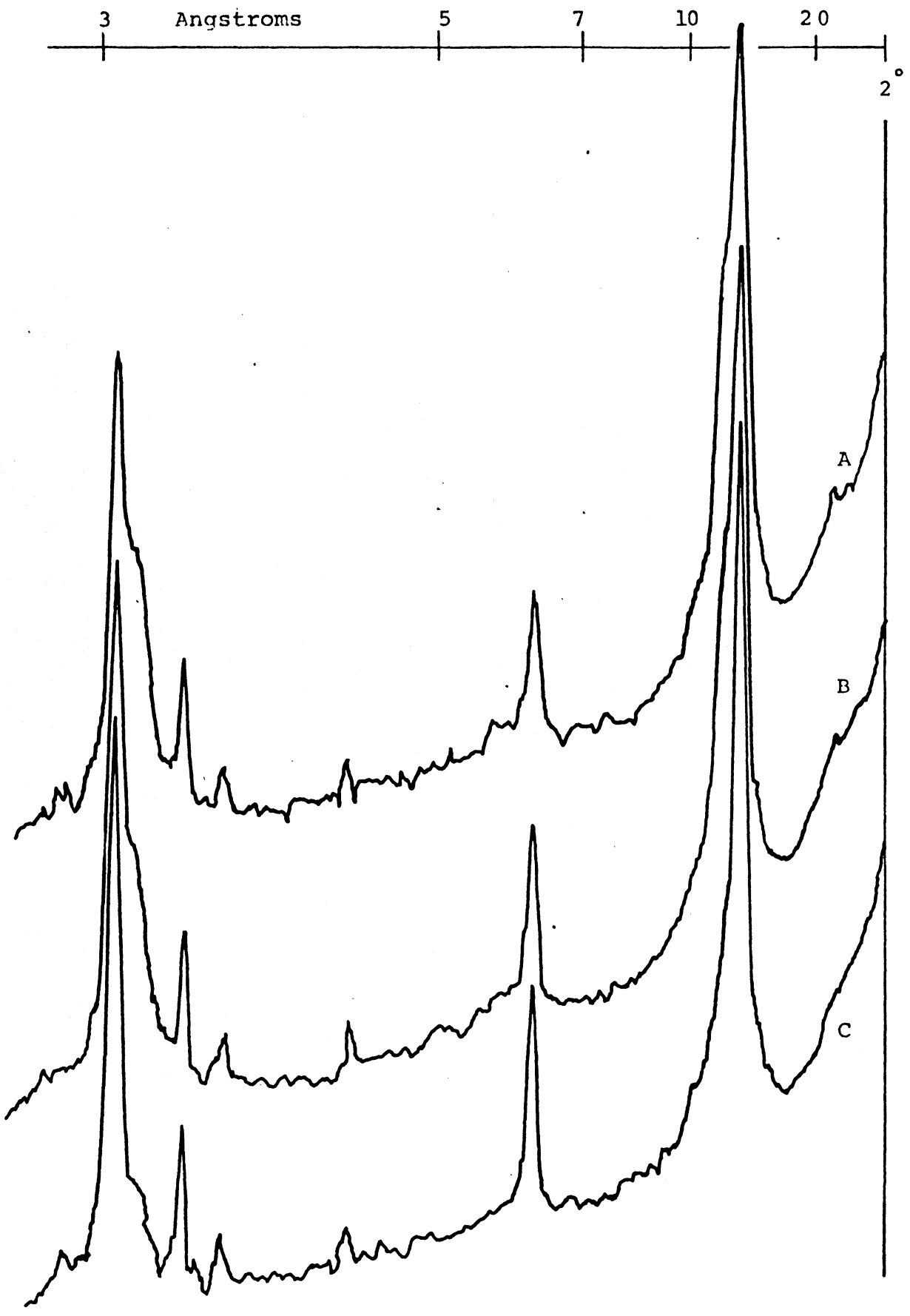
3
Angstroms
5
7
10
20
2°
A
B
C

Figure 12—Nason IIC, 5-2 micron fraction, purified, partially expanded by a single barium chloride treatment (A), five barium chloride treatments (B), eight barium chloride treatments (C).

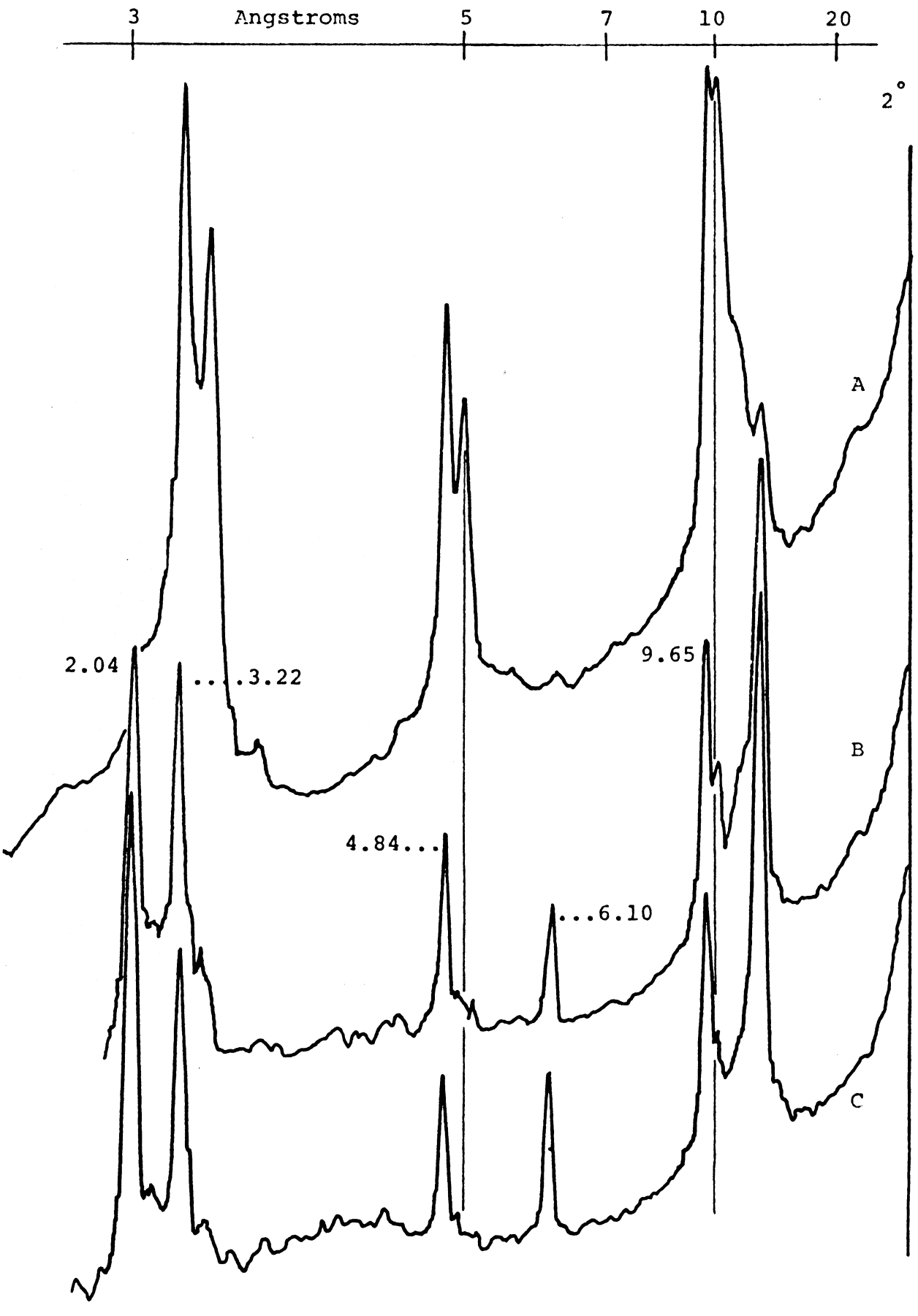
3
Angstroms
5
7
10
20
2°
A
B
C
2.04
...3.22
9.65
4.84...
...6.10

indicates that some of the paragonite is being converted to the 12 A material, since the second order paragonite peak decreases as the second order vermiculite peak increases. Other attempts to expand the paragonite were made using small samples and large volumes, but there appeared to be a point beyond which no more expansion took place. Because of the interference of the 003 reflection of the paragonite impurity, this material was judged unsatisfactory for further structural study of dioctahedral vermiculite.

Nason IC and Ontario Muscovite: In order to supplement the supply of sample which was severely limiting further work, the 5-2 micron fraction was separated from the horizon above that from which Nason IC was obtained. The behavior of this sample, Nason IB, was indistinguishable from that of Nason IC up through the barium chloride expansion treatments. It was practical to use the patterns from the barium saturated samples to follow the expansion and these are presented in Figures 13 and 14. Also included at the bottom of Figure 13 is the diffraction pattern showing the effect of five barium chloride treatments on Ontario Muscovite. The only effect noted was slight broadening of the 10 A reflection, and the conclusion was that this material would not expand to by this method within the time available.

Barium Chloride Mica Expansion: That autoclave treatments with normal barium chloride will expand any kind of mica completely is a discovery in itself. That the treatment will expand potassium mica and not sodium mica reveals something of the mechanism of the reaction.

Figure 13—Nason 1B, 5-2 micron fraction, purified by twenty-four hour acid fluoride batch treatment (A), and given five barium chloride autoclave treatments (B); Ontario muscovite given five barium chloride treatments (C).

Figure 14—Nason 1B, 5-2 micron fraction, purified, given batch barium chloride treatments six times (A), seven times (B), and nine times (C).

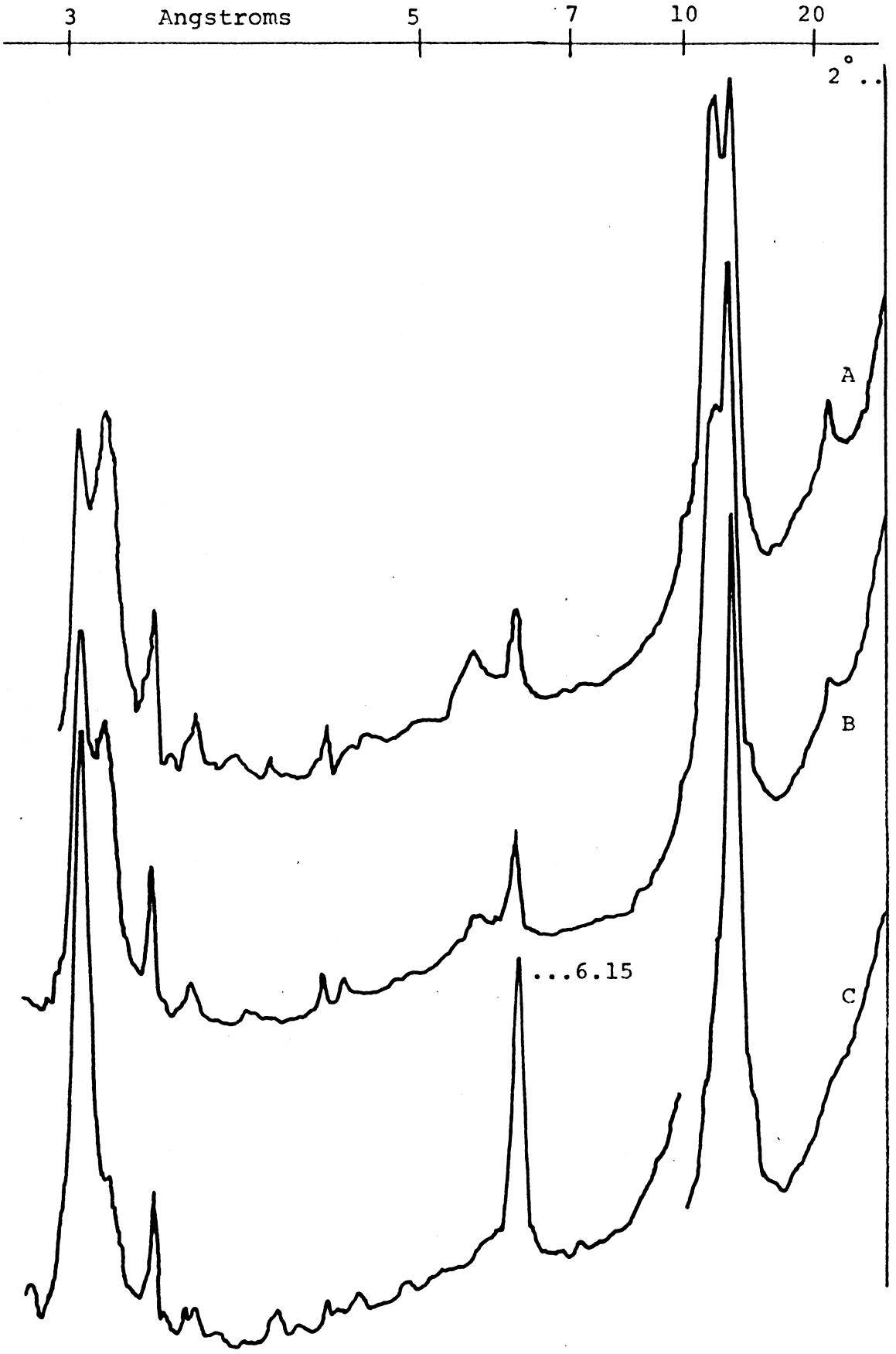
3
Angstroms
5
7
10
20
2°..
A
B
...6.15
C

The barium ion and potassium ion differ in ionic radius by only three percent, barium having a radius of 1.29 and potassium having a radius of 1.33, whereas sodium and barium differ by twenty-four percent if sodium is considered to have a radius of 0.98. An additional consideration is that the barium ion is divalent and will be more highly hydrated than potassium, though the water of hydration will not be held very tightly because of the large size of the barium ion. Thus, though barium can proxy for potassium in size, its charge relationships and hydration relationships to the exchanger surface will not be the same. These differences are indeed fortunate with respect to the present objective, for, if the barium ion did not have any tendency to hydrate, the barium saturated mica would collapse to 10 A at room temperature in the same fashion as potassium saturated mica; then the barium ion would be hard to replace from the collapsed mica. The divalent character is also helpful, for if the charge distribution on the mica basal oxygen surfaces is considered to be localized in such a fashion that is best balanced by potassium ions located partially in the "hexagonal holes" in 12 fold coordination, then barium ions will not balance the negative charge as well as single charge ion because they will be occupying only every other site. If each charge is somewhat localized in the area of "hexagonal holes" filled by potassium, the most probable place to find double charged ions should be between the negatively charged sites rather than on every other one. This condition would permit barium to be more easily replaced than potassium, as is the case.

To understand why the sodium mica is not expanded by the same treatment that expands the potassium mica, more than the mica structure must be considered. The adjacent basal oxygen layers are more than 0.3 A further apart in potassium mica than in sodium mica, but it would be difficult for the barium ion (2.58 A) to work its way between sheets that are less than 0.7 A (10.1 minus 9.4) apart. Furthermore, some of the sodium mica is expanded. Helfferich (1962, p. 162) indicates that polarizability of ions influences exchange reactions. Ions of greater polarizability are favored in an exchange reaction because of the greater electrostatic attraction possible when the distance of closest approach is smaller. Greater electrostatic attraction also favors smaller ions in exchange reactions. The barium ion is not only smaller than potassium and double charged but it has greater polarizability, being two periods further down in the periodic table. The greater difficulty in replacement of sodium must result from the added electrostatic attraction to the silicate network resulting from the smaller size of the sodium ion.

The mechanism of expansion must involve the diffusion of the unhydrated barium ion between partially expanded mica layers, neutralization of charge in its immediate area, followed by replacement of potassium. The higher temperature in the autoclave and the mass action effect add to the electrostatic attraction in forming the driving force of the reaction. The weak tendency for the barium ion to hydrate must expand the mica to a spacing comparable to one layer of water in the interlayer once the mica is sufficiently depleted of potassium.

Total Analysis

Once a reasonably pure sample of dioctahedral vermiculite was obtained, its composition was determined by total analysis. The structural formula of the mineral was inferred by adapting the accepted methods of structural formula calculation presented by Foster (1960).

Water Content: First consideration was given to the drying temperature to be used to obtain the base weight for the analysis. Since a temperature high enough to remove all interlayer water, and not high enough to remove octahedral water was desired, a heat treatment of 350 C for eight hours was chosen. Water loss data at this and other temperatures are presented in Table 15. These data conform with the data found in the literature, with six percent and twelve percent water loss corresponding to one and two layers of interlayer water. Since the samples were not equilibrated at a specific relative humidity prior to initial weighing, only approximate correspondence with values found in the literature was expected. The behavior of the lithium saturated samples was unexpected, and it appears that differences in the prior treatment of lithium saturated samples has an effect on the temperature of water loss. X-ray diffraction analysis of different hydration states of lithium saturated samples was attempted, and discrete spacings were difficult to maintain. The air dry sample appeared to be randomly interstratified mixture of 12 A and 14 A layers and the sample was interstratified

Table 15—Percentage water contained in dioctahedral vermiculite

Cation saturation	Treatment	Sample	Dehydration temperature			
			110 C	350 C	450 C	550 C
				%		
		Nason 1B				
NH_4		1		1.6	4.2	
NH_4		2		0.7		7.1 (6.5)**
Ba		1	6.0	6.3	8.8	
Ba		2		6.7		
Ba		3		6.2		9.6 (3.6)*
Mg		1	none	12.4		
Mg		2		12.6		16.1 (3.9)*
Ca			1.3	13.3		
Na			1.6	4.8		
Na	Boiled in $NaNO_3$			5.1		
Na	Boiled in NaCl			4.0		
Li			3.6	12.8	14.0	
Li	Boiled in Li-citrate	1		9.7	12.0	
Li	Boiled in Li-citrate	2		9.4		
		Nason 1C				
Al		1	0.7	12.6		
Al		2		13.8		17.0 (3.5)*
Al	Hydrolyzed			13.5		
Mg				15.2		

* Figures in parentheses are weight loss percentages based on 350 C sample weight equivalent to structural water loss.

** $NH_3 + H_2O$ loss.

with a spacing larger than 14 A at one hundred percent relative humidity. Random change in layer charge caused by something more than cation exchange can explain both the change to random patterns of a well defined material and the unusual water content found.

The water loss occurring between 350 C and 550 C was used as an estimate of structural water, and the determinations presented in Table 15. One determination of water loss between 550 C and 800 C was made for a magnesium saturated sample of Nason IB and the value of one percent obtained. The values between 3.5 to 4.0 percent obtained for structural water are high for pure mica, but not unexpected for a soil material. One determination was not considered sufficient evidence to add the additional one percent to the structural water content reported in the total analysis.

Magnesium Content: Total analysis was carried out on samples of Nason IB saturated with different cations, with the intent that such a procedure would reveal any errors in the analysis better than repetitions of the analysis of a single sample. The analyses of identical materials were reproducible. That there were differences between the same material saturated with different cations soon became apparent, as can be seen from the data presented in Table 16. These data indicate that the standard method of cation saturation does not appear to work, and that the careful differentiation between structural and "exchangeable" magnesium is required. Even prolonged boiling in sodium nitrate and sodium chloride did not reduce the

Table 16—Partitioning of exchangeable and structural magnesium by total analysis

Treatment	MgO	Moles per unit cell	Al_2O_3	CEC	K_2O
	%		%	meq/100 g	%
		Nason 1B			
Acid fluoride, NH_4 saturated	2.2	--	20.9	48	3.87
Ba saturated	2.6	0.60	19.9	119	0.097
	2.6	0.60	21.2		0.10
Mg saturated	8.8	1.19	23.1		0.090
Ca saturated	4.7	0.92	22.8	137	0.077
Na saturated	4.1	0.80	22.8		0.071
Li saturated	4.2	0.79	21.2	150	0.035
Boiled in $NaNO_3$, Na saturated	3.5	0.71	20.7		1.76
Boiled in $NaNO_3$, Na saturated	3.7	0.73	22.1		1.55
Boiled in Li-citrate, Li saturated	3.0	0.56	24.1	171	0.058
	2.9	0.54	24.0	167	0.076
		Nason 1C			
Al saturated					0.19
Al hydrolyzed					0.089
Mg saturated					0.12

magnesium to its initial level. This was only achieved by boiling in lithium citrate, as can be seen by comparing the figures indicating the molecular weights of magnesium found per formula weight of vermiculite. That the value found in the material that had never been in contact with a magnesium salt was eventually achieved was considered a sufficient evidence that this value accurately estimated the structural magnesium content of dioctahedral vermiculite.

Potassium Content: Information on the potassium content was required not only for a complete structural formula, but also to substantiate the conclusions from the x-ray diffraction studies already discussed. Inspection of Table 16 reveals 0.035 percent as the lowest content found; this is approximately 1/100 of the original potassium content and 0.3 percent of the ideal muscovite content. Other workers have had difficulty obtaining potassium free samples and have attributed the difficulty to contamination of the reagents. Boiling vermiculite samples in sodium chloride and sodium nitrate to remove magnesium caused the potassium content to increase approximately twenty fold as the result of the potassium content of the reagents (Table 16). Some representative potassium contents of salts are reported in Table 17. In order to maintain low potassium contents, only reagents selected for their purity could be used; lithium citrate made from lithium hydroxide and citric acid and lithium chloride were the reagents found to be lowest in potassium. Achievement of low potassium values was associated with the potassium free

Table 17—Potassium content of N salt solutions

Solution	Chart readings with slit setting 0.1			K in solution
	Salt	Salt with 1 ppm K	Chart units per ppm K	
	Chart units			ppm
$LiNO_3$	12.3	15.8	3.5	3.7
LiCl	2.0	14.0	12.0	0.17
Citric acid	2.5	5.2	2.7	0.94
Sodium citrate	51.0			9.5
NaOH + citric acid	10.4	15.8	5.4	1.9
NaCl	2.7	7.2	4.5	0.60
Li-citrate	16.6	44.2	27.6	0.60
EDTA	59.8	69.0	9.2	6.5
NaCl	23.2	32.0	9.2	2.4
LiOH				trace
LiOH + citric acid			70.0*	0.13

* Slit setting 0.2.

salts, but also with the lithium salts. It is possible that lithium ions may be migrating within the sample during prolonged boiling treatment and permitting the release of potassium in a fashion other than the accepted mechanism of cation exchange.

It is evident that the expansion of dioctahedral vermiculite with non-lithium salts by the generally accepted cation exchange is accompanied by the reduction of potassium level to approximately 0.1 percent (2.5 milliequivalents per one hundred grams) or, structurally speaking, one potassium ion for every one hundred unit cells.

Structural Formulas: Structural formulas were calculated from the total analysis data according to the method proposed by Foster (1960). The analysis data and calculated gram equivalents of cationic equivalents, cationic valencies per unit cell, cations per unit cell, and layer charge are presented in Tables 19, 20, and 21. In Table 19, the analysis data for the barium saturated sample is used directly in the calculation, yielding results which are in error. The quartz correction, obtained from the data presented in Table 18, was not used to obtain the results in Table 19. Tables 20 and 21 illustrate the structural formula calculation with a proper correction for quartz.

The data for the Li-vermiculite and Ba-vermiculite presented in Tables 20 and 21 are taken from duplicate analyses of each type and differ considerably. The structural formulas derived from these two sets of data, however, are very similar and the exchangeable cations balance the layer charge resulting from isomorphous

Table 18—Quartz determination

Sample	Observed intensity	Background count	Net count
		cpm	
95% sample + 5% standard	325	95	230
100% sample	210	95	115

Calculation:

Formula: $\frac{I_{o(std)}}{I_{o(sample)}} = \frac{0.95X + 0.50}{X}$

Result: $X = 4.8\%$

Table 19—Structural calculation of Ba-vermiculite without quartz correction

Oxide	Composition	Gram equivalents of cationic constituents		Cationic valencies per unit cell
	%			
SiO_2	50.5	3.36	29.6	7.40
Al_2O_3	19.9	1.17	10.3	3.43
MgO	2.6	0.13	1.14	0.57
Fe_2O_3	5.13	0.193	1.70	0.57
BaO	11.5	0.150	1.32	1.33
K_2O	0.05	0.001	0.009	
H_2O	3.6			
Total	93.3	5.004	44.07	

Tetrahedral	SiO_2	7.40	Octahedral	Al_2O_3	2.83
	Al_2O_3	0.60		MgO	0.57
				Fe_2O_3	0.57
Total population:		8.00			3.97
Negative charge:	1.17	0.60			0.57

Structural formula:

$$(Al_{1.41}Mg_{.28}Fe_{.28})(Si_{3.70}Al_{.30})O_{10}(OH)_2^{-.58}(K_{.01}Ba_{.66})^{+.67}$$

Table 20—Structural calculation of Ba-vermiculite with quartz correction

Oxide	Composition	Gram equivalents of cationic constituents		Cationic valencies per unit cell
	%			
(Quartz)	5.0			
SiO_2	45.5	3.03	28.6	7.15
Al_2O_3	19.9	1.17	11.0	3.67
MgO	2.6	0.13	1.23	0.61
Fe_2O_3	5.13	0.193	1.82	0.61
BaO	11.5	0.150	1.42	1.43
K_2O	0.05	0.001	.010	
H_2O	3.6			
Total	93.3	4.674	44.08	

Tetrahedral	SiO_2	7.15	Octahedral	Al_2O_3	2.82
	Al_2O_3	0.85		MgO	0.61
				Fe_2O_3	0.61
Total		8.00			4.04
Negative charge:		1.46 0.85			0.61

Structural formula:

$$(Al_{1.41}Mg_{.30}Fe_{.30})(Si_{3.57}Al_{.43})O_{10}(OH)_2^{-.72}(K_{.01}Ba_{.72})^{+.73}$$

Table 21—Structural calculation of Li-vermiculite with quartz correction

Oxide	Composition	Gram equivalents of cationic constituents		Cationic valencies per unit cell
	%			
(Quartz)	5.0			
SiO_2	58.0	3.85	29.1	7.28
Al_2O_3	24.1	1.42	10.7	3.56
MgO	2.95	0.146	1.11	0.56
Fe_2O_3	6.00	0.225	1.70	0.57
Li_2O	2.50	0.172	1.30	1.30
K_2O	0.05	0.001	0.008	0.01
H_2O	(3.6)*			
Total	102.2	5.814	43.92	

Tetrahedral	SiO_2	7.28	Octahedral	Al_2O_3	2.84
	Al_2O_3	0.72		MgO	0.56
				Fe_2O_3	0.57
Total		8.00			3.97
Negative charge:	1.28	0.72			0.56

Structural formula:

$$(Al_{1.42}Mg_{.28}Fe_{.29})(Si_{3.64}Al_{.36})O_{10}(OH)_2^{-.65}(Li_{1.30}K_{.01})^{+.66}$$

* Assumed to be the same as Ba-vermiculite.

substitution. The small differences that do exist between the structural formulas of the vermiculite samples can be explained by the difference in treatment they received. The Ba-vermiculite appears to have impurities (possibly fluorides) since only 93.3% was recovered; the method of structure calculation employed eliminates the error introduced by inert impurities not analysed by first reducing the analyses to cationic equivalents and then adjusting these figures to a unit cell of 44 negative charges. The Ba-vermiculite was magnesium saturated, and then given four lithium citrate boiling treatments to produce the Li-vermiculite analysed. This last treatment may explain why the Li-vermiculite is lower in aluminum and iron, and richer in silica, for citrate complexes both iron and aluminun and does not attack silica; lower magnesium content may result from migration of lithium ions promoting the release of octahedral magnesium near the edges of the vermiculite platelets.

That structural formulas with balanced charge can be calculated from such dissimilar data is evidence of the correctness of both the chemical analysis and the theory behind the calculations. That the layer charge averages 1.45 in one case and 1.30 in the other is not too disturbing. The figure of 1.4 characterizes the mineral. Conversion of this figure yields 1.7 me/g exchange capacity, which compares very well with the values ranging from 1.5 to 1.7 obtained by direct determination. It is to be noted further that, once the theoretical assumption of a tetrahedral cation population of 8 per unit cell is

made, the structural formula calculation indicates octahedral population close to the theoretical 4 cations of dioctahedral minerals.

The material under study is a component of a soil and has been exposed to the forces of weathering including oxidation. For this reason, the iron found was assumed to be in the ferric state. That the structural formula charges balance tends to substantiate this assumption. If one considers the iron as being in the octahedral layer and in the ferrous state, a charge imbalance occurs, but the total charge approaches the value of 2 which is the charge theorized for unweathered micas. If it is presumed that the iron was originally in the ferrous state in the unweathered mica, a triggering mechanism for the initiation of weathering of certain micas to dioctahedral vermiculite is immediately apparent. Furthermore, this triggering mechanism (oxidation of iron) is an accepted weathering reaction. The above theory can help explain why some micas approaching theoretical, iron free muscovite, weather to kaolinite, while others yield vermiculite as an end product. The iron free micas do not have this mechanism to dissipate their high charge density, allowing them to expand into hydrous micas. Potassium removal is accomplished by the weathering process through conversion to kaolinite. The micas containing ferrous iron, on the other hand, have a mechanism whereby the loss of a single electron permits the reduction of charge and release of potassium, easily followed by hydration of the basal oxygen surfaces.

The oxidation of ferrous iron was suggested by Murray and

Leininger (1957) as the mechanism involved in the conversion of illite and chlorite to montmorillonite. This mechanism of charge reduction was considered applicable primarily to the conversion of biotite to trioctahedral vermiculite by Rich (1958) in the early studies of this dioctahedral vermiculite. Another mechanism that has been suggested for lowering the charge of layer silicates is the formation of hydroxyls in association with tetrahedral aluminum ions (McConnell, 1950). Though the nature of the phenomena that does exist may not bear much similarity to McConnell's hypothesis, his observation that water lost at high temperature is indicative of extra hydroxyls being present in the mineral structure warrants consideration when dealing with weathered minerals.

Cation Saturation of Dioctahedral Vermiculite

With a purified, homogenized, chemically characterized, barium saturated vermiculite available, the preparation of the different cationic forms of the mineral was initially considered to be a relatively simple task. That this was not true was soon discovered, and the extent to which it was not true was determined only with difficulty. The work was carried out in two studies separated by one year in time; the more detailed examination of the mineral by total analysis just presented was conducted in the interim. The two studies yielded two sets of conclusions about interlayer aluminum which will be presented in chronological order.

Even though the removal of potassium from the exchange sites was accomplished only with great difficulty, it was hoped that standard methods of cation exchange could be employed with the expanded material. Magnesium saturation by the standard procedure of washing five times with the normal chloride salt yielded a sample that produced the x-ray diffraction pattern traced at the bottom of Figure 15. The spacings corresponding to the peaks depicted do not form an integral series; hydration of the sample at 100 percent relative humidity improves the symmetry of the peaks, but the spacings remain non-integral. The hydration of the sample apparently expanded the 12 A component present in the random interstratification of the unhydrated sample. Since calculations indicating percentage composition for 12-14 and 14-15 random interstratification are not available, only an estimate can

Figure 15—Nason 1C, 20-5 micron fraction, magnesium saturated by standard method after the barium expansion treatment, hydrated at 100 percent relative humidity (A); compared to the same sample air dryed at 25 C (B).

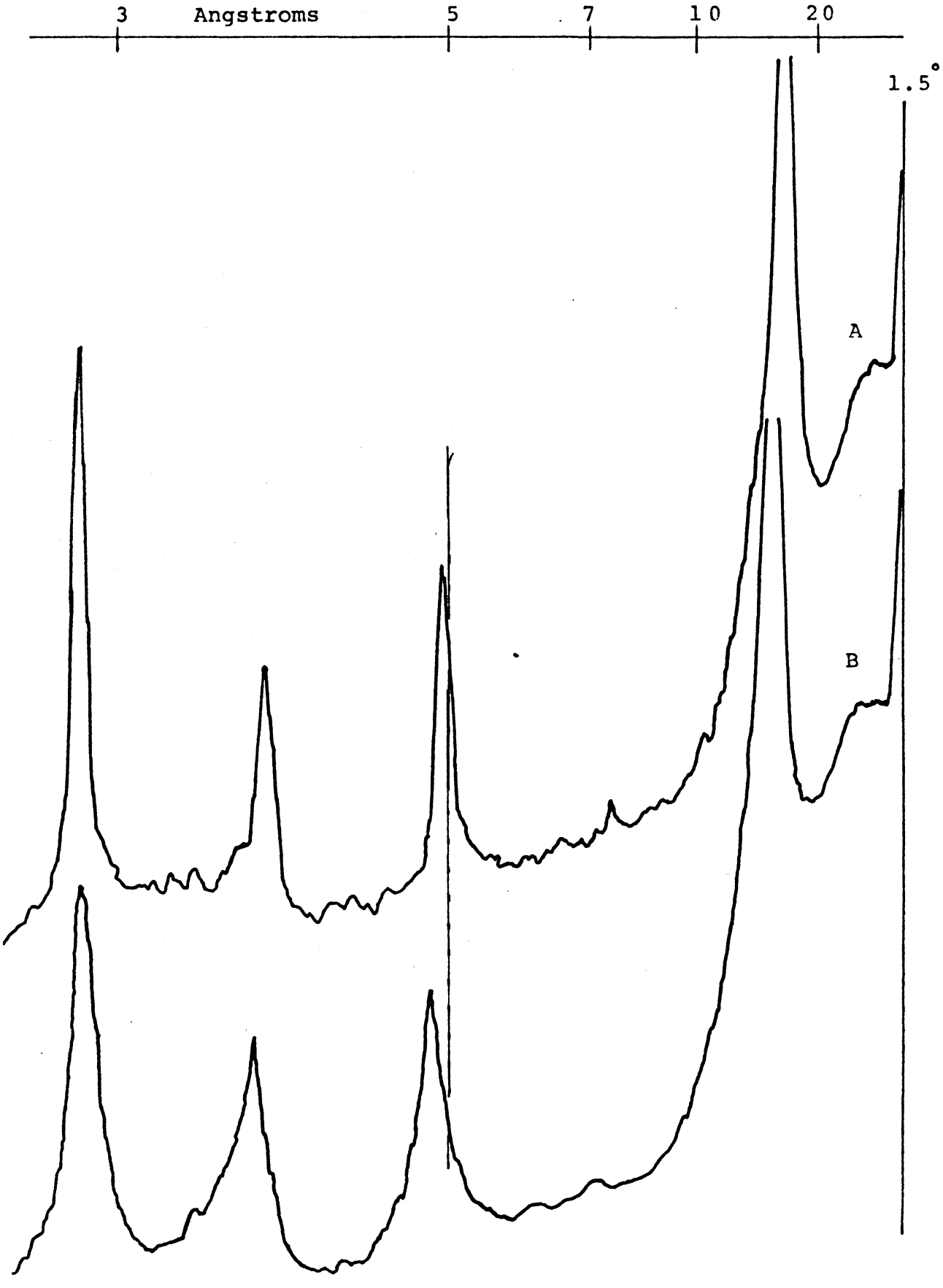
3
Angstroms
5
7
10
20
1.5°
A
B

be made. If we note that the effect on the apparent spacing is small and assume that the barium component is expanding from about 12 A, which is smaller than the unhydrated magnesium spacing, to about 15, which is larger than the unhydrated magnesium spacing, we can estimate that the random interstratification is approximately ten percent barium species. This is the composition which would be sufficient to be noticed by broadening of peaks, particularly for the 12 A phase, and still not have much effect on the apparent interplanar spacing. All in all, the diffraction patterns are a good indication that complete cation exchange is not taking place. To overcome this, magnesium saturation was carried out using autoclave treatments with magnesium chloride, followed with magnesium sulfate to insure the removal of the last traces of barium. A diffraction pattern of the typical product is presented at the bottom of Figure 9.

With the barium removed, additional attempts to effect complete cation exchange were carried out and the results are presented in Figure 16. The topmost pattern depicts a sample that was fully magnesium saturated, then sodium saturated, and then saturated with magnesium. Table 22 indicates the random interstratification present. The charts presented by MacEwan et al. (1961) indicate that both the third and fourth peaks represent 60 percent ten A component interstratified with 40 percent fourteen A component. These estimates are for a 10-14 interstratification and do not include the effect of 12 A layers (Na-saturated) which are undoubtedly present. In

Figure 16—Nason IB, 5-2 micron fraction, fully expanded Mg-vermiculite, sodium saturated by repeated boiling treatments followed by magnesium saturation by the standard method (A); the same Mg-vermiculite lithium saturated with seven washes with normal chloride salt (B).

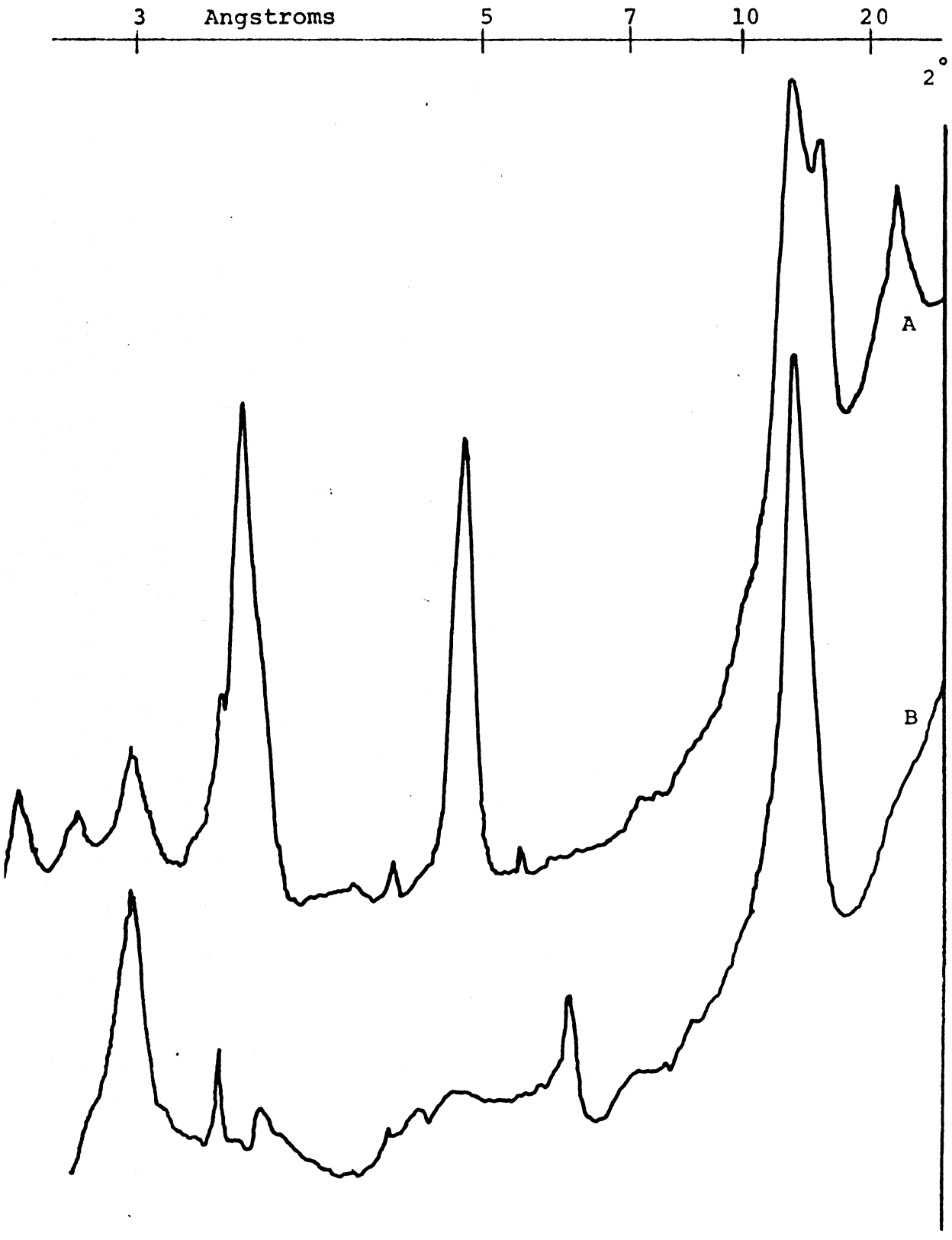
3
Angstroms
5
7
10
20
2°
A
B

Table 22 —Random interstratification in magnesium saturated Nason IB

Apparent spacing	10 A component		14 A component	
A	00	A	00	A
14.0			(001)	14.0
12.1	(001)	10.0		
4.81	(002)	5.0	(003)	4.73
3.44	(003)	3.33	(004)	3.54
2.99	(003)	3.33	(005)	2.84
2.84	(003)	3.33	(006)	2.37
			(005)	2.84
2.40	(004)	2.50	(006)	2.37

retrospect, it must be pointed out that the sample may have contained potassium contamination which further complicates the interpretation.

The lithium saturated sample whose diffraction pattern appears at the bottom of Figure 16 also appears to represent random interstratification. This interpretation is made on the basis of peak broadening alone. The patterns discussed above illustrate the difficulties encountered in replacing the last ten percent of the exchangeable cation. Though other cations are replaced with greater ease than potassium, the vermiculite exhibited a tendency to hold on more strongly to the cations that were present in smallest amount. One interpretation of this phenomenon is that the diffusion required for exchange is more difficult for the ions in the central portion of the clay platelet, and that these are the ions that exchange last. Another interpretation of the observations is that there are areas of the exchanger surface with higher charge density, resulting in different equilibrium constants obtaining in different areas of the mineral for the same exchange reaction. McDowell and Marshall (1962) have pointed out that "a small amount of any cation will seek those positions where it has the highest bonding energy." It is the cations at points with higher than average bonding energies that are the ones that are difficult to replace. This latter interpretation is preferred, though it is hard to substantiate with structural considerations, unless one imagines that in certain parts of the mineral, the iron is not all in the ferrous state, creating greater than average charge density; other parts of the mineral could have a lower than

average charge density resulting from penetration of hydrogen ions into the crystal lattice. Such an explanation would account for the high values found for structural water.

Aluminum Saturation: Since an aluminum saturated sample containing unhydrolyzed aluminum was desired for study, treatment in hot solutions was ruled out because heat promotes hydrolysis; many washes with fresh aluminum chloride was also thought to produce hydrolysis. Since experiments with exchange resins had shown that prolonged treatment in aluminum chloride did not result in hydrolysis, small magnesium saturated samples were soaked in normal aluminum chloride solutions for a week in order to achieve what was thought to be complete aluminum saturation. The second pattern in Figure 17 depicts the product. On hydration at 100 percent relative humidity, the topmost pattern was obtained. The narrow, sharp peaks with integral orders are typical of homoionic material. No evidence of interstratification could be detected. The aluminum saturated sample was clearly different from the random interstratified material shown in Figures 15 and 16. That the Al-vermiculite exhibited different spacings was considered a normal behavior phenomenon, comparable to Ca-vermiculite shown in Figure 18. The aluminum saturated vermiculite prepared by the prolonged contact with one volume of aluminum chloride was considered satisfactory for structural analysis.

Hydrolysis of aluminum - initial interpretation: After the required intensity data were obtained from this sample, it was leached with 250 ml 0.1 N $AlCl_3$ with OH/Al ratio equal to 1.75. The third diffraction pattern in Figure 17 was obtained after this treatment: the bottom pattern was obtained after cation exchange capacity determination had been made on the sample, followed by an additional leaching

Figure 17—Fully expanded vermiculite derived from Nason IC sample, 20-5 micron fraction, aluminum saturated by prolonged soaking, leached with 250 milliliters aluminum solution with OH/Al ratio equal to 0.75, hydrated at 100 percent relative humidity (A); the same sample prior to leaching treatment, air dry, 25 C (B); sample (A), air dry, 25 C (C); same sample after cation exchange capacity determination and aluminum saturation (D).

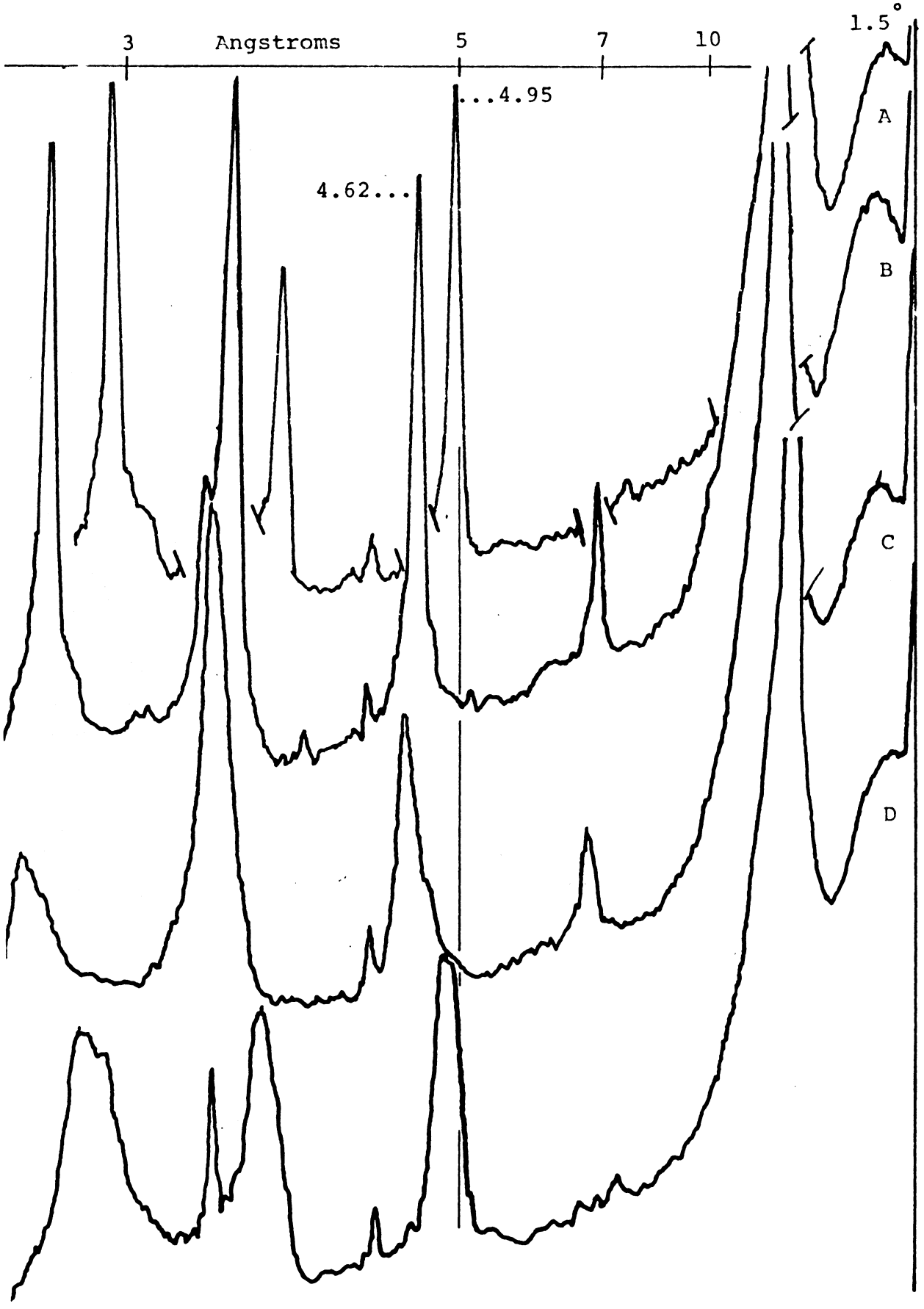
3
Angstroms
5
7
10
1.5°
...4.95
4.62...
A
B
C
D

Figure 18—Fully expanded vermiculite derived from Nason IC, 5-2 micron fraction, magnesium saturated followed by calcium saturation with autoclave treatments air dry, 25 C (A); same sample hydrated at 100 percent relative humidity (B).

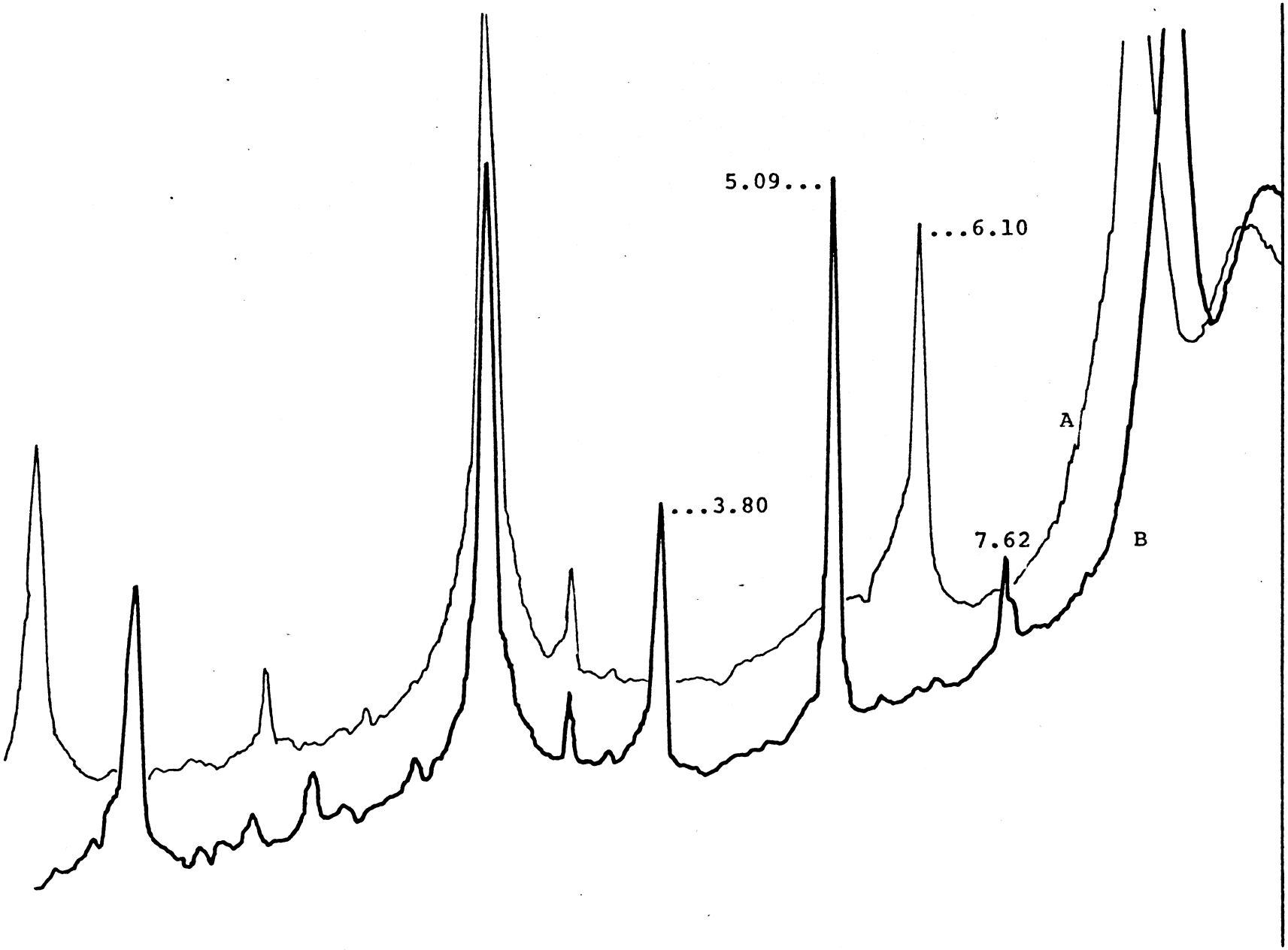
5.09...
...6.10
...3.80
7.62
A
B

treatment. The sequence of patterns was interpreted as representing different stages of hydrolysis of aluminum and the formation of "hexahydronium aluminum polymers". It was easy to visualize the Al-vermiculite fully hydrated, and the exchangeable aluminum being hydrolyzed in place. Once hydrolysis had taken place, the water structure which existed while the aluminum was being hydrolyzed was maintained by hydroxy bridges in the areas where the aluminum was hydrolyzed. The random interstratification of the two components presented at the top of Figure 17 resulted when only part of the aluminum was hydrolyzed, maintaining the higher spacing, while the remainder of the material collapsed to 14 A on dehydration. When the sample whose diffraction pattern appears third was hydrated at 100 percent relative humidity, it exhibited integral reflections similar to hydrated Al-vermiculite at the top of the figure, but differing slightly in intensity. This behavior substantiated the theory that had been developed.

Wyoming bentonite samples boiled in the same hydrolyzing solutions produced diffraction patterns presented in Figure 19. The bentonite maintained the typical hydrated spacing on heating and did not collapse even after 550 C heat treatment. In this system, the water structure involves three layers of water and hydrolysis of aluminum in place maintained the expanded structure by propping it apart with polymeric forms of hydrolyzed aluminum. The structure of interlayer hydrolyzed aluminum was considered to involve a centrally located aluminum ion surrounded by water and some hydroxyls which lower its charge, permitting additional aluminums to enter the interlayer space. Fixation results from these aluminum ions bonding to each other through hydroxy bridges

Figure 19—Wyoming bentonite, boiled in 0.5 N $AlCl_3$, OH/Al ratio equal to 1.75 12 hours, air dry, 25 C (A); 110 C (B); 200 C (C); 550 C (D).

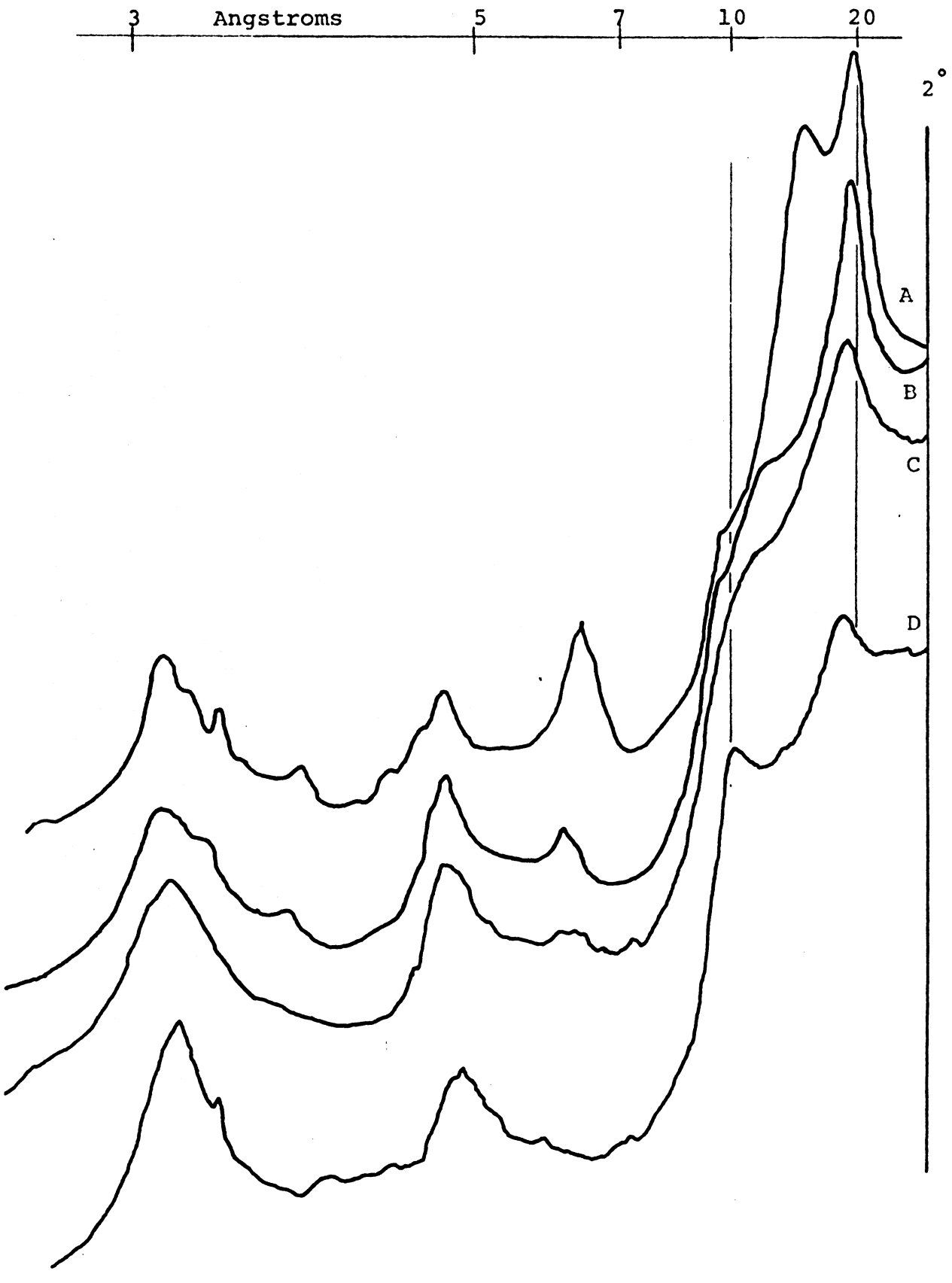
3
Angstroms
5
7
10
20
2°
A
B
C
D

and forming large, highly charged units which were immobilized by their very size and charge. This concept of the structural relationships in the interlayer space was used in structural analysis and is discussed further in the section dealing with structural analysis.

Aluminum saturation; Additional information: The development of the theories just presented was followed by the efforts to obtain additional sample which produced the material called Nason IB. The Nason IB samples were given identical treatments and produced x-ray diffraction patterns that were practically indistinguishable from Nason IC for all but one kind of cation saturation. The exceptional behavior of aluminum saturated Nason IB is illustrated by the diffraction patterns presented in Figure 20. The topmost pattern, made after three aluminum chloride washes, indicates the presence of two phases of the mineral, both somewhat interstratified. One phase consists predominantly of material close to 14 A and the other of material close to 15 A. Repetition of the procedure produced identical results. The data presented in a previous section (Table 16), revealing the difficulty with which magnesium was replaced, indicated that this diffraction pattern should be interpreted as a mixture of materials from which more or less magnesium had been removed. To determine the extent to which magnesium and lithium were replaced by aluminum, analysis of repeated aluminum chloride washes were carried out and the data presented in Table 23. The x-ray diffraction patterns obtained after the terminal treatment of the Nason IB samples are the second and third patterns in Figure 20. Both the elution analyses

Figure 20—Nason 1B, 5-2 micron fraction, fully expanded, Mg-vermiculite aluminum saturated by three washes (A); same sample after eight washes (B); Mg-vermiculite, lithium saturated by boiling in lithium citrate, aluminum saturated by three washes (C); sample (A) heated at 110 C for 15 minutes (D).

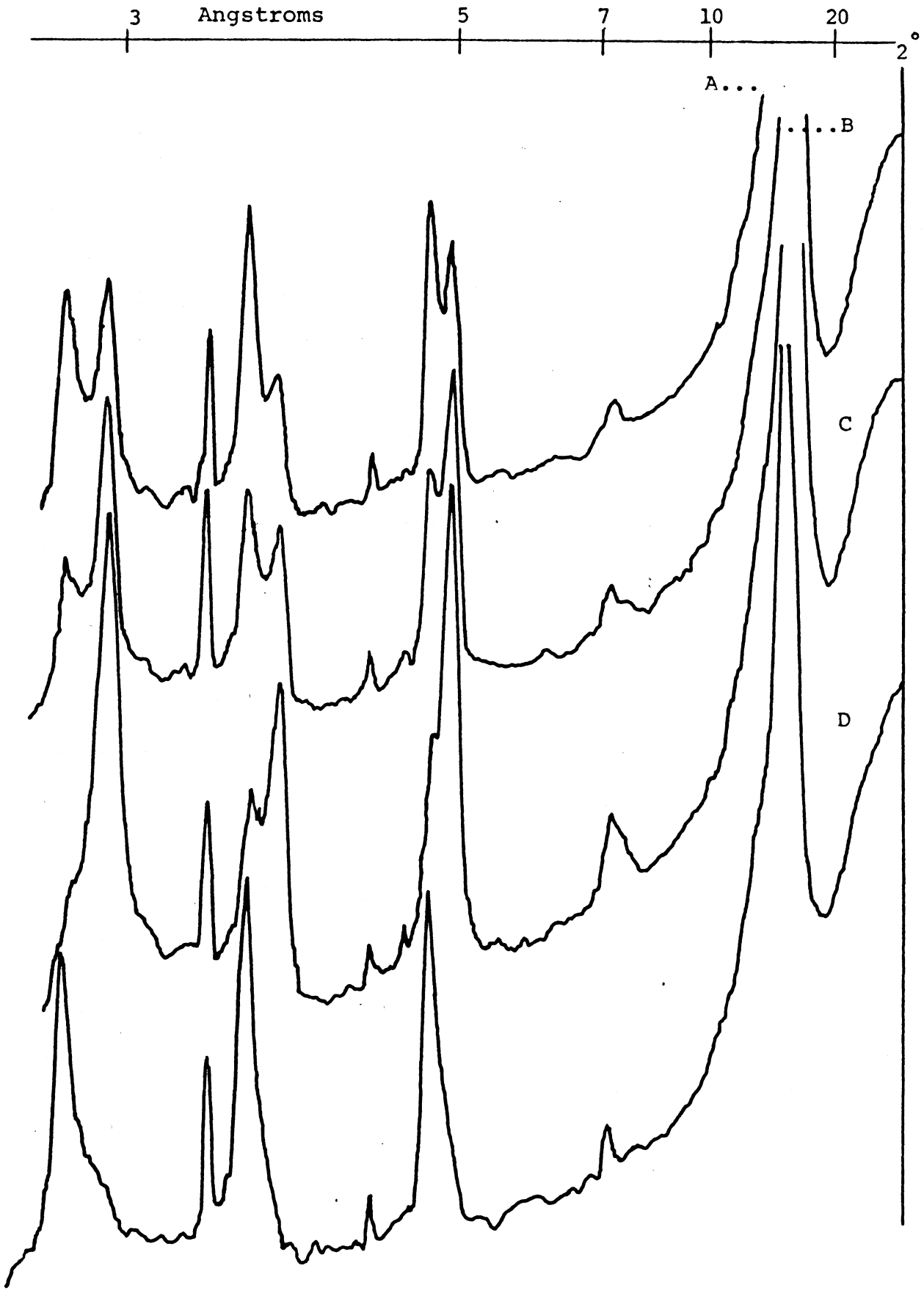
3
Angstroms
5
7
10
20
2°
A...
...B
C
D

Table23 —Elution study of aluminum saturation

Wash number	Lithium removed	Magnesium removed	
	Li-vermiculite Nason IB	Mg-vermiculite Nason IB	Mg-vermiculite Nason IC
		meq/100 g	
1	96.50	153.0	424.0*
2	0.40	1.6	28.2
3	0.13	1.0	4.7
4		1.1	1.9
5		1.3	2.6
6		0.4	0.7
7		0.4	0.8
8	____	0.2	0.4
Total	97.	159.	

* Sample not washed free of salt.

and the diffraction pattern of the Mg-vermiculite indicate that all the magnesium has not been removed, though considerable progress to this end was made. Less lithium was removed from the Li-vermiculite, but the diffraction pattern appears to indicate a better result. Prior lithium saturation removed the magnesium (Table 16) and, though present, lithium may not affect the spacing in a predominantly aluminum saturated vermiculite.

The last pattern in Figure 20 is presented to show that the higher spacing of the aluminum saturated vermiculite is not due to hydrolysis of the aluminum as the theory already presented would indicate, for heating the sample fifteen minutes at 110 C caused collapse to a slightly interstratified 14 A material. The diffraction patterns from the Nason IC sample presented in Figure 21 substantiate this statement. The topmost pattern was made after the magnesium elution data presented in Table 23 was obtained. Even though these data indicate that the process of magnesium removal has not been completed, the diffraction pattern consists of sharp, integral peaks, three of which appear at the top of Figure 21; the complete pattern is traced in Figures 27 and 28. Drying the material in a vacuum desiccator and applying heat treatments collapsed the mineral to the random interstratified components as illustrated by the next two patterns in Figure 21. The sample rehydrated completely after the desiccator drying, but only partially after the 110 C heat treatment as illustrated in the last pattern in Figure 21. These dehydration treatments were performed to insure that room temperature relative

Figure 21—Nason IC, 20-5 micron fraction, fully expanded Mg-vermiculite aluminum saturated by eight washes (A); same sample dried eight hours in a vacuum, silica gel desiccator (B), dried at 110 C (C), and allowed to rehydrate (D).

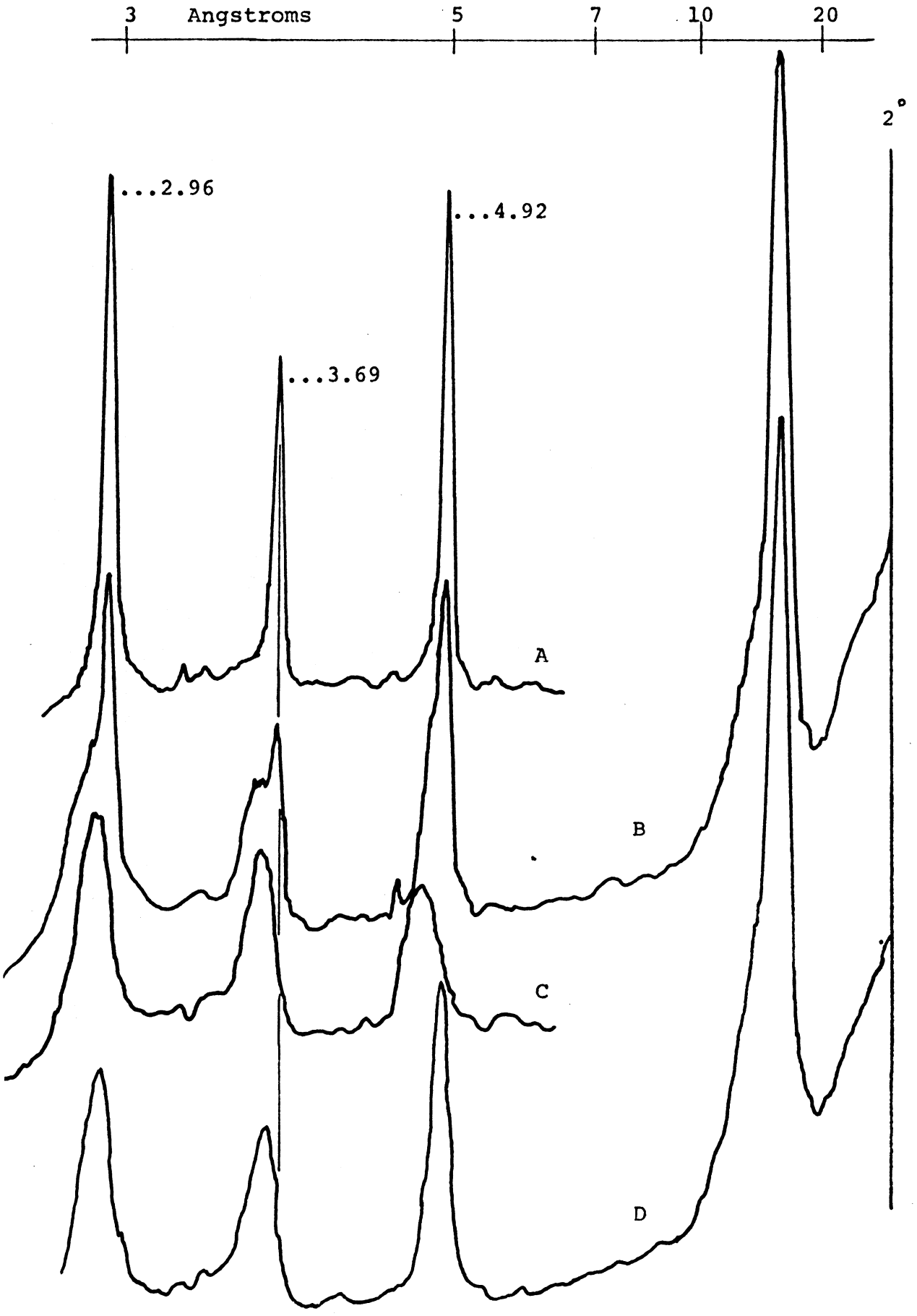
3
Angstroms
5
7
10
20
2°
...2.96
...4.92
...3.69
A
B
C
D

humidity was not responsible for maintaining a spacing that had been observed previously only at 100% relative humidity. The conclusion drawn from these investigations was that a completely aluminum saturated sample had the higher spacing observed and did not have hydrated and dehydrated phases. To confirm this, a sample of the 5-2 micron Nason IC material used to obtain the earlier data was progressively aluminum saturated. The last stages of the saturation are presented in Figure 22 and show that, with repeated washings, this sample also is converted to a high spacing, single phase material. The original slide which yielded the patterns presented in Figure 17 was re-examined after one year of storage. The diffraction patterns are presented for comparison in Figure 23; not only has the material changed in one year of dry storage by apparently collapsing to a smaller spacing, but the material has lost the property of expanding to a higher spacing and producing integral peaks on hydration at 100% relative humidity.

In an attempt to homogenize the Nason IB sample, the finer fraction was concentrated by sedimentation; the diffraction patterns obtained from this material were richer in the material exhibiting the higher spacing. This indicated that the lower spacing magnesium phase persisted longer in the larger particles. Differences in particle size or stages of weathering were responsible for the existence of a mixture of materials that became apparent on aluminum saturation. Because of this lack of homogeneity, the Nason IB sample was judged unsatisfactory for structural analysis.

Figure 22—Nason IC, 5-2 micron fraction fully expanded Mg-vermiculite, aluminum saturated by progressive washings of a small sample; one wash (A), two washes (B), three washes (C).

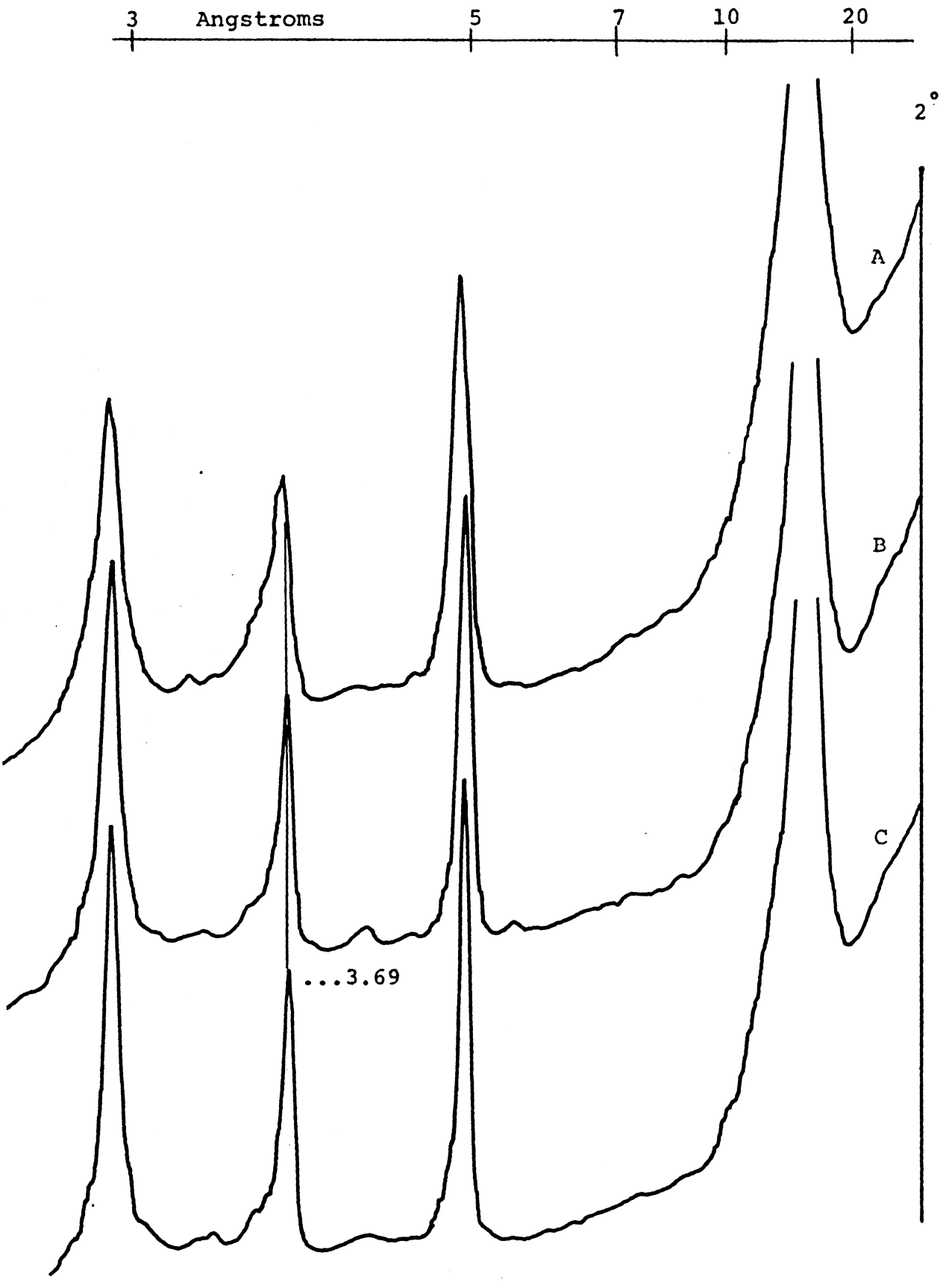
3
Angstroms
5
7
10
20
2°
A
B
C
...3.69

Figure 23—Nason IC, 5-2 micron fraction, fully expanded vermiculite, aluminum saturated by prolonged single treatment, after hydrolysis and determination of cation exchange capacity (A); same slide after one year storage air dry (B); and hydration at 100% relative humidity (C).

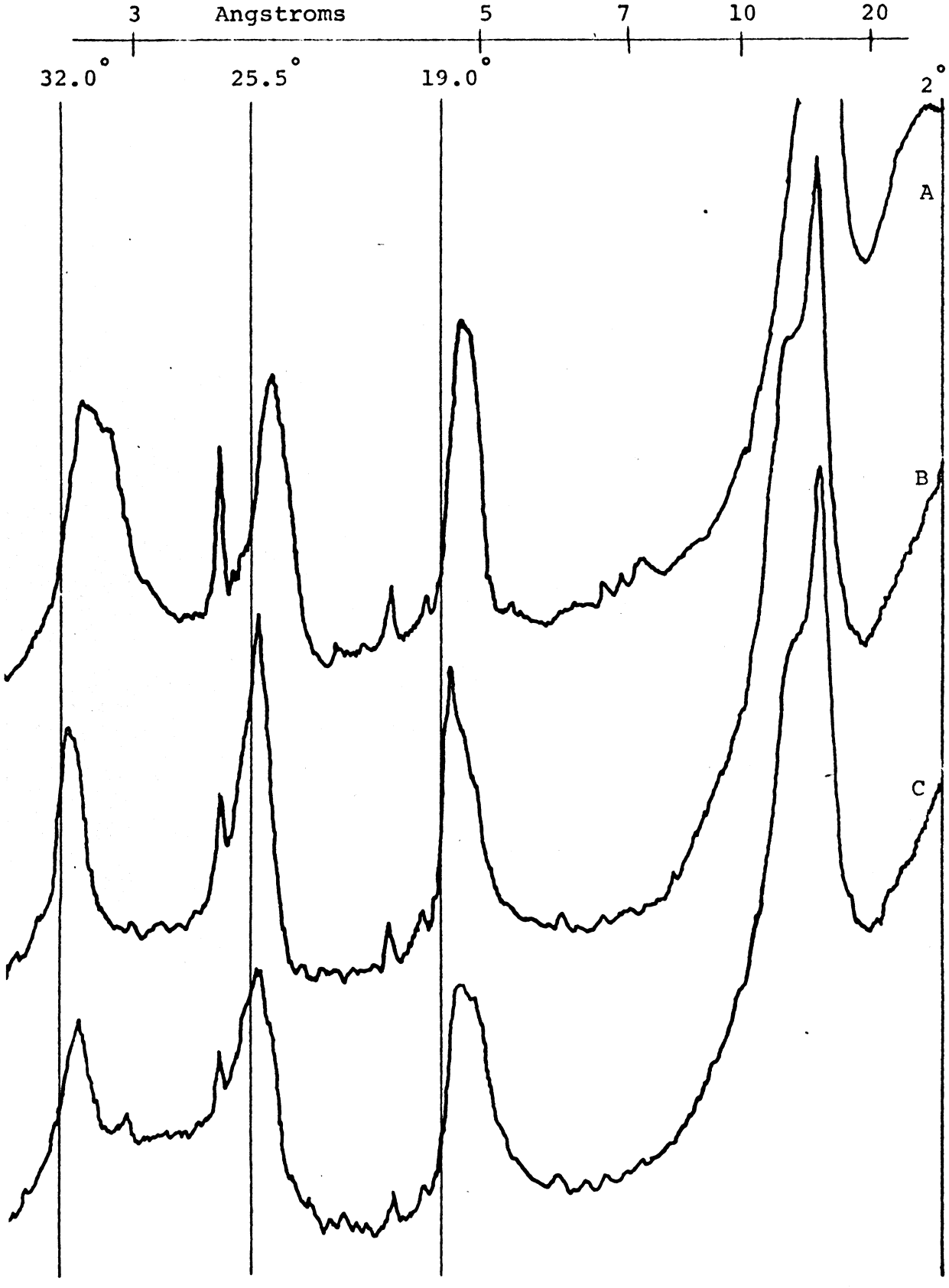
3
Angstroms
5
7
10
20
32.0°
25.5°
19.0°
2°
A
B
C

Hydrolysis of aluminum; additional information: Once the investigation demonstrated that vermiculite with unhydrolyzed aluminum had the higher spacing, an investigation of the progressive hydrolysis of this aluminum was undertaken. Aluminum chloride solutions with OH/Al ratio equal to 1.75 were used in repeated boiling and autoclave treatments. The progressive effect of these treatments on the Nason IB sample is depicted in Figure 24. Comparison of the second pattern in Figure 20 with patterns obtained after hydrolysis shows that the net effect of hydrolysis is to increase the lower spacing 14 A component. The pattern obtained after autoclaving with high OH/Al ratio aluminum chloride solutions representing the highest degree of hydrolysis achieved shows that the high spacing component practically disappeared. Examination of the fifth order peaks in Figure 24 best illustrates this point. Consideration of the calculated interplanar spacings for such patterns alone indicates that the deviation from integral spacings is only slight, but this would be true for 50-50 randomly interstratified 14-15 A material. The unsymmetric nature of the peaks, and broad character and low intensity of the orders higher than the fifth (not shown), indicate random interstratification.

The Nason IC samples behaved in a similar manner. An attempt was made to substantiate the assumption that hydrolysis resulted from the hydrolyzed aluminum treatments using the Nason IC material A small quantity of fully aluminum saturated Nason IC sample shown in Figure 21 was potassium saturated, given the standard heat treatments, and compared to identically treated material after the last progressive

Figure 24—Nason 1B, 5-2 micron fraction, fully expanded Mg-vermiculite aluminum saturated and hydrolyzed by boiling in solutions with OH/Al ratio equal to 1.75 one time (A), twice (B), and autoclave treatment (C)

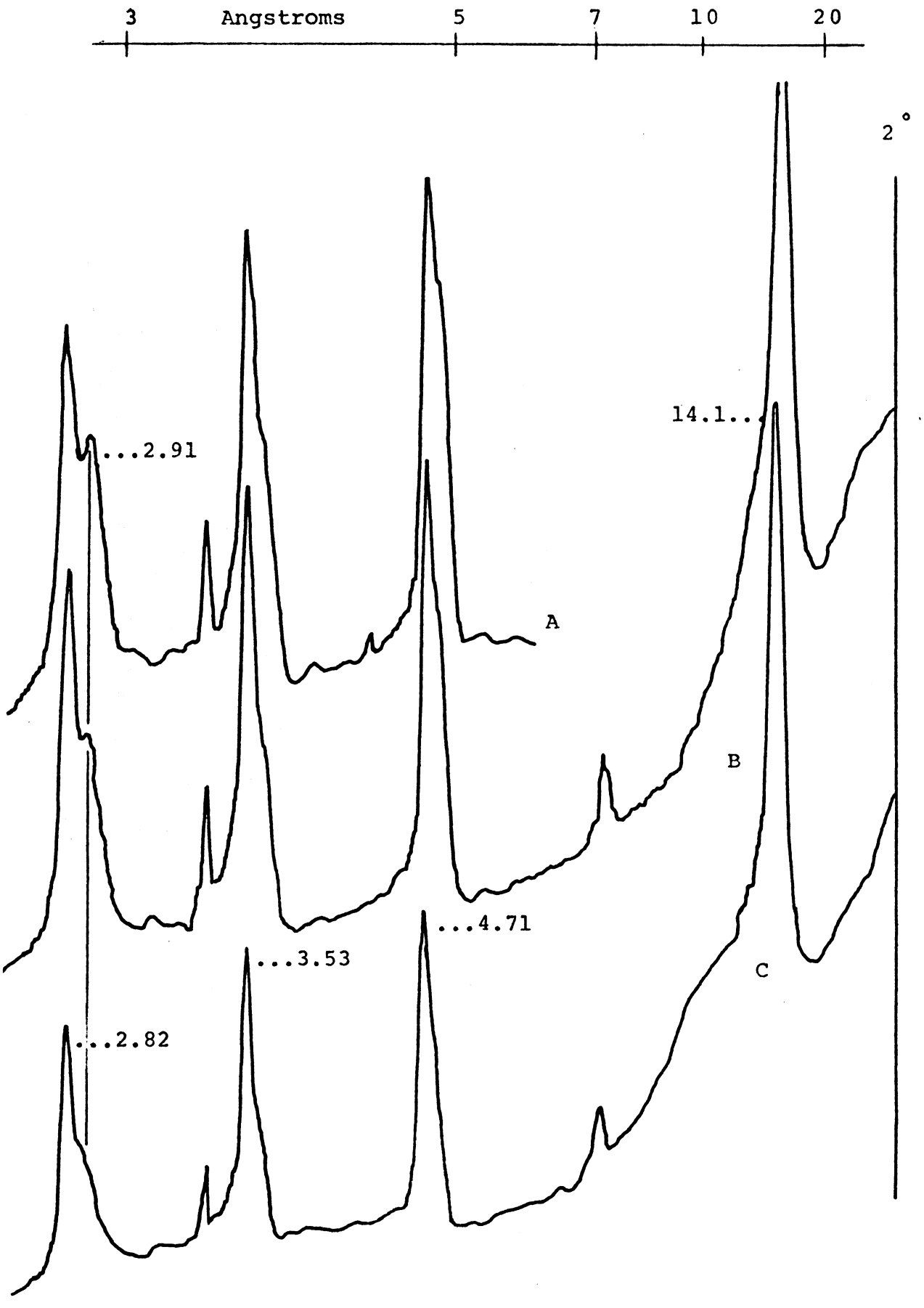
3
Angstroms
5
7
10
20
2°
...2.91
14.1...
A
B
...4.71
...3.53
C
...2.82

hydrolysis treatment. The results are presented in Figures 25 and 26. The evidence for progressive hydrolysis is not limited to the first order peaks maintaining higher spacings on heat treatment; the theories developed in what follows will show that the sharper, more intense, first order peak in the hydrolyzed sample after potassium saturation is also indicative of progressive hydrolysis. The failure of the unhydrolyzed sample to collapse on potassium saturation can not be used as evidence indicating that the aluminum is already hydrolyzed because the hydrolysis that prevents full collapse can take place during the potassium saturation process. The conclusions from these two figures must be limited to comparison of progressive developments.

The qualitative x-ray diffraction data presented in Figures 20-26 and discussed above are not compatible with the theorized structure of hydrolyzed aluminum in the interlayer proposed initially. The earlier theory called for expansion on hydrolysis and the observation is that the aluminum saturated vermiculite collapses to a spacing intermediate between 14 and 15 on hydrolysis. A possible reason for the distinction between the behavior of Wyoming bentonite and the dioctahedral vermiculite is as follows: the former may preserve the water structure present at the time of hydrolysis and the latter, destroys it. Even the concept of the aluminum being surrounded by six water molecules while in the interlayer region must be questioned in a review of the established concepts in light of the new findings. This examination, which is essentially a study of structure, will be presented in the following section.

Figure 25—Nason 1C, 20-5 micron fraction, fully expanded Mg-vermiculit aluminum saturated by eight aluminum chloride washes, potassium saturated 25 C (A), heated to 110 C (B), and 300 C (C).

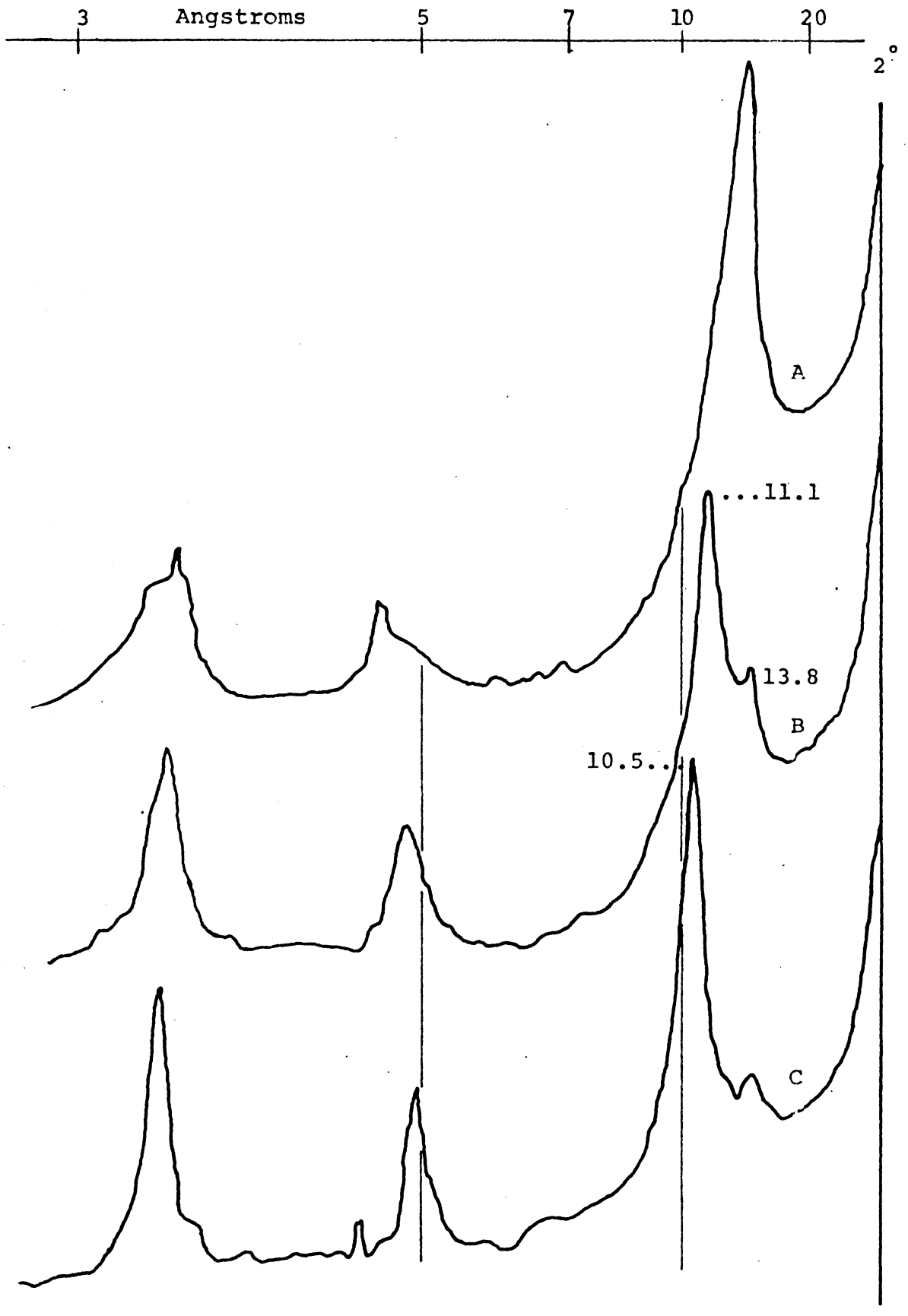
3
Angstroms
5
7
10
20
2°
A
...11.1
13.8
B
10.5...
C

Figure 26—Nason IC, 5-20 micron fraction, fully expanded Mg-vermiculit aluminum saturated by eight washes, hydrolyzed by two washes, and a 24 hour boiling treatment in solutions with OH/Al ratio equal to 1.75, potassium saturated, 25 C (A), 110 C (B), 300 C (C).

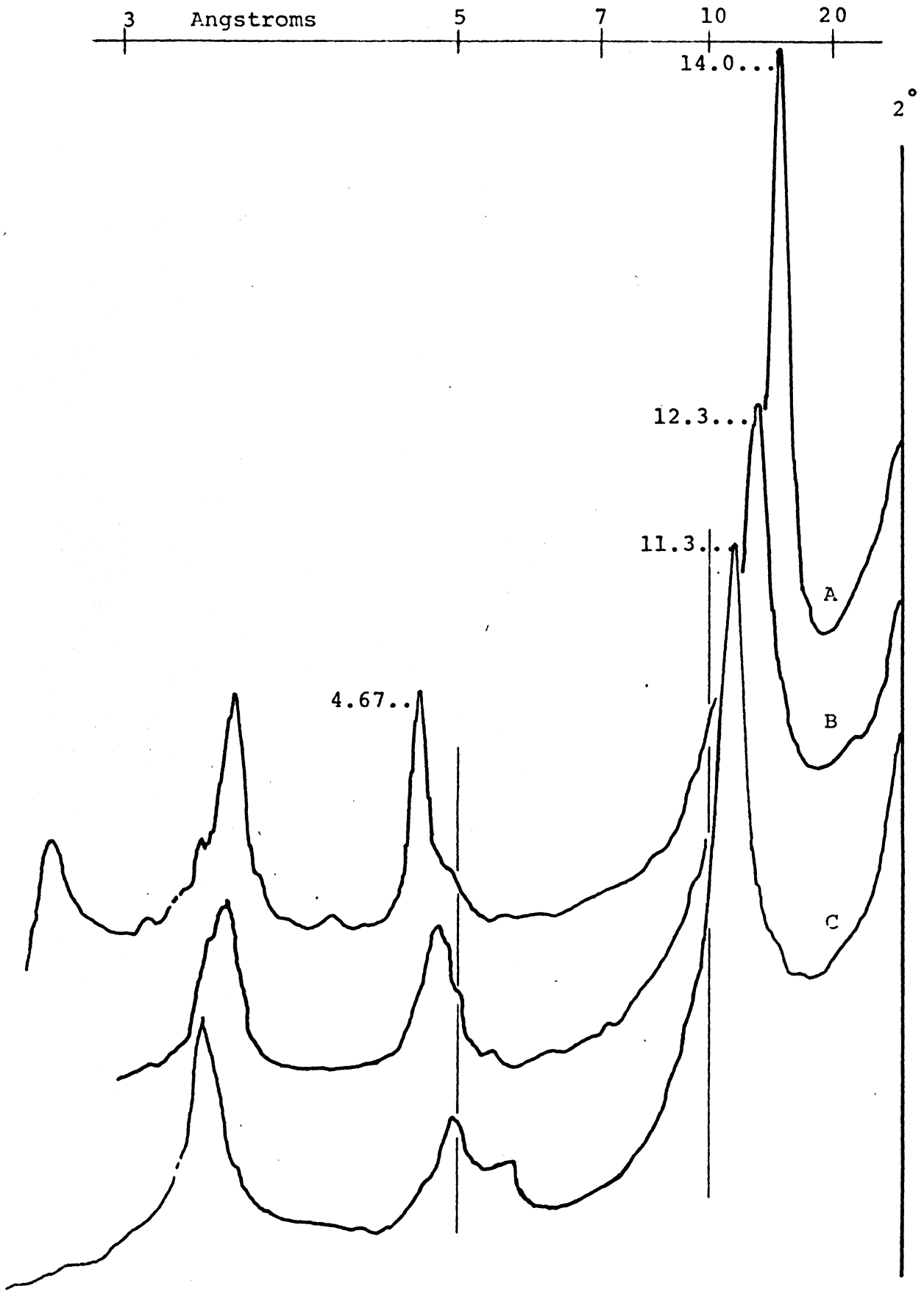
3
Angstroms
5
7
10
20
14.0...
2°
12.3...
11.3...
A
4.67..
B
C

Figure 27—Linearly recorded, x-ray diffractometer pattern of aluminum saturated dioctahedral vermiculite.

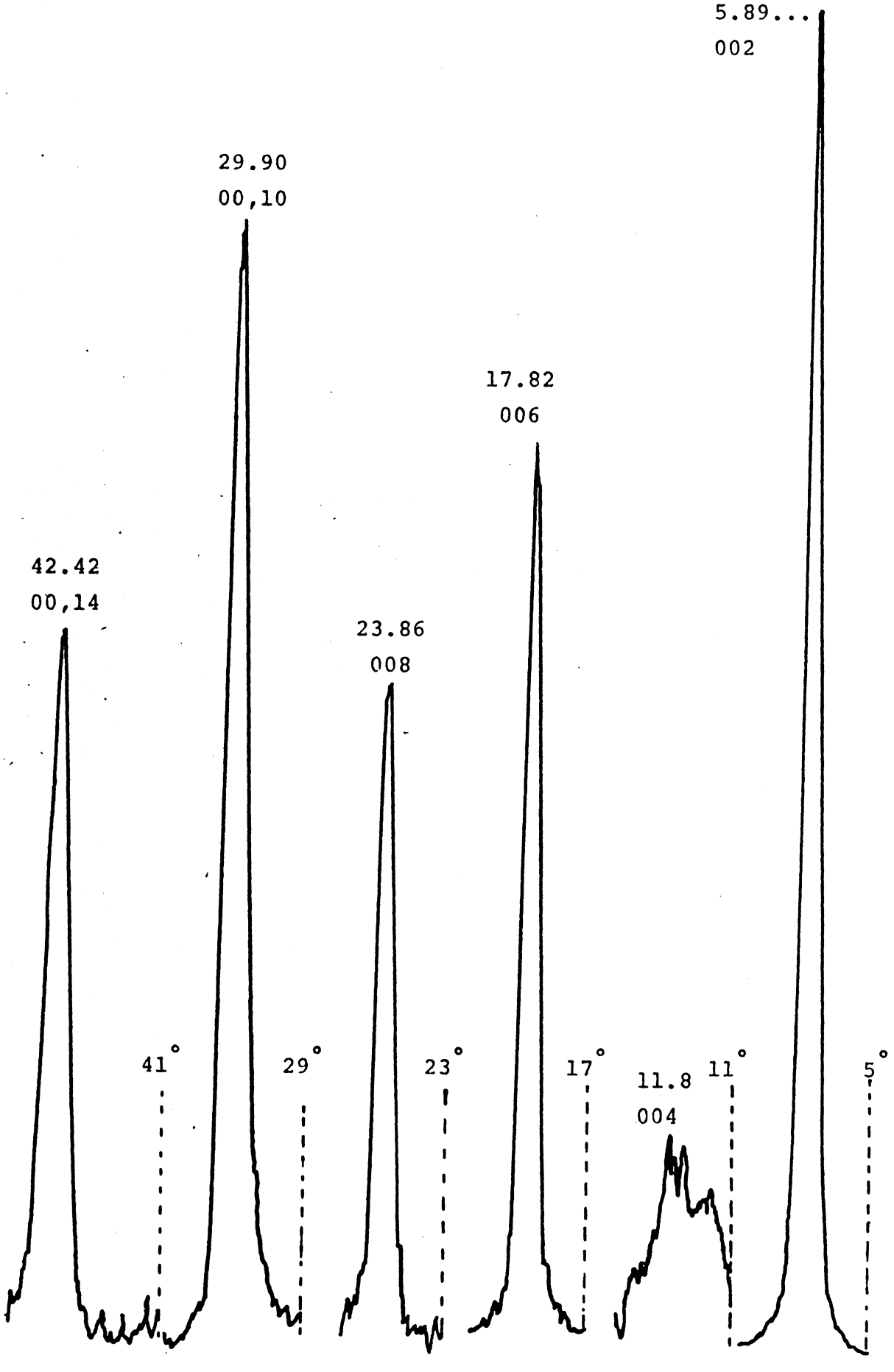
5.89...
002
29.90
00,10
17.82
006
42.42
00,14
23.86
008
11.8
004
41°
29°
23°
17°
11°
5°

Figure 28—Linearly recorded, x-ray diffractometer pattern for aluminum saturated dioctahedral vermiculite.

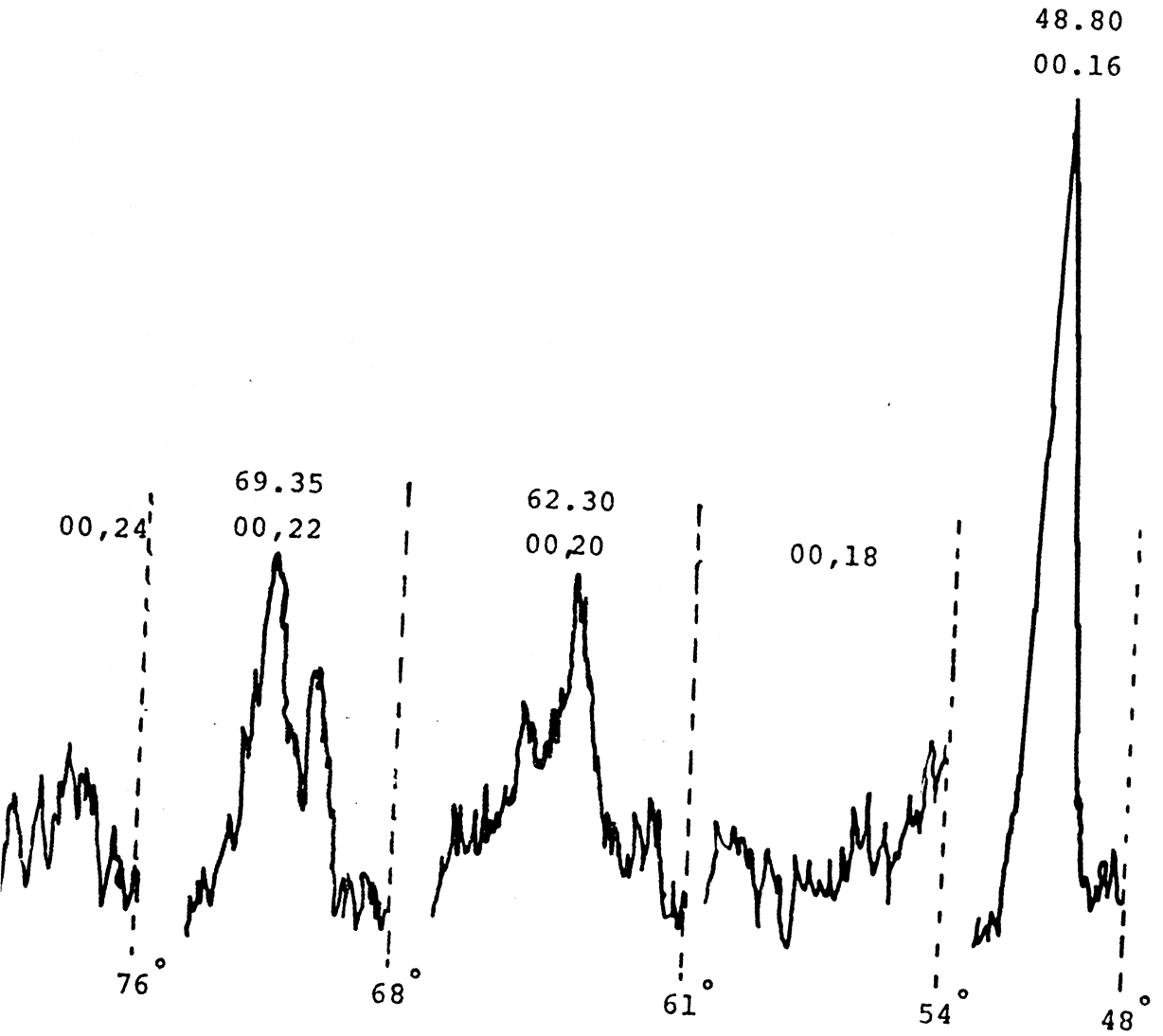
48.80
00.16
69.35
00,22
62.30
00,20
00,24
00,18
76°
68°
61°
54°
48°

ANALYSIS OF DIOCTAHEDRAL VERMICULITE STRUCTURE

Methods and Procedures

The objective of the structure analyses attempted was to characterize the distribution of matter within the dioctahedral vermiculite grain, with particular emphasis on the interlayer region. This was accomplished by using appropriate mathematical tools to interpret data on the angle and intensity of x-ray diffraction maxima resulting when an oriented sample of silt-sized vermiculite was rotated in an x-ray beam about an axis parallel to the crystallographic ab plane of the crystallites.

Structure factor analysis: Existing mathematical interpretation of x-ray diffraction phenomena, comprehensively reviewed by Buerger (1960), make it possible to calculate the theoretical intensity of diffraction maxima for a mineral of known structure. When the composition is known, a reasonable structure can sometimes be assumed, and the resultant calculated intensities compared with the observed intensities. Since considerable information is available on the structure of expansible layer silicates and only intensities resulting from diffraction by the 00ℓ planes were of interest, the task was simplified.

The intensity, (I), of x-ray radiation, which is observed and measured, is proportional to the square of the amplitude (F), which can be calculated. The amplitude can be a positive or negative quantity whereas the intensity can only be positive. For a one dimensional calculation for a centrosymmetrical crystal, the more complicated expression for the structure factor reduces to (Buerger, 1960, p. 264)

$$^{o}F_{c} = \sum_{i} f_{i}(\cos 2\pi \ell z) \qquad (i=1,\ldots,\underline{t}) \qquad (1)$$

where f_i is the atomic scattering factor of the $\underline{i}$th element, $\underline{t}$ is the number of elements in the structure, $^{\circ}F_c$ is the calculated amplitude of the 00ℓ reflection, ℓ is the order, and z is the fractional coordinate equal to r/d where r is the distance of the element from the crystallographic origin and d is the interplanar spacing.

The atomic scattering factors used were those calculated by Berguis (1955) supplemented by those of Klug and Alexander (1954, p. 680). These scattering factors are calculated assuming no thermal motion of the electrons or atoms and must be appropriately corrected before exact comparisons can be made with the observations.

Corrections for certain geometrical and physical factors must also be applied to the data. Theoretical consideration is given to this matter in Buerger (1960, pp. 152 - 241), Bradley (1964, pp. 113 - 117) and MacEwan et al., (1961, p. 406). As suggested by the latter, the Lorentz and polarization factor, (LP), customarily used for single crystals was used.

$$F_{obs} = I^{\frac{1}{2}}/LP \qquad (2)$$

$$LP = \frac{1 + \cos^2 2\theta}{\sin 2\theta} \qquad (3)$$

where LP is the Lorentz and polarization factors combined and 2θ is the angle at which the diffraction maxima occurred. The F_{obs} calculated is on an arbitrary scale depending on the instrument used, and $^{\circ}F_c$, (Eq. 1), is on an absolute scale. For this reason, the theoretical amplitude

and calculated amplitude can be compared only on a relative basis. Such a comparison, reveals gross agreement or disagreement between the proposed structure and the observations. This technique was used extensively in the early phases of the study to evaluate assumptions about the interlayer population.

One dimensional fourier synthesis: This mathematical tool used in the interpretation of intensity data is the inverse of the one discussed above. Just as structure factor analysis calculates values of F from a structure, fourier synthesis generates a representation of the structure from the values of F_{obs}. The values of F_{obs} obtained from the observed intensity as before, are transformed into a representation of electron density according to the relationship presented by Buerger (1961) for a one dimensional synthesis (p. 355) with appropriate simplification for a centrosymmetrical crystal referred to an origin taken at the crystallographic center (p. 368).

$$\rho_z = \sum_{\ell} \pm |F_\ell| \cos 2\pi \ell z \qquad (\ell = 1, \ldots, u) \quad (4)$$

where ρ_z is the electron density at z, F_ℓ is the observed amplitude (F_{obs} of Eq. 2) for the 00ℓ reflection, z is the fractional coordinate, and u is the number of diffraction maxima considered. The relationship is also dealt with by Bradley (1964, p. 122). In words, a single summation is a measure of the relative electron density at the point z required to produce the particular F_ℓ. The summation for all values of ℓ generates a representation of electron density. Similarly, the inverse is true for structure factor analysis: each piece of the

summation (Eq. 1) is the contribution of the electrons (atom) at z to the overall $F_{00\ell}$ being calculated.

As can be seen from Eq. 4, a choice of signs must be made. For the problem at hand, this choice is simplified because enough is known about the general structure of vermiculite (Mathieson, 1958), that the signs obtained by calculating $^{\circ}F_c$ were used.

Paraphrasing Buerger (1961, p. 368), fourier synthesis, in revealing the locations of atoms, provides information which can then be used to make minor corrections in the calculation of a new set of $^{\circ}F_c$ for comparison with the F_{obs}. The fourier syntheses calculated were used in this manner.

Difference synthesis: An additional tool useful in interpreting amplitudes is the difference synthesis outlined by Buerger (1960, p. 603 - 604). With this technique, the difference in observed and calculated amplitudes $(F_o - F_c)$ are used to reveal details of structure causing these differences. Fourier syntheses were made using values of $(F_o - F_c)$ to investigate the use of this approach to locate the distribution of matter in the interlayer of soil-derived dioctahedral vermiculite.

Before such a synthesis can be calculated, the values of $^{\circ}F_c$ and F_o must be placed on the same scale and be comparable. The calculation of $^{\circ}F_c$ (Eq. 1) utilized scattering factors, (f_i), assuming no thermal vibrations (0 Kelvin) and the F_o values were obtained on an arbitrary scale. Corrections for both these quantities can be obtained simultaneously once the structure is sufficiently refined as outlined by Buerger (1960, p. 583) using the following relationships:

$$KF_o = {}^{o}F_c e^{-(B\sin^2\theta)/\lambda^2} \qquad (5)$$

$$\ln(F_{obs}/{}^{o}F_c) = \ln(1/K) - (B\sin^2\theta)/\lambda^2 \qquad (6)$$

where K is the scale correction desired, λ is the wave length of radiation used, and B is the temperature correction factor. The values of ln(1/K), (intercept) and $B\sin\theta$, (slope), were obtained by linear regression analysis. The value used in the difference synthesis is calculated as follows:

$$F_o - F_c = KF_{obs} - {}^{o}F_c e^{-(B\sin^2\theta/\lambda^2)} \qquad (7)$$

The results of the difference synthesis are interpreted (Buerger, 1960, p. 605) using the slopes of the lines on the graphical representation. Calculations to determine the degree of correction were not attempted, but the atomic coordinates were shifted according to an intuitive interpretation of the difference synthesis. These new positions were used to generate new values of ${}^{o}F_c$, which were treated in the same fashion as the ones obtained initially.

Once the observed and calculated amplitudes are on the same scale and comparable, the progress of the structure refinement is measured by calculating the residual (Buerger, 1960, p. 586),

$$R = \frac{\sum_{\ell} \big|\, |F_o| - |F_c| \,\big|}{\sum_{\ell} |F_o|} \qquad (8)$$

The refinement procedure described above was used until a low residual and a low relief difference curve indicated the structures

assumed would require more data for further improvement. These techniques are usually reserved for more sophisticated structural determinations where many more reflections are available and the experimental conditions are controlled to a greater degree, allowing for more accurate corrections to be applied to the data. The maximal use of the data obtained was attempted, recognizing the possibility of error inherent in such a treatment. The structural assumptions made in the analyses attempted were based on the structural formula derived through chemical analysis and presented in the preceding section. The calculation of the number of water molecules per unit cell was based on the water loss as percent of the 350 C weight using 884 as the molecular weight of the mineral.

The linear regressions were accomplished using a desk calculator. The summations for the structure factor calculations and the fourier syntheses were carried out using an IBM-7040 data processing machine programmed with a FORTRAN IV symbolic language source deck developed under the supervision of the author. The source statements for the programs and sample output and input are included with a general description of the use of the programs in the Appendix.

Results and Discussion

Magnesium saturated dioctahedral vermiculite: Magnesium saturated dioctahedral vermiculite differs from the 14.36 A vermiculite analysed by Mathieson and Walker (1954) in that the interplanar spacing was observed to be 13.98 A. In this respect, it more closely resembles the dehydrated phase having a 13.81 A periodicity reported by Walker (1955). Walker suggested that the cations in this phase had migrated to new positions and were octahedrally coordinated by water molecules and basal oxygens. Since there was no reason to preclude a centrally located exchangeable cation with the same octahedral coordination as in the 14.36 A phase, calculations of theoretical amplitudes were made for both structures and compared in Table 24. This comparison illustrates the effectiveness of structure factor analysis, for inspection of the observed and calculated amplitudes indicates the incorrect nature of the structure proposed by Walker. This is substantiated by a larger residual (R = 0.414). The residual for the other structure (R = 0.294) leaves something to be desired, for correct structures usually have residuals less than 0.25 (Buerger, 1960, p. 586).

Inspection of the fourier transformation of the observed amplitudes presented graphically in Figure 29 reveals the nature of the discrepancy in the theoretical structure which results in the high residual. Knowing that the exchangeable cations (0.35 Mg per half unit cell) have approximately 0.35 the electron density of an oxygen in water (both have 10 electrons) and that there are almost two water molecules present per unit cell, it is a surprise to find a higher electron density at the center of the interlayer (z = 0.25). That the remainder of the structure is

Table 24—Comparison of calculated amplitudes and corrected observed amplitudes for 13.98 A Mg-saturated dioctahedral vermiculite with different cation and water positions

Mg^{2} coordinated with 3 basal oxygens and 3 H_2O after Walker (1956)			Mg^{2} centrally located in interlayer, octahedrally coordinated with 6 H_2O		
Atom	Half cell composition	Coordinate	Atom	Composition	Coordinate
Al	1.4	0.0	Al	1.4	0.0
Fe	.30	0.0	Fe	.30	0.0
Mg	.30	0.0	Mg	.30	0.0
O	6.00	1.06	O	6.00	1.06
Si	3.56	2.74	Si	3.56	2.74
Al	.42	2.74	Al	.42	2.74
O	6.00	3.32	O	6.00	3.32
Al	.35	4.46	O	3.60	5.84
O	3.60	5.60	Al	.35	6.98
	R = .414			R = .294	
00ℓ	F_c	KF_o	00ℓ	F_c	KF_o
2	30.7	29.0	2	28.8	35.8
4	- 9.9	- 3.3	4	- 4.2	- 4.1
6	- 1.2	-12.5	6	- 8.2	-15.5
8	14.8	19.0	8	19.8	23.6
10	23.7	14.4	10	22.5	17.7
12	-11.2	- 4.9	12	-12.4	- 6.0
14	-10.8	-10.9	14	- 9.5	-13.5
16	- 2.3	- 1.9	16	- 3.9	- 2.4
18	3.2	2.7	18	4.7	3.4
20	6.7	3.9	20	6.3	4.9
22	1.8	2.7	22	2.1	3.3
24	2.0	2.8	24	2.8	3.5

Figure 29—One dimensional fourier transformation of magnesium saturate dioctahedral vermiculite amplitudes.

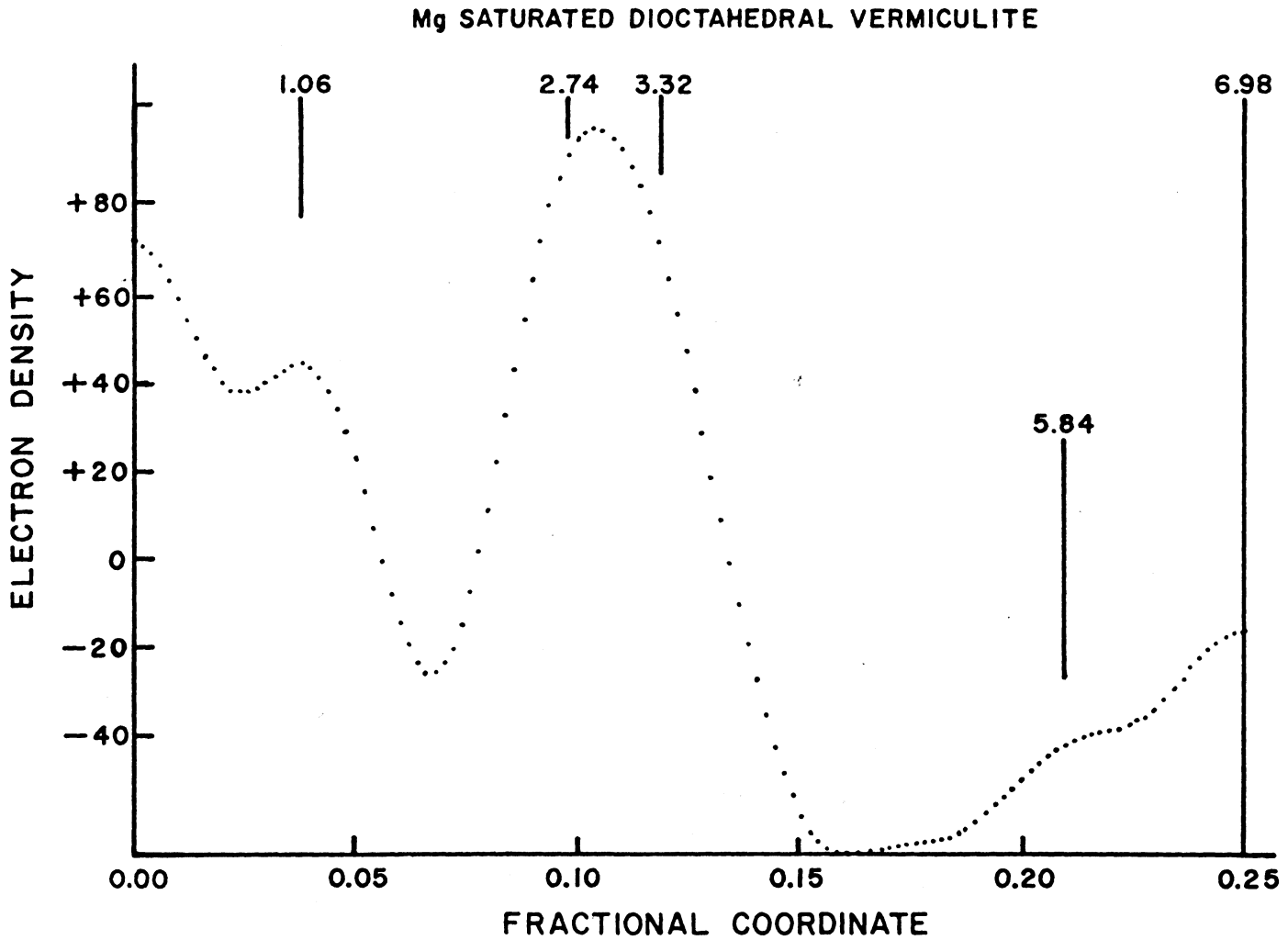
Mg SATURATED DIOCTAHEDRAL VERMICULITE
1.06
2.74
3.32
5.84
6.98
+80
+60
+40
+20
0
−20
−40
ELECTRON DENSITY
0.00
0.05
0.10
0.15
0.20
0.25
FRACTIONAL COORDINATE

essentially correct in the representation lends support to the conclusion that an unforseen structure obtains in the interlayer. The good resolution of the octahedral oxygen at 1.06 A, its exact theoretical position, supports the correctness of the electron density projection. Furthermore, the higher electron density of the tetrahedral layer relative to the octahedral layer lends additional assurance since this is expected for a dioctahedral mica. It is noted that an electron density peak is partially resolved in the 5.8 A position where all the water was expected. The topmost difference synthesis presented in Figure 30 has a steep slope in the area where the water molecules were located in the theoretical structure used to obtain F_c. This slope is preceded by a negative trough. The standard interpretation of this representation as illustrated by Buerger (1960, p. 605), yields the conclusion that the scattering matter situated at z = 0.210 in the assumed structure should be moved to a higher fractional coordinate position. The objective of such an action is to generate a featureless difference synthesis which obtains when the assumed structure is correct.

An intuitive interpretation of the fourier transform in Figure 29 indicated that there was too much scattering matter in the center of the interlayer relative to the water location. Instead of shifting all the scattering matter from its original position toward the center of the interlayer, as would be indicated by the difference synthesis alone, a portion of the water molecules were located at the center of the interlayer and the second difference synthesis presented in Figure 29 was calculated. The reduction of the relief and commensurate decrease in the residual (R = 0.175) resulted.

Figure 30—Difference syntheses obtained comparing data obtained from magnesium saturated dioctahedral vermiculite with various theoretical structures.

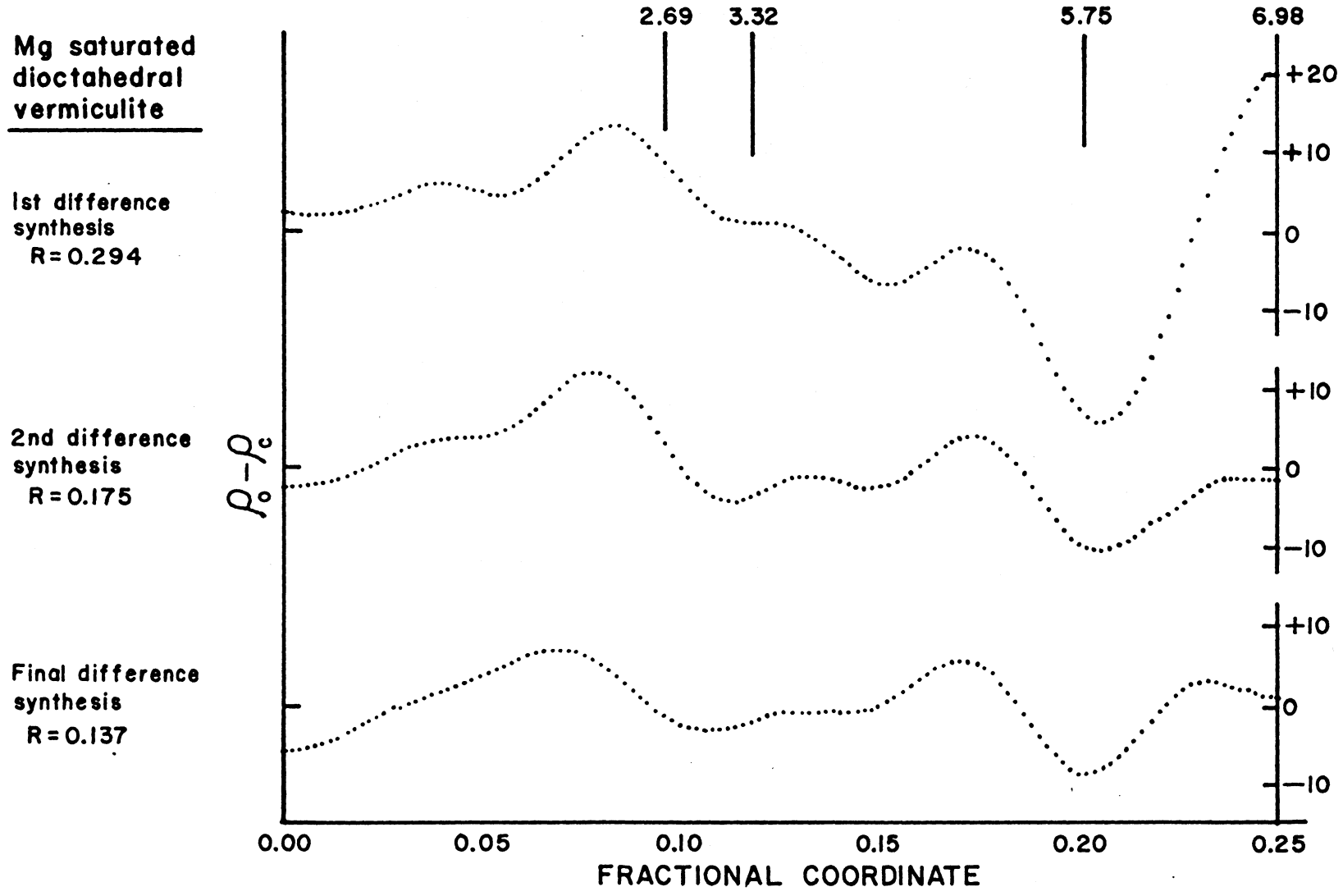
Mg saturated dioctahedral vermiculite
1st difference synthesis R=0.294
2nd difference synthesis R=0.175
Final difference synthesis R=0.137
2.69
3.32
5.75
6.98
+20
+10
0
−10
+10
0
−10
+10
0
−10
$\rho_o - \rho_c$
0.00
0.05
0.10
0.15
0.20
0.25
FRACTIONAL COORDINATE

The repetition of the difference feature in the region of the maximum electron density of the tetrahedral layer indicates that a correction in atomic coordinates is warranted in this region. The slope is opposite in sense to the one discussed above and the standard interpretation calls for a shift toward the crystallographic origin. This is not unexpected since Radoslovich (1960) has shown that the octahedral hydroxyl ion is closer to the origin than the oxygens of the tetrahedrons. Since this vermiculite is soil-derived and lower charged than the pure mica characterized by Radoslovich, more hydroxyls may be present and the average electron density may not be correctly portrayed by the average of the Radoslovich positions that were used in the structural analysis. Since average positions were used for this portion of the structure, the position of all the oxygens was shifted slightly to represent a shift of average electron density.

A slope feature similar to the one above is also repeated in the second difference synthesis at z = 0.190, which is about halfway between the central extension of the basal oxygen radii and the theoretical position of the interlayer water molecules that were not moved to the center of the interlayer. This feature indicates that the remaining water molecules should be shifted toward the basal oxygens. The third difference synthesis presented in Figure 30 reflects the improvement resultant from both the corrections discussed above by a decrease in the relief features and by its associated smaller residual (R = 0.136). The comparison between the observed and calculated amplitudes which generated the third difference synthesis are presented in Table 27 along with the

original data and associated calculations.

The coordinates and composition adopted in the structure compared are presented in Table 29. As can be seen, 1 molecule per half unit cell, along with all the exchangeable magnesium are assumed to be centrally located in the interlayer. The remainder of the 3.6 water molecules thought to be present from water loss calculations are shifted 0.1 A closer to the basal oxygens than would be expected from the dimension of the H_2O - Mg - H_2O distance (2.28) reported by Mathieson (1958) and used in the original calculation. This is not so surprising a result when viewed in the knowledge that the dioctahedral vermiculite investigated had a somewhat higher charge than the vermiculite analysed by Walker (1958). Such a higher charge may induce a shorter H_2O-O hydrogen bond distance. Though this is thought to be the case by the author, it is not a requirement, since the closer packing between the water molecules and the basal oxygen network, not necessarily accompanied by shorter bond distance, is what accounts for the smaller interplanar spacing. The evidence for the stronger hydrogen bond lies in the greater H_2O - H_2O distance apparently associated with the water coordinating magnesium, creating a distorted octahedral coordination. This could result from the H-bonds to the basal oxygens having strength enough to overcome part of the forces associated with hydration of the magnesium. In the realization that what is revealed by the one dimensional synthesis is an average distribution at best, the above argument becomes speculative, though it still is substantiated.

Aluminum saturated dioctahedral vermiculite: The aluminum saturated dioctahedral vermiculite differs from the 14.36 A vermiculite analysed

by Mathieson and Walker (1954) in that the interplanar spacing observed was 14.91 A. It does, however, resemble the hydrated phase (14.81 A) of the mineral reported by Walker (1955). In addition to the 0.1 A difference, the dioctahedral vermiculite differs in behavior from the Mg-saturated trioctahedral one characterized by Walker in that the higher spacing reported by Walker was accomplished with difficulty and days of equilibration with high relative humidity, whereas the 14.91 A spacing is stable at room temperature and humidity in the aluminum saturated specimen analysed.

Walker (1955, p. 105) envisages the swelling of the 14.36 A phase to the 14.8 A phase to involve an increase in the H_2O-O distance from 2.90 A to "about 3.1 A" and he indicates that the slow swelling is regular throughout the crystal. As demonstrated in the previous section, the dehydration of the Al-vermiculite did not proceed in a regular fashion, but led to a random interstratified product which rehydrated readily. The decrease in hydrogen bond energy inherent in the increase in the bond length proposed seems improbable in the Al-vermiculite since the water is held so tightly. A structure incorporating these longer bond lengths was assumed for the calculation of amplitudes for comparison with the observations. Additional structures, characterized as much by imagination as reason, were also studied in this manner. One of these involved the rotation of the coordinating octahedron so that it presented its broadest dimension to the basal oxygen planes rather than its narrowest as proposed by Walker (1955). The difference syntheses produced with these two assumptions are compared in Figure 32. The standard interpretation

of the negative trough at 6.32 A calls for the scattering matter on either side of it to be moved further apart. Since what is at the center cannot be moved without becoming closer to the basal oxygen, the movement of the water originally at 6.32 A can only be closer to the basal oxygen. This is what is accomplished in the structure incorporating the rotated octahedron. The difference synthesis for this structure is somewhat improved in the interlayer region, but the overall structure departs from the true one by a greater extent as indicated by a larger value of the residual. Inspection of the fourier transformation of the observed amplitudes presented in Figure 31 indicates that the scattering matter in the interlayer appears to be spread throughout the region without any distinct maxima. Such would be the case if the water molecules were in many different positions with respect to the crystallographic origin. A coherent diffracting domain would still be presented to the x-ray radiation as long as the basic periodicity obtained. With this in mind, improvement of the theoretical structure was attempted, maintaining the concept of the rotated octahedron and within the restriction of the chemical analysis which required the use of 7.6 water molecules per unit cell. This value of water is much lower than that reported by Walker (1955) for the 14.81 phase of vermiculite, but this low value is born out by the low density of the interlayer region on fourier projection. (Figure 31).

The last difference synthesis attempted is presented at the bottom of Figure 32. This synthesis, incorporating structural changes of the silicate network as well as additional shifts in the location of water,

Figure 31—One dimensional fourier transformation of aluminum saturated dioctahedral vermiculite amplitudes.

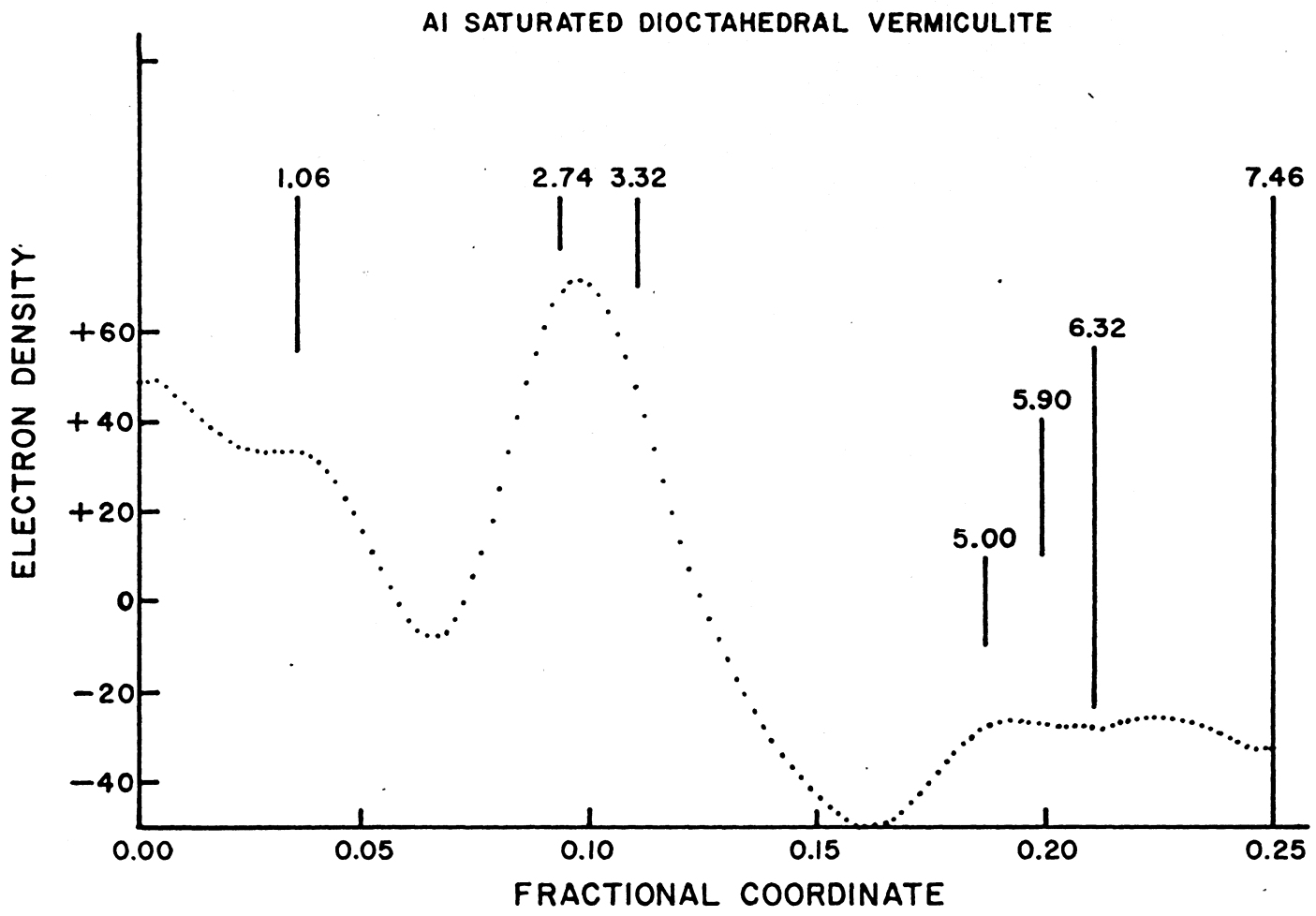
Al SATURATED DIOCTAHEDRAL VERMICULITE
1.06
2.74
3.32
7.46
6.32
5.90
5.00
+60
+40
+20
0
−20
−40
ELECTRON DENSITY
0.00
0.05
0.10
0.15
0.20
0.25
FRACTIONAL COORDINATE

Figure 32—Difference syntheses obtained comparing data obtained from aluminum saturated dioctahedral vermiculite with various theoretical structures.

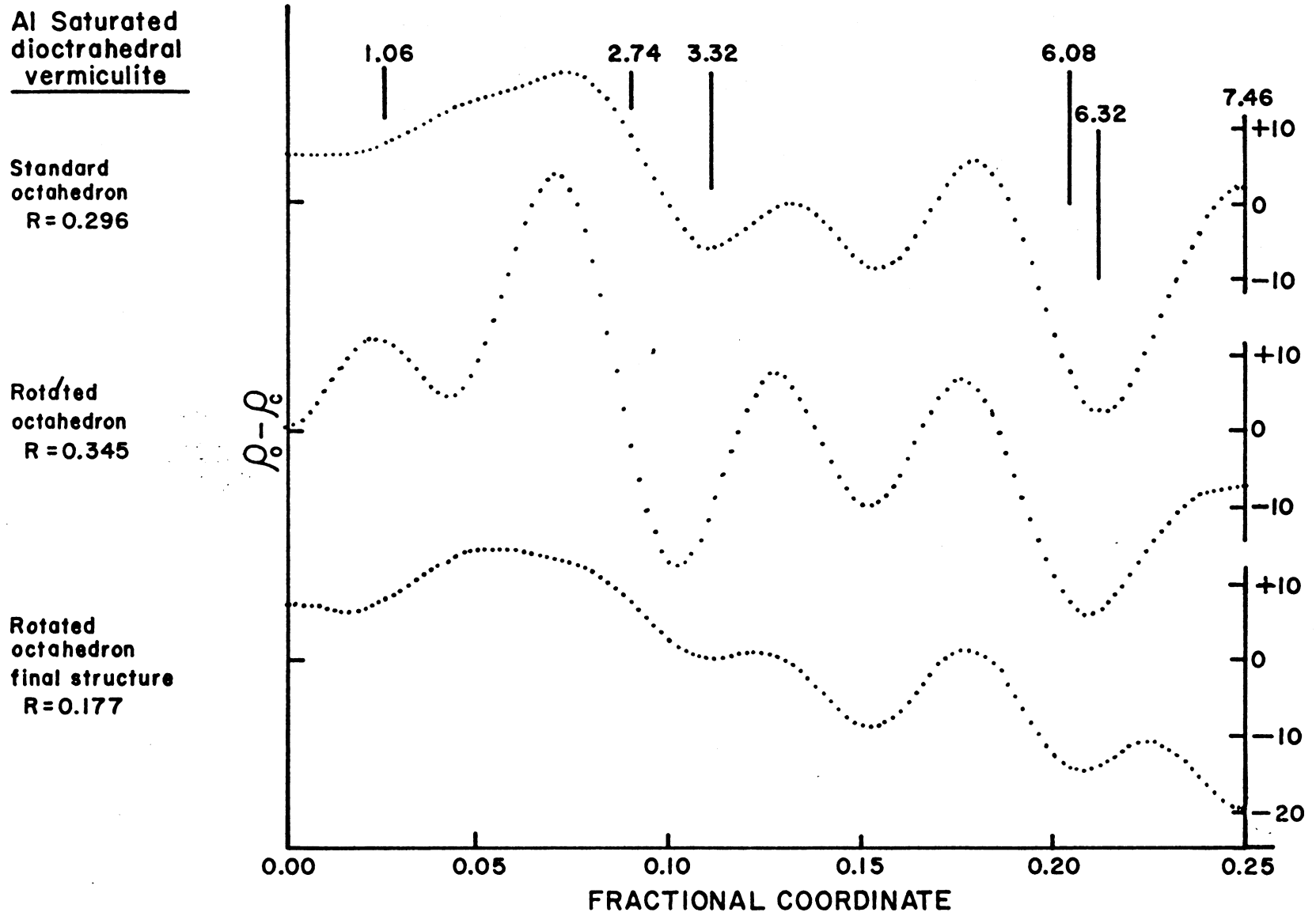
Al Saturated
dioctrahedral
vermiculite
Standard
octahedron
R = 0.296
Rotated
octahedron
R = 0.345
Rotated
octahedron
final structure
R = 0.177
1.06
2.74
3.32
6.08
6.32
7.46
+10
0
−10
+10
0
−10
+10
0
−10
−20
$\rho_o - \rho_c$
0.00
0.05
0.10
0.15
0.20
0.25
FRACTIONAL COORDINATE

still has some relief, though the residual (0.177) is approaching a satisfactory level. If one considers that the scale used in the difference synthesis plots is double that used for plotting the transformation of the data, the final difference synthesis may also be satisfactory. The original data and the calculated and observed amplitudes are presented in Table 28. The final coordinates and composition used in the last difference synthesis are presented in Table 29.

One aspect of the last difference synthesis that requires discussion is the manner in which the interlayer region is far more negative than the origin. Mathematically, this results from the large difference between the observed and calculated amplitudes for the first observable diffraction maxima (Table 28). This is so because its contribution to the difference is at its maximum positive value at the origin and at its maximum negative value at z = 0.25, following the form of the cosine curve by which it is multiplied in the transformation expression (Eq. 4). This phenomenon brings to mind a warning concerning experimental conditions expressed by Bradley (1964, p. 116), who points out that if samples used are not appropriately thick, reflections at lower angles would be enhanced because those at higher angles would effectively have less sample presented to the beam. The inordinately high 002 reflection may have resulted from such an experimental condition, even though specific effort was made to avoid it.

In full recognition of the errors that might be involved, it can be said that the data does not preclude the water molecules coordinating the

aluminum from being in an octahedron rotated sixty degrees relative to its previously accepted position. This orientation would at once explain the higher spacing and still permit shorter H_2O - O bond lengths. It is conceivable that in the negative environment of the interlayer, the waters associated with the aluminum would be at a lower energy state if four out of six could form short hydrogen bonds than six somewhat longer ones. This could be the driving force for the expansion. Since the water is not held as tightly by the magnesium ion, distortion of the octahedra permits adjustments creating shorter H-bonds without requiring their reorientation. Additional evidence for this concept is provided by the behavior of the aluminum saturated vermiculite on hydrolysis of the interlayer aluminum as was demonstrated in the previous section. When the aluminum ion is hydrolyzed, the hydrogen bond structure in which four short bonds are more stable than six, is disrupted and the system reverts to the lower spacing phase. Since only part of the aluminum hydrolyzes in this highly charged medium, the random interstratification (14.9 with 14.0) observed results. When the exchangeable aluminum is removed, the agent responsible for maintaining the 14.9 spacing is removed, and collapse to 14 A occurs as was observed.

Ratio of 7 A to 14 A intensities: Inspection of the data obtained after the aluminum saturated sample had received a single hydrolysis treatment (Table 30) discloses that the 7 A peak, which was absent in the 14.91 A phase, has appeared. This increase in the 7A/14A intensity ratio was used by Rich (1960) for a trioctahedral vermiculite and Frink (1965) for a soil chlorite-vermiculite to indicate an increase in interlayer

aluminum that occurred concurrently with hydrolysis. Since an increase in the 7A/14A intensity ratio was observed, the theoretical changes in intensity for a 14 A mineral of the composition of dioctahedral vermiculite with increases in interlayer aluminum were calculated. The results of these calculations are presented in tabular form in Tables 25 and 26. A comparison is made between a dioctahedral mineral and a trioctahedral mineral of 14 A periodicity with two different interlayer water contents. Of particular note is the calculation for 14 A dioctahedral vermiculite of the composition and water content investigated. The theoretical amplitudes were converted into intensity ratios, the form in which they commonly appear. The tables show that over much of the range of OH/Al ratio the intensity ratio decreases as the interlayer population increases, the opposite of what is commonly assumed to happen. Only at very high OH/Al ratios (high interlayer population) does the trend reverse. It is noted that the trend reverses earlier for the trioctahedral counterpart, possibly within the range that might be encountered. With additional water incorporated into the theoretical structure, this reversal of sign takes place at lower aluminum contents for both types. This reversal of sign as affected by the amount of water in the structure has been dealt with by Bradley and Serratosa (1960, p. 264), substantiating the correct nature of these calculations. The conclusion to be drawn from these calculations is that equating intensity ratios with changes in interlayer population is hazardous at best and can lead to erroneous conclusions when applied to dioctahedral vermiculites similar in composition to the one investigated.

Table 25—Theoretical ratio of 7A/14A peak intensities for Al-saturated vermiculite with 7 H_2O molecules per unit cell for varying degrees of hydrolysis of interlayer aluminum

Interlayer Al	OH/Al ratio	Amplitude sign (7A)	7A/14A ratio x 10^3
atoms per $\frac{1}{2}$ unit cell			
Dioctahedral vermiculite $(Al_{1.41}Mg_{.30}Fe^{3+}_{.30})(Si_{3.56}Al_{.44})O_{10}(OH)_2^{-.70}\ Al_{.232}^{+.70}7H_2O$			
0.23	--	-	15.
0.46	1.0	-	9.8
0.70	2.0	-	1.9
1.16	2.4	-	.5
1.40	2.5	+	.5
Ideal trioctahedral vermiculite $(Mg_{1.5})(Si_{3.30}Al_{.70})O_{10}(OH)_2^{-.70}\ Al_{.232}^{+.70}7H_2O$			
0.23	--	-	2.1
0.46	1.0	-	.5
0.70	2.0	+	.06
1.16	2.4	+	3.6
1.40	2.5	+	8.6

Table 26— Theoretical ratio of 7A/14A peak intensities for Al-saturated vermiculite with 8 H_2O molecules per unit cell for varying degrees of hydrolysis of interlayer aluminum

Interlayer Al	OH/Al ratio	Amplitude sign (7A)	7A/14A ratio x 10^3
atoms per $\frac{1}{2}$ unit cell			
Dioctahedral vermiculite $(Al_{1.41}Mg_{.30}Fe^{3+}_{.30})(Si_{3.56}Al_{.44})O_{10}(OH)_2^{-.70}\ Al_{.232}^{+.70}8H_2O$			
0.23	--	-	10.4
0.46	1.0	-	6.0
0.70	2.0	-	2.3
1.16	2.4	+	1.9
1.40	2.5	+	2.7
Ideal trioctahedral vermiculite $(Mg_{1.5})(Si_{3.30}Al_{.70})O_{10}(OH)_2^{-.70}\ Al_{.232}^{+.70}8H_2O$			
0.23	--	-	0.6
0.46	1.0	+	--
0.70	2.0	+	.9
0.16	2.4	+	9.0
1.40	2.5	+	11.4

The explanation of the increase in intensity ratio (7A/14A = 0.9 x 10^{-3}) is dealt with by Bradley (1964, p. 120-121). The illustration presented illustrates how the "layer of talc" for which his calculation was made contributes increasingly to the second order reflection as the interlayer spacing is varied from 7.45 A (C* = 0.13), reaching a maximum at 6.25 A (C* = 1.6), and then contributes decreasingly for smaller spacings such as 5.0 A (C* = 0.2). It is to be noted in this respect that the contribution of the layer to the 14 A peak is going through a minimum at the same time (C* = 0.08). The steep slope of the curve indicates that small changes in dimension will result in large increases in contribution of the talc layer. It is this increased contribution of the talc layer that is responsible for the increase in the peak ratio observed. Since changes in interlayer population are commonly associated with changes in spacing, the principle illustrated here only adds to the hazards involved in estimating interlayer populations with peak intensities.

Summary: One dimensional fourier synthesis indicated that the lower water contents found by gravimetric analysis for the high charge vermiculite investigated were rational with respect to the overall structure.

The analysis of the structure of a dioctahedral vermiculite derived from a soil revealed that the water appeared to be more randomly distributed in the interlayer region than pictured by ideal structures proposed for vermiculites.

Difference syntheses showed that, superimposed upon the random nature of the interlayer water, more matter was centrally located in the interlayer than could be accounted for by exchangeable cations alone. When this

matter was assumed to be water, a closer representation of the true structure was achieved as revealed by lower calculated residuals.

Investigation of the effect of increasing amounts of aluminum on the relative intensities of the 14 A and 7 A diffraction maxima indicated that this approach to evaluating interlayer populations is subject to error. The decrease in interplanar spacing resulting from hydrolysis of aluminum was explained on the basis of changes in interlayer water configuration and shown to be the cause of the change in 14A/7A intensity ratio observed.

Table 27—Magnesium saturated 5-2 micron dioctahedral vermiculite: original data and final theoretical and corrected amplitudes

00ℓ order	2θ	Interplanar spacing (d)	d/ℓ	Observed intensity	F_{obs}	$^{\circ}F_c$	KF_o	F_c
		A		cpm				
2	6.30	28.06	14.03	46125.0	50.5	29.2	29.5	28.8
4	12.67	27.94	6.986	299.0	- 5.8	- 2.7	- 3.4	- 2.6
6	19.05	27.95	4.659	2746.0	-21.8	-12.4	-12.7	-11.1
8	25.49	27.95	3.494	4647.0	33.2	26.1	19.4	21.3
10	32.05	27.92	2.792	2022.0	25.0	25.0	14.6	18.2
12	38.66	27.95	2.329	184.0	- 8.5	-11.4	- 5.0	- 7.2
14	45.46	27.93	1.995	752.0	-19.0	-19.9	-11.1	-10.7
16	52.20	28.04	1.752	20.0	- 3.4	- 4.7	- 2.0	- 2.1
18	59.30	28.05	1.558	34.0	4.8	5.2	2.8	1.9
20	66.75	28.03	1.401	60.0	6.9	21.3	4.0	6.0
22	74.50	28.02	1.274	25.0	4.7	10.2	2.7	2.2
24	82.70	28.00	1.167	25.0	4.9	18.0	2.9	2.9

Table 28—Aluminum saturated 20-5 micron dioctahedral vermiculite: original data and final theoretical and corrected amplitudes

00ℓ order	2θ	Interplanar spacing (d)	d/ℓ	Observed intensity	F_{obs}	$^{o}F_{c}$	KF_{o}	F_{c}
		A		cpm				
2	5.89	30.01	15.00	29968.0	39.3	33.6	45.9	33.4
4				absent	0.0	1.8	0.0	1.8
6	17.82	29.86	4.977	1361.0	-14.8	-17.9	-17.4	-16.7
8	23.86	29.83	3.729	493.0	10.4	18.5	12.2	16.4
10	29.94	29.84	2.984	1778.0	22.5	32.5	26.5	26.9
12				absent	0.0	- 0.5	0.0	- 0.4
14	42.42	29.83	2.131	272.0	-10.9	-17.5	-12.8	-12.1
16	48.80	29.86	1.866	89.0	- 6.8	-15.2	- 8.0	- 9.3
18				absent	0.0	- 1.6	0.0	- 0.9
20	62.30	29.80	1.490	31.0	4.8	16.7	5.6	7.8
22	69.35	29.81	1.355	38.0	5.6	11.6	6.6	4.6

Table 29—Final composition and coordinates assumed for structural analysis of dioctahedral vermiculite.

Element	Content	Coordinate	Fractional coordinate
	Mg-saturated dioctahedral vermiculite		
Al	0.70	0.00	0.000
Mg	0.15	0.00	0.000
Fe	0.15	0.00	0.000
O	3.00	1.06	0.038
Si	1.78	2.69	0.096
Al	0.21	2.69	0.096
O	3.00	3.32	0.119
O	1.30	5.75	0.206
O	0.50	6.98	0.255
Mg	0.18	6.98	0.255
	Al-saturated dioctahedral vermiculite		
Al	0.70	0.00	0.000
Mg	0.15	0.00	0.000
Fe	0.15	0.00	0.000
O	3.00	1.06	0.036
Si	1.78	2.69	0.090
Al	0.21	2.69	0.090
O	3.00	3.32	0.111
O	0.46	5.90	0.198
O	1.00	6.32	0.212
O	0.43	7.46	0.250
Al	0.12	7.46	0.250

Table 30—Aluminum saturated dioctahedral vermiculite after one wash with hydrolyzed aluminum solution with 1.75 OH/Al ratio

00ℓ order	2θ	Interplanar spacing (d)	d/ℓ	Observed intensity	F_{obs}
		A		cpm	
2	5.89	30.01	15.00	45797.0	48.6
4	11.83	29.92	7.481	41.0	- 2.1
6	17.89	29.75	4.958	1687.0	-16.5
8	23.97	29.70	3.712	646.0	12.0
10	30.08	29.71	2.971	1600.0	21.4
12	42.65	29.68	2.120	229.0	-10.0
14	46.00	31.57	1.973	84.0	- 6.4
16	62.60	29.68	1.484	19.0	3.7
18	69.90	29.60	1.346	25.0	4.6
20	76.50	29.88	1.245	7.0	2.5

CONCLUSIONS

The study of aluminum hydrolysis involving synthetic cation exchange resins indicated that the OH/Al ratio of the units that make up the fixed aluminum is related to charge density. As the pH of a system increases, the triple charged hydrated aluminum ion is more stable in the presence of exchange material of higher charge density. As the charge density decreases, aluminum ions may hydrolyze, forming double, or preferably, single charged units that may be joined to other single charged units through an Al-O-Al bridge. These units are thought to grow into larger structures with continued hydrolysis.

In a typical clay mineral and in an exchange resin, variation of charge density is presumed to exist, yielding zones where the charge density is lower or higher than the average. In the Dowex X8 resin, areas that have a charge density too high to permit hydrolysis may exist. Experimentally, this was demonstrated by the limited extent to which the cation exchange capacity was reduced by hydrolysis treatments using solutions increasing in OH/Al ratio. In dioctahedral vermiculite, this same phenomenon was observed. After extensive hydrolysis treatment, the random interstratified material produced still contained exchangeable aluminum and was observed to collapse to a 14 A phase on removal of this exchangeable aluminum. The analogous behavior of these two dissimilar materials is better understood when it is noted that the charge density calculated on the basis of the interlayer volume is 4.6 meq/cc for a 14.8 A vermiculite. This value compares favorably with the 3.4 meq/cc calculated for the X8 resin

on the basis of internal water.

In the lower charge density Dowex X1 resin, hydrolysis was observed to progress to a greater extent, producing fixed aluminum with higher OH/Al ratios. Units with higher OH/Al ratios have a lower charge density per unit of volume and are more compatible with, and more easily accomodated by, surfaces with lower charge density. A mineral counterpart to this low charge density resin is the mineral montmorillonite. The charge density of the interlayer volume of an 18 A montmorillonite was calculated to be 1.8 meq/cc, a value which campares favorably with the one obtained for the X4 resin (1.9 meq/cc). The larger aluminum hydroxide units found associated with this mineral by Shen and Rich (1962) and Barnhisel and Rich (1963) are not unexpected in this light. Under certain conditions (high OH/Al ratio and dilute solutions) obtaining in the experiments conducted by Barnhisel and Rich, these larger units were separated from the interlayer surfaces. In the light of what has been presented, this can be visualized as the non-aluminous cations present in the dilute salt solutions acting as agents to reduce the charge density in the environment of the large hydrolyzed aluminum units by countering the layer charge. This would free the aluminum units to continue the hydrolysis process to the thermodynamically stable gibbsite (Peech and Frink, 1963, and Garrells, 1960, p. 221). In the experiments of Shen and Rich, the conditions were not proper for the expansion of the montmorillonite and release of the aluminum hydroxide formed, so it remained in the interlayer. Only the aluminum which was directly

associated with countering the interlayer charge was released by the action of the dilute acid on the two Al-O bonds (clay-$Al^{-O-}_{-O-}Al_x(OH)_y$) yielding the one mole of aluminum found for each equivalent of exchange capacity recovered.

The use of different salts in exchangeable aluminum replacement solutions resulted in the production of a portion of the fixed aluminum as a direct result of the salt used. The OH/Al ratio of the fixed aluminum depended on the resin used (charge density) and not on the solution (OH/Al) ratio in the range studied or the manner in which the fixed aluminum was produced. These findings do not support the reports (Hsu and Bates, 1964) of the fixation of polymers of definite composition, but indicate the formation in place of hydrolyzed aluminum units, whose size and related OH/Al ratio are controlled in part by the charge density of the environment. Fixation was concluded to result from stearic hindrance, since the exchange of hydrolyzed aluminum from low charge density resins (X1) of a more porous nature was observed in the presence of other cations.

The study of different methods of sample preparation indicated that removal of aluminum interlayers and kaolinite, along with a reduction in quartz content can be accomplished by the fluoride treatment method proposed by Rich and Cook (1963) with less alteration of the mica structure than possible with other methods. The hydrous mica samples were successfully expanded by repeated treatments with $\underline{N}$ $BaCl_2$, lowering the potassium level to 0.05 percent, a level which corresponds to one potassium ion for every one hundred unit cells. These treatments

provided the first soil derived dioctahedral vermiculite in pure enough form for more precise characterizations of this important soil constituent.

The structural formula calculated from the results of total analyses revealed the mineral to be a high charge dioctahedral vermiculite with the general formula $(Al_{1.4}Mg_{.3}Fe_{.3})(Si_{3.7}Al_{.3})O_{10}(OH)_2^{-.70}X^{+.70}8H_2O$. This structural formula suggests that the lowering of the charge from the theoretical one per half unit cell to 0.7 was accomplished by oxidation of iron. This is concluded to be the mechanism initiating the weathering of this type micaceous material to dioctahedral vermiculite. The iron content is thought to be the property that differentiates the micas that yield dioctahedral vermiculite from those that yield kaolinite on weathering.

The dioctahedral vermiculite obtained on purification, produced sufficient x-ray diffraction maxima to warrant structural analysis based upon the intensity of these maxima. Calculated crystal structure factors and one dimensional fourier syntheses, in conjunction with difference syntheses, indicate a different arrangement of water than anticipated on the basis of the structures postulated by Walker (1956). That this soil derived vermiculite has a lower water content is substantiated by both chemical analysis and one dimensional electron density projections. The scattering matter centrally located in the interlayer is in excess of what can be accounted for by the exchangeable cations present. Furthermore, the analyses indicate that the water was not regularly distributed in the interlayer. A closer approach between some of the water and the basal oxygens was the assumption

required to explain the intensities observed for diffraction maxima. This suggests a shorter and stronger hydrogen bond between the waters coordinating aluminum ions than reported for minerals of comparable spacing. This involvement of the hydrogen ions in bonding in high charge density, aluminum-saturated vermiculites may be related to the difficulty with which aluminum undergoes hydrolysis in this highly charged mineral and in all high charge density evnironments.

Both the experiments with synthetic cation exchange resins and the structural analysis of the soil-derived vermiculite indicate that, contrary to the reports of Dixon and Jackson (1962), the amount of hydrolysis and the amount of aluminum that can be added through hydrolysis is limited in this highly charged material. If a mechanisn for reduction of charge, such as proposed by MacDonnell (1950), operates in addition to the oxidation of iron mentioned above, weathering products of lower charge density may be formed from dioctahedral vermiculite in which hydrolysis of aluminum could progress to a greater extent. It is doubtful if this hydrolysis proceeds to a point much beyond that which yields an OH/Al ratio equal to 2 in soil dioctahedral vermiculite and closely related materials. It is concluded that, even in the lower charge density materials, the formation of fixed aluminum results, not from the migration and subsequent fixation of "aluminum polymers" in the interlayer region, but rather from the hydrolysis and fixation of aluminum in place.

ACKNOWLEDGEMENTS

The author wishes to express his appreciation to the members of his graduate committee for their willingness to discuss problems that arose during the course of the investigation. Those who contributed willingly, but are no longer at Virginia Polytechnic Institute, include Dr. B. W. Nelson, Dr. J. A. Redden, and Dr. G. W. Thomas. Dr. Nelson was instrumental in teaching the author the principles of structural analysis through his patient effort. The author is grateful to Dr. L. K. Brice and Dr. R. V. Dietrich, the remaining members of the graduate committee, for their continuing help throughout the investigation, and to Dr. T. B. Hutcheson and Dr. H. L. Dunton for serving on the committee.

The author is particularly indebted to his major professor, Dr. Charles I. Rich, for many helpful discussions and continuing encouragement throughout the past years. He wishes to acknowledge Dr. Rich for providing many key suggestions which helped immeasurably to bring this study to its present conclusion, and is grateful for his continued interest and personal friendship.

Recognition is extended to Cecile Korsmeyer Cotton, the author's wife, for writing the program which made possible the calculations included in this work. He also commends her for her patience with, and tolerance of, all the many hardships involved in bringing this work to fruition.

The financial support of the National Science Foundation under grant number G-11402 is gratefully acknowledged. The Virginia Agricultural Experiment Station is also gratefully acknowledged for the financial support needed for computer services.

LITERATURE CITED

Aguilera, N. H. and Jackson, M. L. 1953. Iron oxide removal from soils and clays. Soil Sci. Soc. Am. Proc. 17:359-364.

Barnhisel, R. I. 1962. Unpublished M.S. Thesis. Interlayer Aluminum in Montmorillonite. Virginia Polytechnic Institute, Blacksburg, Va.

Barnhisel, R. I. and Rich, C. I. 1963. Gibbsite formation from aluminum-interlayers in montmorillonite. Soil Sci. Soc. Am. Proc. 27:632-635.

Bassett, W. A. 1958. Copper vermiculites from Northern Rhodesia. Am. Min. 43:1112-1133.

Berghuio, J., Haanappel, I.J.M., Potters, M., Loopstra, B.O., MacGillavvy, C.H., and Veehendaal, A. L. 1955. New calculations of atomic sattering factors. Acta Cryst. 8; 478-483

Bernal, J. D. and Fowler, R. H. 1963. A theory of water and ionic solution, with particular reference to hydrogen and hydroxyl ions. J. Chem. Phys. 1:515-548.

Black, R. L. and Rich, C. I. 1963. Agronomy Abstracts. A.S.A. Annual Meeting, Denver, Colo.

Bradley, W. F. 1953. Analysis of mixed-layer clay mineral structures. Anal. Chem. 25:727-730.

Bradley, W. F. 1964. X-ray diffraction analysis of soil clays and structures of clay minerals. In Soil Clay Mineralogy, (C. I. Rich and G. W. Kunfe, Editors). Univ. of N. C. Press, Chapel Hill, N. C., Ch. 111, pp. 113-124.

Bradley, W. F. and Serratosa, J. M. 1960. A discussion of the water content of vermiculite. In Clays and Clay Minerals, Proc. 7th Natl. Clay Conf., Natl. Acad. Sci.-Natl. Res. Coun., Pergamon Press, New York, pp. 260-270.

Bradley, W. F., Weiss, E. J., and Rowland, R. A. 1961. A glycol-solium vermiculite complex. In Clays and Clay Minerals, Proc. 10th Natl. Clay Conf., Natl. Acad. Sci.-Nation. Res. Coun., Pergamon Press, New York, pp. 117-122.

Brosset, C. 1952. On the reactions of the aluminum ion with water. Acta Chem. Scand. 6:910-940.

Brosset, C., Biedermann, G., and Sillen, L. G. 1954. Studies on the hydrolysis of metal ions. XI. The Aluminum ion, Al^{3+}. Acta Chem. Scand. 8:1917-1926.

Brown, G. 1954. Soil morphology and minerology. A qualitative study of some gleyed soils from North-West England. J. Soil Sci. 5:145-155. (original not seen).

Brown, G. 1953. The dioctahedral analogue of vermiculite. Clay Minerals Bull. 2:64-70.

Brydon, J. E. and Heystek, H. 1958. A mineralogical and chemical study of the dikeland soils of Nova Scotia. Can. J. Soil Sci. 38:171-186.

Buerger, M. J. 1960. Crystal-Structure Analysis. John Wiley and Sons, New York.

Coleman, N. T., Thomas, G. W. LeRoux, F. H., and Bredell, G. 1964. Salt-exchangeable and titratable acidity in bentonite-sesquioxide mixtures. Soil Sci. Soc. Am. Proc. 28:35-37.

Coleman, N. T., Ragland, J. L., and Craig, D. 1960. An unexpected reaction between Al-clay or Al-soil and $CaCl_2$. Soil Sci. Soc. Am. Proc. 24:419-420.

Cook, M. G. 1962. Unpublished Ph.D. Thesis. Alteration of Dioctahedral Micas in Soils. Virginia Polytechnic Institute, Blacksburg, Va.

Cook, M. G. and Rich, C. I. 1962. Weathering of sodium-potassium mica in soils of the Virginia Piedmont. Soil Sci. Soc. Am. Proc. 26:591-595.

Dowex: Ion Exchange. 1958. The Dow Chemical Company, Midland, Mich.

Dixon, J. B. and Jackson, M. L. 1962. Properties of intergradient chlorite-expansible layer silicates of soils. Soil Sci. Soc. Am. Proc. 26:358-362.

Fink, D. H. and Thomas, G. W. 1963. A technique for low angle x-ray diffraction studies on expanded three layer clays. Soil Sci. Soc. Am. Proc. 27:241-242.

Foster, M. D. 1960. Interpretation of the composition of trioctahedral micas. Geol. Surv. Prof. Paper 354-B. U. S. Gov. Printing Off.. Wash. D. C.

Frink, C. R. 1965. Characterization of aluminum interlayers in soil clays. Soil Sci. Soc. Am. Proc. (In press - manuscript seen).

Frink, C. R. and Peech, M. 1963. Hydrolysis of the aluminum ion in dilute aqueous solutions. Inorg. Chem. 2:473-478.

Garrells, R. M. 1960. Mineral Equilibria at Low Temperature and Pressure. Harper and Brothers, New York.

Hashimoto, I. and Jackson, M. L. 1960. Rapid dissolution of allophane and kaolinite-halloysite after dehydration. In Clays and Clay Minerals, Proc. 7th Natl. Clay Conf., Natl. Acad. Sci.-Natl. Res. Coun. Pergamon Press, New York, pp. 102-113.

Helfferich, F. 1962. Ion Exchange. McGraw-Hill Book Co., New York.

Hendricks, S. B. and Jefferson, M. E. 1938. Structures of kaolin and talc-pyrophyllite hydrates and their bearing on water sorption on clays. Am. Min. 23:863-875.

Hono, G. and Shimaoka, K. 1957. Electron Diffraction of cubic ice. Acta Cryst. 10:710-711.

Hsu, P. H. 1957. Unpublished M.S. Thesis. Aluminum Fixation in a Synthetic Cation Exchanger. Virginia Polytechnic Institute, Blacksburg, Va.

Hsu, P. H. and Bates, T. F. 1964. Fixation of hydroxy-aluminum polymers by vermiculite. Soil Sci. Soc. Am. Proc. 28:763-768.

Hsu, P. H. and Rich, C. I. 1960. Aluminum fixation in a synthetic cation exchanger. Soil Sci. Soc. Am. Proc. 24:21-25.

Jenny, H. 1961. Reflections on the soil acidity merry-go-round. Soil Sci. Soc. Am. Proc. 25:428-432.

Jackson, M. L. 1956. Soil Chemical Analysis. Advanced Course. Mimeograph published by the author. Madison, Wisconsin.

Jackson, M. L. 1958. Soil Chemical Analysis. Prentice-Hall, Englewood Cliffs, N. J.

Jackson, M. L. 1959. Frequency distribution of clay minerals in major great soil groups as related to factors of soil formation. In Clays and Clay Minerals, Proc. 6th Natl. Clay Conf., Natl. Acad. Sci.-Natl. Res. Coun., Pergamon Press, New York, pp. 133-143.

Jackson, M. L. 1963. Aluminum bonding in soils: a unifying principle in soil science. Soil Sci. Soc. Am. Proc. 27:1-10.

Jeffries, C. D., Rolfe, B. N., and Kunze, G. W. 1953. Mica weathering sequence in the Highfield and Chester soil profiles. Soil Sci. Soc. Am. Proc. 17:337-339.

Jones, L. T. and Thurman, D. A. 1957. The determination of aluminum soil, ash, and plant materials using Erichrome-Cyanine-R. Plant and Soil 9:131-142.

Keay, J. and Wild, A. 1961. Hydration properties of vermiculite. Clay Minerals Bull. 4:221-228.

Keay, J. and Wild, A. 1961. The kinetics of cation exchange in vermiculite. Soil Sci. 92:54-60.

Kiely, P. V. and Jackson, M. L. 1965. Quartz, feldspar, and mica determination for soils by sodium pyrosulfate fusion. Soil Sci. Soc. Am. Proc. 29:159-163.

Klages, M. G. and White, J. L. 1957. A chlorite-like mineral in Indiana soils. Soil Sci. Soc. Am. Proc. 21:16-20.

Klug, H. P. and Alexander, L. E. 1954. X-ray Diffraction Prodedures. John Wiley and Sons, N. Y.

Krupskii, N. K., Alexsondrova, A. M., and Khizhnyak, A. I. 1961. Determination of available aluminum in soils. Pochnovedeniye 10:93-96.

Kunin, R. 1958. Ion Exchange Resins. John Wiley and Sons, Inc. N. Y.

Low, P. F. 1955. The role of aluminum in the titration of bentonite. Soil.Sci. Soc. Am. Proc. 19:135-139.

MacEwan, D.M.C. 1961. X-ray Identification and Crystal Structures of Clay Minerals. (G. Brown, Editor) Mineralogical Society, London, Ch. IV, pp. 143-204.

MacEwan, D. M. C., Amil, A. R., and Brown, G. 1961. X-ray Identification and Crystal Structures of Clay Minerals. (G. Brown, Editor) Mineralogical Society, London, Ch. XI, pp. 393-445.

Marshall, C. E. 1949. The Colloid Chemistry of the Silicate Minerals. Academic Press Inc., New York.

Mathieson, A. McL. 1958. Mg-vermiculite: a refinement and reexamination of the crystal structure of the 14.36 A phase. Am. Min. 43:216-227.

Mathieson, A. McL. and Walker, G. F. 1954. Crystal structure of magnesium-vermiculite. Am. Min. 39:231-255.

Matijevic', E. and Tezak, B. 1953. Detection of polynuclear complex aluminum ions by means of coagulation measurement. J. Phys. Chem. 57:951-954.

McConnell, D. 1950. The crystal chemistry of montmorillonite. Am. Min. 35:166-172.

Murray, H. H. and Leininger, R. K. 1957. Effect of weathering on clay minerals. In Clays and Clay Minerals, Proc. 4th Natl. Conf., Natl. Acad. Sci.-Natl. Res. Coun., Pub. 456:340-347.

Norrish, K. and Rausell-Colom, J. A. 1961. Low angle x-ray diffraction studies of the swelling of montmorillonite and vermiculite. In Clays and Clay Minerals, Proc. 10th Natl. Clay Conf., Natl. Acad. Sci.-Natl. Res. Coun., Pergamon Press, New York, pp. 123-149.

Pimentel, G. C. and McClellan, A. L. 1960. The Hydrogen Bond. Reinhold Publishing Corp., New York.

Pearson, R. W. and Ensminger, L. E. 1949. Types of clay minerals in Alabama soils. Soil Sci. Soc. Am. Proc. 13:153-156.

Peech, M., Cowan, R. L., and Baker, J. H. 1961. A critical study of the $BaCl_2$-triethanolamine and the ammonium acetate methods for determining the exchangeable hydrogen content of soils. Soil Sci. Soc. Am. Proc. 26:37-40.

Pimentel, G. C. and McClellan, A. L. 1960. The Hydrogen Bond. Reinhold Publishing Corp., New York, pp. 255-295.

Pratt, P. F. and Bair, L. F. 1961. A comparison of three reagents for extraction of aluminum from soils. Soil Sci. 91:357-359.

Radoslovich, E. W. 1960. The structure of muscovite. Acta Cryst. 13:919-932.

Ragland, J. L. and Coleman, N. T. 1960. The hydrolysis of aluminum salts in clay and soil systems. Soil Sci. Soc. Am. Proc. 24:457-460.

Rich, C. I. 1958. Muscovite weathering in a soil developed in the Virginia Piedmont. In Clays and Clay Minerals, Proc. 5th Natl. Conf., Natl. Acad. Sci.-Natl. Res. Coun., Pub. 566: pp. 203-212.

Rich, C. I. 1960. Aluminum in interlayers of vermiculite. Soil Sci. Soc. Am. Proc. 24:26-32.

Rich, C. I. and Cook, M. G. 1963. Formation of dioctahedral vermiculite in Virginia soils. In Clays and Clay Minerals, Proc. 10th Natl. Clay Conf., Natl. Acad. Sci.-Natl. Res. Coun., Pergamon Press, New York, pp. 96-106.

Rich, C. I. and Obenshain, S. S. 1955. Chemical and clay mineral properties of a red-yellow podzolic soil derived from muscovite schist. Soil Sci. Soc. Am. Proc. 19:334-339.

Rich, C. I. 1955. Unpublished report for years 1952-1954. Department of Agronomy, Virginia Agricultural Experiment Station, Blacksburg, Va.

Ruff, J. K. and Tyree, S. Y. 1958. Light-scattering studies on aqueous aluminum nitrate solutions. J. Am. Chem. Soc. 80:1523-1526.

Schofield, R. K. and Taylor, A. W. 1954. Hydrolysis of aluminum salt solutions. J. Chem. Soc. (London) 4445-4448.

Scott, A. D. and Reed, M. G. 1960. Determination of precipitate potassium in sodium tetraphenylboron-micaceous mineral systems. Soil Sci. Soc. Am. Proc. 24:326-327.

Shallcross, F. U. and Carpenter, G. B. 1957. X-ray: crystal structure of cubic ice, -190°C. J. Chem. Phys. 26:782-784.

Shen, M. J. 1960. Unpublished M. S. Thesis. Aluminum Fixation in Montmorillonite. Virginia Polytechnic Institute, Blacksburg, Va.

Shen, M. J. and Rich, C. I. 1962. Aluminum fixation in montmorillonite. Soil Sci. Soc. Am. Proc. 26:33-36.

Slaughter, M. and Milne, J. H. 1960. The formation of chlorite-like structures in montmorillonite. In Clays and Clay Minerals, Proc. 7th Natl. Clay Min. Conf., Natl. Acad. Sci.-Natl. Res. Coun., Pergamon Press, New York, pp. 114-124.

Tanabe, H. 1954. Composition of basic aluminum solution, J. Pharm. Soc. Japan. 74:866-872, (original not seen).

Thomas, G. W. 1960. Forms of aluminum in cation exchangers. Trans. 7th Intern. Cong. Soil Sci. 2:364-369.

Walker, G. F. 1951. X-ray Identification and Crystal Structures of Clay Minerals. (G. W. Brindley, Editor), Mineralogical Society, London, Ch. VII, pp. 199-223.

Walker, G. F. 1956. The mechanism of dehydration of Mg-vermiculite. In Clays and Clay Minerals, Proc. 4th Natl. Clay Conf., Natl. Acad. Sci.-Natl. Res. Coun., Pub. No. 456, pp. 101-115.

Walker, G. F. 1961. X-ray Identification and Crystal Structures of Clay Minerals. (G. Brown, Editor), Mineralogical Society, London, Ch. VII, pp. 297-324.

Weiss, A. and Kantner, I. 1960. Uber eine einfache moglichkeit zur abschatzung der schichladung glimmerartiyer schichtsilicate. Zaitscrift fur natuv: 5b:804-807.

Wells, A. F. 1950. Structural Inorganic Chemistry. Oxford Univ. Press, London. (Original not seen).

Wells, A. F. 1962. Structural Inorganic Chemistry. Oxford Univ. Press, London.

White, J. L. 1958. Layer charge and interlamellar expansion in a muscovite. In Clays and Clay Minerals, Proc. 5th Natl. Clay Conf., Natl. Acad. Sci.-Natl. Res. Coun., Pub. No. 566, pp. 289-294.

Yuan, T. L. 1959. Determination of exchangeable hydrogen by a titration method. Soil Sci. 88:164-167.

The vita has been removed from the scanned document

APPENDIX

The two programs developed for structural analysis are presented in this appendix along with the precise instructions as to the proper format for the preparation of the input and an illustrative example of the output. The two programs, Structure Factor Analysis and One Dimensional Fourier Synthesis, do what their respective names imply.

The structure factor analysis program performs the summations required to calculate up to 20 00ℓ reflections for a centrosymmetrical crystal containing elements in up to twenty different positions according to the following relationship:

$$^{o}F_{c} = \sum_{i} f_{i}(\cos 2\pi \ell z) \qquad (i=1,\ldots,t)$$

where f_i is the atomic scattering factor of the ith element, t is the number of elements in the structure, $^{o}F_{c}$ is the calculated amplitude of the 00ℓ reflection, ℓ is the order, and z is the fractional coordinate equal to r/d where r is the distance of the element from the crystallographic origin and d is the interplanar spacing. The atomic scattering factors (f_i), for 14 elements are included in the program and are selected by choosing appropriate code numbers. Provision is made to make calculations using other elements without altering the program by including the desired scattering factors as part of the input. Also an option permitting the use of fractional coordinates instead of the coordinates in angstrom units is provided.

In using this program to make calculations for layer silicates, it must be remembered that the true crystallographic dimensions and

orders must be used (i.e., the first observable order for a mica is 002 and the d-spacing is 20 A).

The one dimensional fourier synthesis program performs the summations required to generate an electron density projection along a line perpendicular to the ab plane utilizing intensity data from up to 20 reflections, according to the following equation:

$$\rho_z = \sum_{\ell} \pm |F_\ell| \cos 2\pi \ell z \qquad (\ell = 1, \ldots, u)$$

where ρ_z is the electron density at z, F_ℓ is the observed amplitude for the 00ℓ reflection, z is the fractional coordinate, and u is the number of diffraction maxima considered. The electron density is calculated for every 0.001 fraction of a unit cell and the results are given in the output for 1/4 unit cell.

In using this program to make calculations for layer silicates, it must be remembered that the true crystallographic dimensions and orders must be used (i.e., the first observable order of a mica is the 002 and the d-spacing is 20 A).

The essential input data required is: order number, sign of the respective amplitude, observed intensity, and the diffractometer angle at which the maxima occurred (2θ). An option permitting the use of the amplitude instead of intensity is incorporated into the program. The Lorentz and polarization factor for single crystals ($LP=(1+\cos^2 2\theta)/\sin 2\theta$) is also incorporated into the program.

STRUCTURE FACTOR ANALYSIS
Data is prepared in the following manner.

Two Description Cards:

Each Description Card contains the following:

card columns	
1 - 78	any information desired
79 - 80	not used

Parameter Card:

card columns	
1 - 5	number of elements
6 - 10	number of reflections
11 - 15	largest element code number used
16 - 20	place a 1 if columns 4-13 of Data Cards contain coordinates place a 2 if columns 4-13 of Data Cards contain fractional coordinates
21 - 30	wave length in angstroms
31 - 40	d-spacing in angstroms
41 - 80	not used

Right justify the first 4 items, such as 00007 for 7 elements.

Wave length and d-spacing should have decimals punched.

Data Cards:

A Data Card is prepared for each element as follows:

card columns	
1 - 3	element code number
4 - 13	coordinate or fractional coordinate in angstroms
14 - 23	content

24 - 80 not used

Right justify the element code number. Punch decimals for the coordinate or fractional coordinate and the content.

Elements are coded in the following manner:

Element	Code Number
Li^{+}	1
C	2
N	3
O^{2-}	4
Na^{+}	5
Mg^{2+}	6
Al^{3+}	7
Si^{4+}	8
Fe^{2+}	9
Fe^{3+}	10
Ba^{2+}	11
K^{+}	12
Ca^{2+}	13
Rb^{+},Sr^{2+}	14

If elements other than those specifically listed are required, the following should be done:

Assign code numbers to each unlisted element starting with 15. A maximum of six unlisted elements may be used per data set, and would have the code numbers 15 through 20.

For each unlisted element, two Factor Cards must be made out in

addition to its Data Card (described above).

Factor Card 1:

card columns

1 - 5	the scattering factor of this element at $\sin\theta/\lambda = 0.00$
6 - 10	the scattering factor of this element at $\sin\theta/\lambda = 0.05$
11 - 15	the scattering factor of this element at $\sin\theta/\lambda = 0.10$
16 - 20	the scattering factor of this element at $\sin\theta/\lambda = 0.15$
.	.
.	.
.	.
.	.
.	.
.	.
76 - 80	the scattering factor of this element at $\sin\theta/\lambda = 0.75$

Factor Card 2:

card columns

1 - 5	the scattering factor of this element at $\sin\theta/\lambda = 0.80$
6 - 10	the scattering factor of this element at $\sin\theta/\lambda = 0.85$
11 - 15	the scattering factor of this element at $\sin\theta/\lambda = 0.90$
16 - 20	the scattering factor of this element at $\sin\theta/\lambda = 0.95$
21 - 25	the scattering factor of this element at $\sin\theta/\lambda = 1.00$
26 - 80	not used

Decimals should be punched for each scattering factor.

Factor Card sets should be entered in the same order as their respective element Data Cards are entered.

Deck Sequence:

1. Appropriate Control Cards
2. Fortran Source Deck
3. Data Set
    a. Two Description Cards
    b. Parameter Card
    c. Data Cards
    d. Factor Cards (when required)

To run more than one set of data simply place Data Sets (a. through d.) one behind the other.

ONE DIMENSIONAL FOURIER SYNTHESIS
Data is prepared in the following manner:

Two Description Cards:

Each Description Card contains the following:

card columns	
1 - 78	any information desired
79 - 80	not used

Parameter Card:

card columns	
1 - 10	wave lenght in angstroms
11 - 12	number of reflections used
13	place a +
14	place a 1 if columns 13-22 of Data Cards contain observed intensities place a 2 if columns 13-22 of Data Cards contain observed amplitudes
15 - 80	not used

A decimal should be punched for the wave length, and the number of reflections should be right justified, such as 02 for 2 reflections.

Data Cards:

card columns	
1 - 2	order
3 - 12	2θ
13 - 22	observed intensity or observed amplitude
23	sign
24 - 80	not used

Right justify order. Decimals should be punched for 2θ and the

observed amplitude or intensity.

Deck Sequence:

1. Appropriate Control Cards
2. Fortran Source Deck
3. Data Set
    a. Two Description Cards
    b. Parameter Card
    c. Data Cards

To run more than one set of data simply place one Data Set (a. through c.) behind the other.

STRUCTURE FACTOR CALCULATION

```
      DIMENSION T(20,21),T1(20,3),T2(20,3),T3(20,3),T4(20,3),T5(20,3),T6
     1(20,3),T7(20,3)
      EQUIVALENCE (T(1,1),T1(1,1)),(T(1,4),T2(1,1)),(T(1,7),T3(1,1)),(T(
     11,10),T4(1,1)),(T(1,13),T5(1,1)),(T(1,16),T6(1,1)),(T(1,19),T7(1,1
     2))
      DATA T1/2.,6.,7.,10.,10.,10.,10.,10.,24.,23.,54.,18.,18.,36.,0.,0.
     1,0.,0.,0.,0.,1.81,5.76,6.78,9.10,9.81,9.91,9.93,9.95,23.62,22.63,5
     23.02,17.65,17.65,35.35,0.,0.,0.,0.,0.,0.,1.48,5.14,6.20,8.00,9.29,
     39.66,9.72,9.79,22.55,21.61,50.41,16.68,16.68,33.61,0.,0.,0.,0.,0.,
     40./
      DATA T2/1.27,4.36,5.42,6.70,8.55,9.26,9.38,9.54,21.02,20.15,46.92,
     115.30,15.30,31.28,0.,0.,0.,0.,0.,0.,1.16,3.61,4.60,5.50,7.66,8.75,
     28.94,9.20,19.27,18.47,43.26,13.76,13.76,28.85,0.,0.,0.,0.,0.,0.,1.
     308,3.,3.86,4.50,6.77,8.15,8.42,8.79,17.46,16.74,39.91,12.27,12.27,
     426.61,0.,0.,0.,0.,0.,0./
      DATA T3/1.01,2.54,3.24,3.80,5.91,7.51,7.85,8.33,15.82,15.16,37.02,
     110.96,10.96,24.68,0.,0.,0.,0.,0.,0.,.929,2.22,2.76,3.18,5.13,6.85,
     27.26,7.83,14.29,13.70,34.53,9.89,9.89,23.02,0.,0.,0.,0.,0.,0.,.844
     3,1.98,2.40,2.70,4.45,6.20,6.65,7.31,12.95,12.41,32.35,9.04,9.04,21
     4.57,0.,0.,0.,0.,0.,0./
      DATA T4/.766,1.85,2.17,2.35,3.92,5.59,6.08,6.78,11.89,11.40,30.48,
     18.45,8.45,20.32,0.,0.,0.,0.,0.,0.,.688,1.71,1.94,2.10,3.40,4.99,5.
     251,6.26,10.83,10.38,28.60,7.86,7.86,19.07,0.,0.,0.,0.,0.,0.,.618,1
     3.63,1.84,1.96,3.04,4.51,5.02,5.77,10.10,9.69,26.91,7.49,7.49,17.94
     4,0.,0.,0.,0.,0.,0./
      DATA T5/.549,1.55,1.70,1.80,2.69,4.03,4.53,5.28,9.38,8.99,25.23,7.
     111,7.11,16.82,0.,0.,0.,0.,0.,0.,.491,1.48,1.62,1.65,2.46,3.65,4.13
     2,4.85,8.89,8.69,23.68,6.81,6.81,15.79,0.,0.,0.,0.,0.,0.,.433,1.42,
     31.55,1.50,2.23,3.28,3.72,4.42,8.39,8.39,22.12,6.51,6.51,14.75,0.,0
     4.,0.,0.,0.,0./
      DATA T6/.387,1.37,1.50,1.45,2.08,3.00,3.41,4.06,8.04,7.88,20.72,6.
     122,6.22,13.82,0.,0.,0.,0.,0.,0.,.342,1.31,1.44,1.39,1.93,2.71,3.10
     2,3.71,7.70,7.38,19.32,5.94,5.94,12.88,0.,0.,0.,0.,0.,0.,.305,1.25,
     31.40,1.34,1.84,2.50,2.86,3.42,7.43,7.12,18.12,5.67,5.67,12.08,0.,0
     4.,0.,0.,0.,0./
      DATA T7/.269,1.20,1.35,1.28,1.74,2.30,2.62,3.13,7.16,6.86,16.92,5.
     139,5.39,11.28,0.,0.,0.,0.,0.,0.,.241,1.15,1.30,1.23,1.67,2.16,2.44
     2,2.90,6.93,6.42,15.93,5.12,5.12,10.62,0.,0.,0.,0.,0.,0.,.213,1.10,
     31.26,1.17,1.60,2.01,2.27,2.68,6.69,5.98,14.94,4.84,4.84,9.96,0.,0.
     4,0.,0.,0.,0./
      DIMENSION U(20),ICODE(20),C(20),R(20),Z(20),F(20),PL(20),P(20),B(2
     10),G(20),DSCRIP(26)
      EQUIVALENCE (C,P),(U,B),(PL,G)
    1 READ 2, DSCRIP
    2 FORMAT (13A6/13A6)
      PRINT 3
```

```
  3 FORMAT (1H1,52X,25HSTRUCTURE FACTOR ANALYSIS)
    PRINT 4, DSCRIP
  4 FORMAT (1H0,27X,13A6/1H,27X,13A6)
    READ 5,N,L,LC,ICZ,ALAM,D
  5 FORMAT (4I5,2F10.0)
    DO 6 I=1,N
  6 READ 7, ICODE(I),C(I),R(I)
  7 FORMAT (I3,2F10.0)
    IF (ICZ.EQ.1) GO TO 100
    DO 102 I=1,N
    Z(I) = C(I)
102 C(I) = Z(I)*D
    GO TO 103
100 DO 101 I=1,N
101 Z(I) = C(I)/D
103 PRINT 8,D,ALAM,L,N
  8 FORMAT (1H0/1H0,8X,9HD-SPACING,F9.3,1X,5HANGS.,8X,11HWAVE LENGTH,F
   19.4,2X,5HANGS.,8X,11HREFLECTIONS,I5,8X,8HELEMENTS,I5/1H0/1H059X,11
   2HCOMPOSITION/1H0/1H ,29X,7HELEMENT,9X,7HCONTENT,6X18HCOORDINATE (A
   3NGS.),6X,21HFRACTIONAL COORDINATE/1H )
    DO 9 I=1,N
    IF (ICODE(I).EQ.1) GO TO 40
    IF (ICODE(I).EQ.2) GO TO 42
    IF (ICODE(I).EQ.3) GO TO 44
    IF (ICODE(I).EQ.4) GO TO 46
    IF (ICODE(I).EQ.5) GO TO 48
    IF (ICODE(I).EQ.6) GO TO 50
    IF (ICODE(I).EQ.7) GO TO 52
    IF (ICODE(I).EQ.8) GO TO 54
    IF (ICODE(I).EQ.9) GO TO 56
    IF (ICODE(I).EQ.10)GO TO 58
    IF (ICODE(I).EQ.11)GO TO 60
    IF (ICODE(I).EQ.12)GO TO 62
    IF (ICODE(I).EQ.13)GO TO 64
    IF (ICODE(I).EQ.14)GO TO 66
    IF (ICODE(I).GT.14)GO TO 68
 40 PRINT 41, R(I),C(I),Z(I)
    GO TO 9
 42 PRINT 43, R(I),C(I),Z(I)
    GO TO 9
 44 PRINT 45, R(I),C(I),Z(I)
    GO TO 9
 46 PRINT 47, R(I),C(I),Z(I)
    GO TO 9
 48 PRINT 49, R(I),C(I),Z(I)
    GO TO 9
 50 PRINT 51, R(I),C(I),Z(I)
    GO TO 9
 52 PRINT 53, R(I),C(I),Z(I)
```

```
   GO TO 9
54 PRINT 55, R(I),C(I),Z(I)
   GO TO 9
56 PRINT 57, R(I),C(I),Z(I)
   GO TO 9
58 PRINT 59, R(I),C(I),Z(I)
   GO TO 9
60 PRINT 61, R(I),C(I),Z(I)
   GO TO 9
62 PRINT 63, R(I),C(I),Z(I)
   GO TO 9
64 PRINT 65, R(I),C(I),Z(I)
   GO TO 9
66 PRINT 67, R(I),C(I),Z(I)
   GO TO 9
68 PRINT 69, R(I),C(I),Z(I)
41 FORMAT (1H ,27X,8H     LI+,8X,F7.3,11X,F7.3,16X,F10.4)
43 FORMAT (1H ,27X,8H       C,8X,F7.3,11X,F7.3,16X,F10.4)
45 FORMAT (1H ,27X,8H       N,8X,F7.3,11X,F7.3,16X,F10.4)
47 FORMAT (1H ,27X,8H     O-2,8X,F7.3,11X,F7.3,16X,F10.4)
49 FORMAT (1H ,27X,8H     NA+,8X,F7.3,11X,F7.3,16X,F10.4)
51 FORMAT (1H ,27X,8H    MG+2,8X,F7.3,11X,F7.3,16X,F10.4)
53 FORMAT (1H ,27X,8H    AL+3,8X,F7.3,11X,F7.3,16X,F10.4)
55 FORMAT (1H ,27X,8H    SI+4,8X,F7.3,11X,F7.3,16X,F10.4)
57 FORMAT (1H ,27X,8H    FE+2,8X,F7.3,11X,F7.3,16X,F10.4)
59 FORMAT (1H ,27X,8H    FE+3,8X,F7.3,11X,F7.3,16X,F10.4)
61 FORMAT (1H ,27X,8H    BA+2,8X,F7.3,11X,F7.3,16X,F10.4)
63 FORMAT (1H ,27X,8H      K+,8X,F7.3,11X,F7.3,16X,F10.4)
65 FORMAT (1H ,27X,8H    CA+2,8X,F7.3,11X,F7.3,16X,F10.4)
67 FORMAT (1H ,27X,8HRB+,SR+2,8X,F7.3,11X,F7.3,16X,F10.4)
69 FORMAT (1H ,27X,8H        ,8X,F7.3,11X,F7.3,16X,F10.4)
 9 CONTINUE
   DO 18 I=1,N
   M=ICODE(I)
   IF (M.LE.14) GO TO 18
   READ 19,(T(M,IJ),IJ=1,21)
19 FORMAT (16F5.0/5F5.0)
18 CONTINUE
   DO 11 J=1,L
   A=J+J
   F(J)=0.0
   W=A/(2.*D)
   IF (W.LE.1.) GO TO 13
   PRINT 14
14 FORMAT (1H0/1H0,10X,30HSCATTERING FACTOR NOT IN TABLE)
   GO TO 1
13 DO 12 I=1,N
   M=ICODE(I)
   DO 130 K=2,21
```

```
      X=K-1
      IF (W.LE.X*.05) GO TO 20
  130 CONTINUE
   20 Y=K-2
      V=(W-.05*Y)*20.*(T(M,K-1)-T(M,K))
      Q=T(M,K-1)-V
  120 P(I)=R(I)*Q*COS(6.2832*A*Z(I))
   12 F(J)=F(J)+P(I)
   11 CONTINUE
      DO 21 J=1,L
      A=J
      U(J)=ARSIN((A*ALAM)/D)
      PL(J)=(1.+COS(2.*U(J))**2)/SIN(2.*U(J))
   21 B(J)=F(J)*F(J)*PL(J)
      H=-100.
      S=100.
      DO 22 J=1,L
      H=AMAX1(F(J),H)
   22 S=AMIN1(F(J),S)
      IF (H.GT.ABS(S))GO TO 23
      H=ABS(S)
   23 PRINT 24
   24 FORMAT(1H0/1H0,29X,11H(001) ORDER,6X,9HAMPLITUDE,6X,18HRELATIVE AM
     1PLITUDE,6X,18HRELATIVE INTENSITY/1H0)
      DO 25 J=1,L
      M=J+J
      G(J) = 100.*F(J)/H
   25 PRINT 26,M,F(J),G(J),B(J)
   26 FORMAT (1H ,34X,I2,8X,F9.1,9X,F9.1,10X,F15.1)
      GO TO 1
      END
```

STRUCTURE FACTOR ANALYSIS

STUART COTTON JUNE 21 FINAL COMPOSITION AND COORDINATES ASSUMED FOR STRUCTURAL ANALYSIS OF DIOCTAHEDRAL VERMICULITE

D-SPACING 27.920 ANGS. WAVE LENGTH 1.5418 ANGS. REFLECTIONS 12 ELEMENTS 10

COMPOSITION

ELEMENT	CONTENT	COORDINATE (ANGS.)	FRACTIONAL COORDINATE
AL+3	0.700	0.000	0.0000
MG+2	0.150	0.000	0.0000
FE+3	0.150	0.000	0.0000
O-2	3.000	1.060	0.0380
SI+4	1.780	2.690	0.0963
AL+3	0.210	2.690	0.0963
O-2	3.000	3.320	0.1189
O-2	1.300	5.750	0.2059
O-2	0.500	6.980	0.2500
MG+2	0.175	6.980	0.2500

(001) ORDER	AMPLITUDE	RELATIVE AMPLITUDE	RELATIVE INTENSITY
2	29.2	100.0	15334.2
4	-2.7	-9.1	62.7
6	-12.4	-42.6	895.0
8	26.1	89.4	2860.4
10	25.0	85.7	2020.7
12	-11.4	-39.1	334.8
14	-19.9	-68.3	830.5
16	-4.7	-16.2	38.7
18	5.2	17.7	38.8
20	21.3	72.9	566.4
22	10.2	35.0	115.4
24	18.0	61.7	330.7

-OF-DATA ENCOUNTERED ON SYSTEM INPUT FILE.

ONE-DIMENSIONAL FOURIER SYNTHESIS

```
   DIMENSION THETA2(20),OBSIN(20),NSIGN(20),THETAR(20),OBSAMP(20),REL
  1AMP(20),D(20),DN(20),SINSQ(20),SNLMSQ(20),ORDER(20),DSCRIP(26),R(2
  252),IORD(20),BASE0(252)
 1 READ 2, DSCRIP
 2 FORMAT (13A6/13A6)
   PRINT 3
 3 FORMAT (1H1,49X,33HONE-DIMENSIONAL FOURIER SYNTHESIS)
   PRINT 4, DSCRIP
 4 FORMAT (1H0,27X,13A6/1H ,27X,13A6)
   READ 5, ALAM,N,NPOS,IA
 5 FORMAT (F10.0,I2,A1,I1)
   DO 6 I=1,N
   READ 7, ORDER(I),THETA2(I),OBSIN(I),NSIGN(I)
 7 FORMAT (F2.0,2F10.0,A1)
 6 THETAR(I)=(3.1416*THETA2(I))/360.
   IF (IA.EQ.1) GO TO 20
   DO 35 I=1,N
   OBSAMP(I)=OBSIN(I)
35 OBSIN(I)= OBSAMP(I)**2*(1.+COS(2.*THETAR(I))**2) /SIN(2.*THETAR(I)
  1)
   GO TO 40
20 DO 30 I=1,N
30 OBSAMP(I)=SQRT((SIN(2.*THETAR(I))*OBSIN(I))/(1.+COS(2.*THETAR(I))*
  1*2))
40 DO 41 I=1,N
   D(I)=(.5*ALAM*ORDER(I))/SIN(THETAR(I))
   DN(I)=D(I)/ORDER(I)
   SINSQ(I)=SIN(THETAR(I))**2
41 SNLMSQ(I)=SINSQ(I)/(ALAM*ALAM)
   H=-1.0
   DO 8 I=1,N
 8 H=AMAX1(OBSAMP(I),H)
   DO 9 I=1,N
   IF (NSIGN(I).EQ.NPOS) GO TO 9
   OBSAMP(I) = OBSAMP(I)*(-1.)
 9 RELAMP(I)=(100.*OBSAMP(I))/H
   PRINT 10
10 FORMAT (1H0/1H0,3X,5H(001),7X,3HTWO,7X,8HOBSERVED,15X,8HOBSERVED,7
  1X,8HRELATIVE,22X,5H  D/ ,6X,9HSIN THETA,6X,8HSIN SQD//1H ,3X,5HORD
  2ER,6X,5HTHETA,6X,9HINTENSITY,5X,4HSIGN,5X,9HAMPLITUDE,6X,9HAMPLITU
  3DE,6X,9HD-SPACING,6X,5HORDER,7X,7HSQUARED,6X,10HLAMBDA SQD/1H )
   DO 11 I=1,N
   IORD(I)=ORDER(I)
11 PRINT 12,IORD(I),THETA2(I),OBSIN(I),NSIGN(I),OBSAMP(I),RELAMP(I),
  1D(I),DN(I),SINSQ(I),SNLMSQ(I)
12 FORMAT(1H ,4X,I2,5X,F8.2,3X,F12.1,7X,A1,4X,F9.1,7X,F8.1,6X,F10.4,3
```

```
  1X,F10.4,5X,F7.4,6X,F8.4)
   DO 13 J=1,252
   Z=J-1
   Z=.001*Z
   R(J)=0.0
   DO 13 I=1,N
13 R(J)=R(J) + OBSAMP(I)*(COS(6.28318531*Z*ORDER(I)))
   S=10000.
   DO 14 J=1,252
14 S=AMIN1(R(J),S)
   DO 15 J=1,252
15 BASE0(J)=R(J)-S
   PRINT 16
16 FORMAT(1H0/1H0/1H ,25X,4HZERO,3(28X,4HZERO)/1H ,6X,1HZ,6X,8HELECTR
  1ON,4X,4HBASE,3(9X,1HZ,6X,8HELECTRON,4X,4HBASE)/1H ,4X,6HCOORD.,3X,
  27HDENSITY,4X,7HDENSITY,3(5X,6HCOORD.,3X,7HDENSITY,4X,7HDENSITY)/1H
  30/1H )
   DO 17 I=1,63
   FC1=I-1
   FC2=I+62
   FC3=I+125
   FC4=I+188
   FC1=.001*FC1
   FC2=.001*FC2
   FC3=.001*FC3
   FC4=.001*FC4
17 PRINT 18, FC1,R(I),BASE0(I),FC2,R(I+63),BASE0(I+63),FC3,R(I+126),B
  1ASE0(I+126),FC4,R(I+189),BASE0(I+189)
18 FORMAT(1H ,2X,F7.3,3X,F8.1,2X,F8.1,3(4X,F7.3,2X,F9.1,2X,F8.1))
   GO TO 1
   END
```

ABSTRACT

Hydrolysis of Aluminum in Synthetic Cation Exchange Resins and Dioctahedral Vermiculite, by Stuart B. Cotton, July, 1965.

The hydrolysis of aluminum in synthetic cation exchange resins differing in charge density was evaluated after treating aluminum and potassium saturated resins with solutions of hydrolyzed aluminum. Fixed aluminum and decrease in exchange capacity were used to calculate the OH/Al ratio of the fixed aluminum. Dowex 50 X1, the resin with lowest charge density, was found to have fixed aluminum with the highest OH/Al ratio. The highest charge density resin tested, Dowex 50 X8, was found to have a limited decrease in exchange capacity. Aluminum was exchanged from potassium saturated resins of low charge density in excess of available negative charge, yielding the conclusion that hydrolyzed forms of aluminum were exchangeable.

Purified dioctahedral vermiculite from a Nason soil was expanded using successive treatments of N $BaCl_2$, reducing the potassium level in the sample to 0.05 percent. Total analysis yielded the average formula $(Al_{1.4}Mg_{.3}Fe_{.3})(Si_{3.7}Al_{.3})O_{10}(OH)_2^{-.70}X^{+.70}\ 8H_2O$. This structural formula suggested that the lowering of the charge from the theoretical one per half cell to 0.7 was accomplished by oxidation of the iron. This was concluded to be the mechanism initiating the weathering of this type of micaceous material to dioctahedral vermiculite.

Structural analyses of both magnesium (13.98 A) and aluminum (14.91 A) saturated dioctahedral vermiculite were carried out using structure factor calculations, one dimensional fourier synthesis, and difference

synthesis. Structure factor calculation for the dioctahedral vermiculite studied indicate that the ratio of the intensities of diffraction maxima corresponding to 7 A and 14 A interplanar spacings (7A/14A ratio) should decrease as scattering matter is added to the interlayer region through hydrolysis of aluminum. Fourier synthesis and difference synthesis indicate that scattering matter was centrally located in the interlayer in excess of what could be accounted for by exchangeable cations present. It was concluded that a portion of the water was centrally located. A close approach between the remainder of the water and the basal oxygens was the assumption required to explain the observed intensities. The aluminum saturated dioctahedral vermiculite (14.91 A) was observed to collapse in a random interstratified fashion upon hydrolysis treatments with solutions of hydrolyzed aluminum. Upon potassium saturation, the collapse progressed, yielding a 14 A material. Orientation of interlayer water associated with triple charged aluminum ion (Al^{3+}) was theorized to be the cause of the stable high spacing and the hydrolysis and/or removal of the triple charge ion thought to result in the diminishing spacing.

Both the experiments with synthetic cation exchange resins and the structural analysis of soil-derived vermiculite indicate that the amount of aluminum that can be added through hydrolysis to the higher charged resins and to dioctahedral vermiculite was limited. It was theorized that hydrolyzed aluminum units could grow in association with a negatively charged surface until the diminishing charge density of the growing hydrolyzed aluminum unit approached that of the associated surface.